



**Excitotoxic Model of Posttraumatic Syringomyelia  
in the Rat**

by

**Liqun Yang**

*Department of Surgery (Neurosurgery)*

*University of Adelaide*

Submitted as part requirement for the degree of Master of Surgery, July 1999

## TABLE OF CONTENTS

ABSTRACT	iii
DECLARATION	v
ACKNOWLEDGEMENTS	vi
ABBREVIATIONS	vii
LIST OF TABLES	viii
LIST OF FIGURES	ix

### INTRODUCTION **1**

<b>1. SYRINGOMYELIA</b>	<b>1</b>
1.1 DEFINITION AND CLASSIFICATION	1
1.2 HISTORICAL INTRODUCTION	1
1.3 EPIDEMIOLOGY	3
1.4 CLINICAL PRESENTATION	4
1.5 NEUROPATHOLOGY	6
1.6 THEORIES OF PATHOGENESIS	8
1.7 ANIMAL MODELS	29
<b>2. EXCITATORY AMINO ACIDS</b>	<b>37</b>
2.1 STRUCTURE AND CLASSIFICATION	37
2.2 SYNAPTIC TRANSMISSION AND NEUROTOXICITY	41
2.3 NEURODEGENERATIVE DISEASES	52

### AIMS AND HYPOTHESES **53**

### METHODOLOGY **54**

<b>1. ANIMALS USED AND ETHICS APPROVAL</b>	<b>54</b>
<b>2. PREPARATION OF QUISQUALIC ACID SOLUTION AND SUSPENSION</b>	<b>55</b>
<b>3. PREPARATION OF KAOLIN SUSPENSION</b>	<b>56</b>
<b>4. ANESTHESIA</b>	<b>56</b>
<b>5. SURGICAL PROCEDURE</b>	<b>56</b>
5.1 QUISQUALIC ACID INJECTION	56
5.2 KAOLIN INJECTION	57
5.3 COMBINED INJECTION OF QA AND KAOLIN	57
5.4 SALINE INJECTION	58
<b>6. PERFUSION-FIXATION</b>	<b>58</b>
<b>7. TISSUE PROCESSING</b>	<b>58</b>
7.1 REMOVAL OF SPINAL COLUMNS FROM RATS	58
7.2 PARAFFIN SECTIONS	59
7.3 IMMUNOHISTOCHEMICAL TECHNIQUES	59
<b>8. PHOTOGRAPHY</b>	<b>61</b>

<b>RESULTS</b>	<b>62</b>
1. NORMAL RATS (GROUP A)	62
2. SALINE CONTROL RATS (GROUP B)	65
3. SUBARACHNOID KAOLIN INJECTION (GROUP C)	69
4. INTRAMEDULLARY QA INJECTION (GROUP D AND E)	71
4.1 LOW CONCENTRATION QA INJECTION (GROUP D)	71
4.2 HIGH CONCENTRATION QA INJECTION (GROUP E)	74
5. INTRAMEDULLARY QA INJECTION WITH SUBARACHNOID KAOLIN INJECTION (GROUP F)	77
<b>DISCUSSION</b>	<b>95</b>
1. QA AS A TOOL IN A RAT MODEL FOR TRAUMATIC SCI	95
2. THE ROLE OF SUBARACHNOID BLOCK IN POSTTRAUMATIC SYRINGOMYELIA	98
3. EXCITOTOXIC MODEL FOR TRAUMATIC SCI	101
4. QA PREPARATIONS AND INJECTION METHOD	102
5. LIMITATION OF THIS PROJECT AND FUTURE WORK	104
<b>CONCLUSIONS</b>	<b>106</b>
<b>APPENDICES</b>	<b>107</b>
<b>REFERENCES</b>	<b>112</b>

## **ABSTRACT**

It has been proposed that in posttraumatic syringomyelia, primary injury and excitotoxic cell death occurring secondary to elevated levels of EAAs initiate a pathologic process leading to the formation of spinal cavities. An animal model was devised to elucidate the role of EAAs and spinal subarachnoid blockade in posttraumatic syringomyelia. Forty-two male Sprague-Dawley rats were used in this study. The animals were divided into six groups. Group A comprised one normal rat. In Group B, three control rats received a unilateral injection of 2  $\mu$ l normal saline into the spinal cord. In Group C, five rats received an injection of 5  $\mu$ l 250mg/ml kaolin into the subarachnoid space. In Group D, ten rats received a unilateral injection of 2  $\mu$ l 8.3 mM (1.6mg/ml) QA, the EAA receptor agonist, into the spinal cord. In Group E, ten rats received a unilateral injection of 2  $\mu$ l 23.7 mg/ml QA into the spinal cord. In Group F, thirteen rats received a unilateral injection of 2  $\mu$ l 23.7 mg QA into the spinal cord following injection of 2  $\mu$ l 250 mg/ml kaolin into the subarachnoid space.

In the saline injection group (Group B) and kaolin injection only group (Group C), no animal developed a parenchymal cyst during the experimental period. Inflammatory response, neuronal degeneration and spinal cavitation were observed in 16/19 animals following the intraspinal injection of QA in Groups D and E. In these two groups, high concentration QA (23.7 mg/ml) produced larger cystic spaces and more extensive pathological changes compared to low concentration QA (8.3 mM or 1.6 mg/ml). Syring formation was seen in 9/11 animals in Group F and the combination of intrathecal kaolin and intraspinal QA was shown to produce cavities that were much larger than those found in animals injected with QA alone in Group D and E. The results of this study support the

proposal that in posttraumatic spinal cord injury, primary injury and excitotoxic cell death occurring secondary to elevated levels of EAAs contribute to a pathologic process leading to the formation of spinal cavities and a subarachnoid block by arachnoiditis is one of the pathogenic factors most responsible for initiating extension of the cavity. This excitotoxic model of posttraumatic syringomyelia in the rat may offer a useful method to study the etiology of spinal cavitation and cavity expansion.

## DECLARATION

This work contains no material that has been accepted for the award of any other degree or diploma in any university or tertiary institution and , to the best of my knowledge and belief, contains no material previously published or written by another person, except where due reference has been made in the text.

I give consent for this copy of my thesis to be made available for loan and photocopying when this copy is placed in the Barr Smith Library.

Liqun Yang

August, 1999

## ACKNOWLEDGEMENTS

I would like to thank all of the people in the University of Adelaide and Institute of Medical and Veterinary Science who gave their valuable time to assist me in my research.

Chris Brown gave his time generously to advise and assist in all aspects of my research. Glenda Summersides assisted in all aspects of animal care and theatre preparation. Melanie Smith was invaluable in conducting the immunohistochemical experiments. Dr Matthew McDonald and Dr Kingsley Storer provided expertise in the surgical technique in the rat. Lyn Cockram often helped in the administrative aspects of my research. Dr. Jennifer Brown provided a great help in revising my thesis even though she is not familiar with this research field.

I would like to thank my wife and my parents for the support that is required to leave China for research in Australia.

Finally, I would like to express my ineffable gratitude to my supervisor, Professor Nigel Jones. This work would not have been possible without the support and encouragement of my supervisor. He is one of the best supervisors I have known.

## ABBREVIATIONS

CNS	Central nervous system
HRP	Horseradish peroxidase
EAA	Excitatory amino acid
MRI	Magnetic resonance imaging
CT	Computerized tomography
NMDA	N-methyl-D-aspartate
MK-801	Dizocilpine
SCI	Spinal cord injury
KA	Kainic acid
AMPA	$\alpha$ -amino-3-hydroxy-5-methylisoxazole-4-propionic acid
QA	Quisqualic acid
NO	Nitric Oxide
PCP	Phencyclidine
ATP	Adenosine triphosphate
GFAP	Glial fibrillary acidic protein
APT	3-Aminopropyl-triethoxysilane
PBS	Phosphate-buffered saline
DAB	3, 3'- Diaminobenzidine
$\beta$ -APP	$\beta$ -Amyloid Precursor Protein
H&E	Hematoxylin and eosin
NHS	Normal horse serum

## LIST OF TABLES

<b>Table 1.</b> Classification of syringomyelia .....	2
<b>Table 2.</b> Secondary mechanisms of acute spinal cord injury .....	19
<b>Table 3.</b> Summary of characteristics and distribution of excitatory amino acid receptor .....	42
<b>Table 4.</b> Rats used to study posttraumatic syringomyelia.....	55
<b>Table 5.</b> Injection, survival, and pathology in six groups of rats .....	94

## LIST OF FIGURES

<b>Figure 1.</b> General structure of excitatory amino acids .....	38
<b>Figure 2.</b> The structures of some excitatory amino acids .....	39
<b>Figure 3.</b> Ionic structure of quisqualic acid.....	39
<b>Figure 4.</b> A schematic glutamergic synapse.....	46
<b>Figure 5.</b> Schematic diagram of an influx of $Ca^{2+}$ .....	48
<b>Figure 6.</b> Irreversible neuronal damage as a result of sustained influx of $Ca^{2+}$ .....	49
<b>Figure 7.</b> Transverse sections of spinal cord from a normal rat .....	63
<b>Figure 8.</b> Transverse spinal cord sections 4 weeks post normal saline injection .....	66
<b>Figure 9.</b> Transverse spinal cord sections 4 weeks post normal saline injection .....	67
<b>Figure 10.</b> Transverse spinal cord sections 4 weeks post subarachnoid kaolin injection .....	70
<b>Figure 11.</b> Transverse spinal cord sections 4 weeks post intraspinal 8.3 mM QA injection .....	72
<b>Figure 12.</b> Transverse spinal cord sections 4 weeks post 23.7 mg/ml QA injection .....	75
<b>Figure 13.</b> Transverse spinal cord sections 3 weeks post QA and kaolin injection .....	78
<b>Figure 14.</b> Transverse spinal cord sections 3 weeks post QA and kaolin injection .....	81
<b>Figure 15.</b> Transverse spinal cord sections 3 weeks post QA and kaolin injection .....	84
<b>Figure 16.</b> Transverse spinal cord sections 3 weeks post QA and kaolin injection .....	87
<b>Figure 17.</b> Transverse spinal cord sections 3 weeks post QA and kaolin injection .....	88
<b>Figure 18.</b> Transverse spinal cord sections 3 weeks post QA and kaolin injection .....	89
<b>Figure 19.</b> Transverse spinal cord sections 3 weeks post QA and kaolin injection .....	91
<b>Figure 20.</b> Transverse spinal cord sections 3 weeks post QA and kaolin injection .....	92
<b>Figure 21.</b> Transverse spinal cord sections 3 weeks post QA and kaolin injection .....	93
<b>Figure 22.</b> A diagram of mechanisms of “slosh” & “suck” .....	100



## **INTRODUCTION**

In this review of the literature on syringomyelia, specific consideration has been paid to syrinxes occurring as a sequel to spinal cord trauma, i.e., posttraumatic syringomyelia.

### **1. Syringomyelia**

#### ***1.1 Definition and classification***

The word syringomyelia was coined by Charles P. Ollivier d' Angers from the fusion of the Greek words for pipe and marrow in an 1827 publication.<sup>1</sup> Now syringomyelia is defined by The Oxford English Dictionary<sup>2</sup> as a "dilation of the central canal of the spinal cord or formation of abnormal tubular cavities in its substance". Therefore, the term 'syringomyelia' in this thesis will be used for all longitudinal fluid-filled cavities within the spinal cord that extend over two segments rather than minor cystic changes at the injury site, which usually do not extend more than one vertebra beyond the level of the injury and are usually termed 'cystic myelopathy'.

Several classifications of syringomyelia have been introduced.<sup>3-5</sup> Barnett<sup>5</sup> classified syringomyelia into five types according to the postulated pathophysiologic mechanisms. The classification presented in Table 1 is adapted from Barnett's classification.

#### ***1.2 Historical introduction***

Estienne in 1546 was the first to describe pathologic cavitation of the spinal cord.<sup>6</sup> A linkage between the presence of the lesion and the expression of clinical

**Table 1. Classification of syringomyelia.**

- 
1. Communicating syringomyelia
    - a. Congenital deformities at the craniocervical junction
    - b. Acquired abnormalities at the craniocervical junction
  2. Noncommunicating syringomyelia
    - a. Congenital deformities at the craniocervical junction
    - b. Postinflammatory syringomyelia
    - c. Syringomyelia related to spinal cord tumors
    - d. Syringomyelia as a late sequel to trauma (posttraumatic syringomyelia)
- 

signs (paralysis) was established by Portal in 1804.<sup>7</sup> After Stilling in 1859 described a persistent dilatation of the central canal in the adult and Hallopeau in 1870 demonstrated pathologic cavitation which was anatomically separate from the central canal, most investigators applied the term 'syringomyelia' to a condition of pathologic cavitation separate from the central canal whereas those cavities that were a pathologic dilation of the central canal were termed 'hydromyelia'.<sup>8</sup> Ballantine et al.<sup>9</sup> in 1971 proposed that these two forms of pathologic cavitation in the spinal cord should be grouped into a single entity, 'syringohydromyelia'.

Posttraumatic syringomyelia is a serious late complication of spinal injury, which was first described by Bastian in 1867.<sup>10</sup> Soon, Holmes<sup>11</sup> reported that an intramedullary spinal cord lesion was found occurring at a distance from the site of severe spinal cord injury. Later, Barnett et al.<sup>12</sup> described the development of spinal cord cavities which were separate from the central canal following serious

spinal cord injury. Other similar findings were reported by Freeman<sup>13</sup> and Rossier<sup>14</sup>. They regarded these cases as cystic degeneration of the spinal cord resulting from spinal cord trauma. The introduction of MRI and modern autopsy studies have shown an increasing frequency of posttraumatic syringomyelia.<sup>8</sup>

Schultze in 1887 and Kahler in 1888 described the classic presentation of syringomyelia.<sup>1</sup> They proposed that a dissociated sensory deficit involving the upper extremity was diagnostic of syringomyelia. The treatment of syringomyelia has essentially been surgical since Puusepp<sup>15</sup> in 1926 performed the first shunting of a syrinx in the spinal cord.

It has been more than three centuries since Estienne<sup>6</sup> in 1546 first described pathologic cavitation of the spinal cord, but the pathophysiologic mechanism of syringomyelia still remains so controversial that the development of effective methods of treatment is impeded.

### ***1.3 Epidemiology***

Syringomyelia is an uncommon disease whose true incidence is unclear. In a nationwide survey of syringomyelia in Japan, a prevalence rate of 1 per 100,000 was reported.<sup>16,17</sup> There is no sex predilection in the development of syringomyelia.<sup>18</sup> An apparent increasing prevalence of syringomyelia due to the introduction of MRI and the prolonged survival of patients with spinal cord injury has been observed.<sup>8</sup>

Previous studies, based on clinical examination and spinal CT, showed that the incidence of posttraumatic syringomyelia in patients with spinal cord trauma was low, between 1% and 5%,<sup>19,20</sup> but incidences of 12-22% have been reported since the introduction of MRI.<sup>20</sup> This figure is close to the 17% found in the only

large published postmortem study of 120 cases.<sup>21</sup> The annual rate of acute spinal cord trauma in most countries is 20-40 persons per million. Traffic accidents, sports and recreational activities, accidents at work and falls at home are the main causes of spinal cord trauma. In addition, one half of the patients with spinal cord trauma have complete injuries of the spinal cord with no preservation of voluntary motor or sensory function below the level of the lesion and the levels of lesions in two-thirds of the patients are in the cervical region.<sup>22</sup>

#### ***1.4 Clinical presentation***

The clinical presentation of syringomyelia is considerably varied, depending on the location of the spinal cord cavitation and consequent gliosis of the spinal cord parenchyma. The predominant clinical course is slowly progressive.<sup>16</sup> The clinical features usually include an insidious onset of a dissociated sensory deficit involving the upper extremity, lower limb stiffness, pain and numbness of the hands, oscillopsia, diplopia, dysesthesia, ataxia and urinary incontinence.<sup>18</sup>

Various forms of development in posttraumatic syringomyelia have been described, including progressive evolution, acute phase and stabilisation, and remission.<sup>10</sup> It was indicated by Quencer et al.<sup>23</sup> that posttraumatic spinal cord cysts were common in patients with new and/or progressively worsening neurological symptoms who, in the past, had suffered significant cervical or thoracic spinal trauma. Moreover, a prospective study of 449 traumatic paraplegic and tetraplegic patients with spinal cord injury demonstrated that neurological worsening or improvement was attributed to the enlargement or collapse of the cystic cavity in the spinal cord.<sup>10</sup> The interval between spinal trauma and the appearance of neurological symptoms varied from 2 months to 36 years.<sup>24</sup>

The most common first symptom, which occurs as early as two months and as late as 30 years after injury, is usually pain,<sup>10,25</sup> which is usually induced by coughing, straining or moving.<sup>26</sup> Thirty-four to 94% of people develop pain following SCI and the pain is described as severe by one-third of these. This has been classified into several categories including musculoskeletal, visceral and neuropathic. The pain may present in different ways, such as a burning or a sharp shooting pain either at the level of the spinal cord injury or diffusely below the level of injury. Increased sensitivity to light touch (allodynia) in the dermatomes may be present at or just above the level of injury.<sup>27</sup> The phenomenon of pain can, in part, be attributed to deafferentation hyperactivity.<sup>28</sup>

The progressive type of posttraumatic syringomyelia is characterized by pain at the onset, followed by objective motor, sensory and reflex changes.<sup>12</sup> The most common presenting symptoms are pain, spasticity, sensory loss, hyperhidrosis, and weakness and the usual physical findings are spasticity, hypesthesia, and weakness.<sup>13</sup>

However, in many cases of posttraumatic syringomyelia, few neurologic deficits may be noted and the physical examination is insufficiently sensitive and nonspecific even when posttraumatic syrinxes extend over many cord segments rostral to a spinal cord injury and produce extensive neuronal loss, especially in the intermediate to intermedio-lateral gray matter.<sup>19</sup> Obvious sensory and/or motor changes and functional decline may only occur late in the development of posttraumatic syringomyelia.

Taken together, these observations suggest that the progression of symptoms is unpredictable and patients may gradually deteriorate over several years to decades. Paraplegia often develops in the later stage.

### ***1.5 Neuropathology***

Syringomyelia is a disorder characterized by the development of an abnormal fluid-filled cyst in the spinal cord. Syringomyelia, which may be congenital or acquired, most commonly occurs in the cervical spinal cord but can involve the entire length of the spinal cord. In some instances, the syrinx may occur in or extend into the brain stem (syringobulbia).<sup>4</sup> The histological changes of syrinxes in humans vary greatly from case to case. Syringomyelia can be classified into three pathologic types: 1) central canal syrinxes communicating with the fourth ventricle in association with hydrocephalus; 2) noncommunicating central canal syrinxes that occur with a wide variety of congenital and acquired disorders such as Chiari malformations, arachnoiditis, and extramedullary compressive lesions; and 3) parenchymal syrinxes that are associated with conditions that directly injure spinal cord tissue, including trauma and hemorrhage.<sup>3</sup>

Communicating central canal syrinxes may be lined wholly by ependyma or by ependyma and a feltwork of glial fibers and collagen. Serial histological sections in these cases show that the central canal at C1 is patent and it is in continuity with the fourth ventricle and that the syrinxes are defined at their caudal end by age-related stenosis of the central canal.<sup>29</sup> The central canal of the spinal cord normally undergoes some degree of stenosis with aging in 70% to 80% of the general population. This is attributed to common viral infections producing ependymitis.<sup>4</sup>

Noncommunicating central canal syrinxes are usually lined by glial and connective tissue and are found at a variable distance from the fourth ventricle. This type of syrinx is usually a dilation of the central canal which is anatomically

not continuous with the fourth ventricle or the subarachnoid space and which is usually defined rostrally and caudally by canal stenosis. The syrinxes are complex, including extensive ependymal denuding, septations and paracentral dissection. Approximately 40% of central canal syrinxes are found to rupture paracentrally and dissect into the parenchymal tissues, which may cause segmental neurological deficits.<sup>3,4</sup>

Extracanalicular syrinxes are associated with conditions which have injured spinal cord tissue (trauma, infarction and hemorrhage). The syrinxes may be present at any level and occur most frequently in the dorsal part of the cord.<sup>23</sup> Histologically, extracanalicular syrinxes are lined by glial or fibroglial tissue and are characterized by the presence of central chromatolysis, neuronophagia and Wallerian degeneration.<sup>3</sup> Recently, on the basis of their observations on the pathology of human spinal cord injury, Bunge et al.<sup>30</sup> reported that the main focus of injury appeared to be in the dorsal part of the lateral white matter in the midcervical level, where a focus of substantial axon loss was seen. In addition, their study showed substantial focal demyelination following chronic spinal cord compression in humans, which is well known in experimental lesions in animals.

Usually cavities in posttraumatic syringomyelia are not connected with the central canal and the central canal is normal. Multiple cavities may or may not inter-communicate. The cavity usually occupies the gray matter in the spinal cord and may develop rostrally or caudally from the site of the injury in the spinal cord and the medulla.<sup>25,26</sup> Light microscopic studies of posttraumatic syringomyelia have demonstrated that the cavity is lined by glia or collagen with little or no ependymal component<sup>26</sup> and early reactive edema and necrosis in the surrounding neural tissue are followed by macrophage infiltration, capillary proliferation and

reactive gliosis which predominates in the late phase after injury. Atrophy of long tracts, enlarged perivasular spaces, perivasular inflammation, perivasular collagen and schwannosis are also often observed.<sup>19</sup> Using electron microscopy, it is demonstrated that the syrinxes are lined largely by cell processes of astrocytes and a small portion of the lining consists of ependymal cells without surface processes. The cystic cavities may develop as early as six weeks after traumatic injury.<sup>20</sup> The pathological changes in the spinal cord after acute traumatic injury, including hemorrhage, edema, neuronal necrosis and demyelination, are followed by cyst formation and infarction. The central zone occupied by hemorrhage at the injury site is necrotic by 24 to 48 hours after major trauma. Several days later, the hemorrhagic zone shows cavitation and the adjacent areas exhibit patchy necrosis.<sup>22,25</sup> Finally, the spinal cord becomes relatively fixed at the site of trauma by arachnoidal adhesions and complete subarachnoid block is often demonstrated. Several studies have shown that the pathological changes after trauma, a process of autodestruction, worsened with time. The pathological studies by electron microscopy also showed progressive changes including granular dissolution of the axoplasm and vesicular disruption of myelin after traumatic injury.<sup>22</sup>

### ***1.6 Theories of pathogenesis***

Although cavitation of the spinal cord has been recognized for more than three centuries as a pathologic entity, considerable controversy regarding the pathophysiologic basis of the disorder continues. Syringomyelia was originally described as a developmental abnormality.<sup>31</sup> Subsequently, it has been proposed that tumors, vascular changes, infective processes, extramedullary compressive lesions and congenital anomalies are associated with syrinx formation.<sup>8</sup> In the

sections that follow, each of the theories will be discussed according to the classification system in this thesis (see *Classification*, page 2).

#### **1.6.1. Communicating syringomyelia: congenital**

Communicating syringomyelia means that there is a communication between the syrinx and the fourth ventricle. Most cases of communicating syringomyelia are associated with congenital deformities at the craniocervical junction, including the Chiari malformation and the Dandy-Walker malformation.<sup>4</sup>

Chiari in 1891 divided hindbrain abnormalities associated with hydrocephalus into three types:<sup>32</sup>

- I Displacement of the cerebellar tonsils into the cervical spinal canal, without caudal displacement of the medulla,
- II Displacement of the inferior vermis into the cervical canal and caudal displacement of the lower pons and medulla, with elongation of the fourth ventricle, and
- III Herniation of the cerebellum in a meningoencephalocele combined with caudal displacement of the brainstem and medulla.

The Dandy-Walker deformity is described as a communicating hydrocephalus due to obstruction from birth of the foramina of Magendie and Luschka. Additionally, all the cerebral ventricles are enlarged and the posterior fossa of the skull is small.<sup>33</sup>

The common feature of these malformations is obstruction of the outlets of the fourth ventricle. From this common feature, hydrodynamic theories have been proposed.

It was demonstrated by Gardner et al.<sup>34</sup> during operation in 1957 that a communication between the fourth ventricle and the upper cervical cavitory lesion in the spinal cord existed in patients with the Chiari malformation. McLaurin et al. in 1954 reported that dilatation of the central canal and the cerebral ventricles was produced by intracisternal injection of kaolin. A radiopaque medium injected into the ventricles of their animals did not escape from the foramina into the subarachnoid space but passed from the fourth ventricle into a dilated central canal. Therefore, from previous experimental studies and observations during surgery, Gardner<sup>35</sup> in 1965 proposed the hydrodynamic mechanism of syringomyelia, namely the gentle, repeated ventricular fluid hammer effect of its pulse pressure, which was transmitted from the beating of the choroid plexus, drove the fluid wave down into the central canal of the spinal cord via an opening at or adjacent to the obex when the foramina of the fourth ventricle were blocked. The ependymal lining of the central canal was ruptured by the consequent hydromyelia, and fluid then continued to force its way through the gray matter of the cord, resulting in syringomyelia. According to this theory, the formation of a syrinx was a process of slow dissection by the pulsatile hydrodynamic force. The hydrodynamic mechanism with respect to the pathogenesis of communicating syringomyelia associated with congenital malformation was first proposed by Gardner.<sup>35</sup> Later Becker et al.<sup>36</sup> and other researchers found dilation of the central canal at the thoracic cord level in kaolin-induced hydrocephalic animals and they also suggested that the central canal was distended in the hydrocephalic condition by the CSF pulse-pressure wave from the fourth ventricle based on the observation that no central canal dilation existed without significant ventricular enlargement. In addition, Eisenberg et al. and other investigators<sup>37</sup> used a

radioisotope to demonstrate downward movement of CSF from the fourth ventricle into the spinal central canal in kaolin-induced hydrocephalic animals. A clinical study by Ghanem et al.<sup>38</sup> in 1997 reported that improvement of syringomyelia and neurologic deficit was observed with suboccipital foraminotomy for the treatment of syringomyelia associated with Chiari I malformation in 12 children, supporting Gardner's hydrodynamic theory. This sequence of observations was consistent with a hydrodynamic mechanism proposed by Gardner. Currently, the hydrodynamic mechanism is widely accepted, according to which CSF from the fourth ventricle passes through the obex down into the spinal central canal and, consequently, distends the canal (hydromyelia) and disrupts the canal into the parenchyma (syringomyelia). The validity of the hydrodynamic theory is dependent upon the presence of communication between the syrinx and the fourth ventricle.

#### **1.6.2. Communicating syringomyelia: acquired**

Some cases of communicating syringomyelia are associated with acquired abnormalities at the craniocervical junction, such as tonsillar herniation secondary to intracranial mass lesions<sup>39</sup>, basilar impression<sup>40</sup> and Lhermitte-Duclos disease of the cerebellar vermis.<sup>41</sup>

To study the mechanism of this type of syringomyelia, researchers usually inject some irritating substances, including kaolin, into the cisterna magna in animals to mimic acquired abnormalities at the skull base. In 1954, McLaurin et al.<sup>42</sup> reported that both hydrocephalus and cavitory lesions in the spinal cord were produced in a model of chronic arachnoiditis by injecting kaolin into the cisterna magna of dogs. Further, they observed a dense adhesive arachnoiditis which

completely surrounded the spinal cord with a paucity of inflammatory cells and this suggested that the vessels of the affected subarachnoid space were constricted by the hypertrophic tissue. Therefore, they concluded that the cavitory lesion was the result of ischemia. The ischemic hypothesis for experimental syrinx formation was supported by the experimental work of Dohrmann.<sup>8</sup> However, the ischemic hypothesis is still in dispute. The evidence disputing the ischemic hypothesis was provided by both Hall et al.<sup>36</sup> and Williams et al.<sup>43</sup>, who found no ischemic changes in their experimental animals prepared by the technique of McLaurin et al. In a further step, Hall et al.<sup>36</sup> reported that the neurons and glial tissue in the immediate vicinity of the kaolin-induced cysts were perfectly preserved, contradicting the ischemic hypothesis. Becker et al.<sup>8</sup> performed cisternal injection of kaolin to produce a syrinx in the spinal cord and arrested the syrinx by blockage of the obex and filum. This study supported the hydrodynamic theory of syrinx formation proposed by Gardner.<sup>35</sup>

Subsequently, experimental work of James et al.<sup>8</sup> and Williams et al.<sup>43</sup> modified the hydrodynamic theory. They used silicone rubber rather than kaolin as the cisternal injection agent. The difference between these two agents was that the former produced a significant hydrocephalus without causing the dense inflammatory reaction of the cervical spinal cord meninges, which was characteristically caused by the latter. In that study, there existed a patent communication between the central canal and the enlarged ventricular system, but no syrinx or dilation of the central canal was observed. Two years later, Williams et al.<sup>43</sup> performed cisternal injection of kaolin by the same technique to demonstrate enlargement of the central canal in 11 animals and found cavities in the spinal cord in 7 of these animals. The results of these two research groups

demonstrated that hydrocephalus was a necessary but not sufficient cause of spinal cord cavitation and a spinal meningeal inflammatory reaction resulting in subarachnoid scarring and local ischemia may be of special importance in the development of a syrinx in the spinal cord.

### **1.6.3 Non-communicating Syringomyelia: congenital**

Based on previous pathological investigations, syringomyelia associated with the Chiari I malformation is characterized by dilation of the central canal (hydromyelia) and/or paracentral intramedullary cavitation (syringomyelia) located in the posterior horn and/or the posterior column of the cervical cord,<sup>3,17</sup> which appears to be an initial process in the occurrence of this spinal cord lesion. Recent MRI and pathological investigations of syringomyelia associated with Chiari I malformation have clearly demonstrated that no definite CSF communication between the central canal syrinxes and the fourth ventricle is established in the majority of patients. The mechanism of the central canal dilation can be well explained by the hydrodynamic theory, whereas the formation of non-communicating cavities can not be explained by this theory.

McLaurin et al.<sup>42</sup> and other investigators<sup>37</sup> discovered that myelomalacia which was located in the posterior half of the cervical spinal cord correlated with prominent spinal arachnoid granuloma, arterial narrowing, and thrombus formation in kaolin-hydrocephalic animals. Additionally, the posterior half of the cervical spinal cord, which is supplied by the terminal branches of the anterior and posterior spinal arteries, is highly vulnerable to vascular impairment. Therefore, they proposed that vascular impairment caused by spinal arachnoiditis might be responsible for cervical cord cavitation. However, subsequent studies<sup>37,43</sup>

have shown that vascular impairment of the cervical cord is not closely correlated with spinal arachnoiditis induced by kaolin, so kaolin-induced inflammation does not play a key role in cervical myelomalacia. Rather, a close correlation between cervical insufficient blood supply and tonsillar herniation resulting from gross hydrocephalus has been observed. Experimental work of Yamada et al.<sup>37</sup> in a perfusion study revealed insufficient blood flow within the cervical cord at the level of the intramedullary cavities. They found that the vascular insufficiency of the cervical cord was closely correlated to the tonsillar herniation resulting from significant hydrocephalus and therefore postulated that cervicomedullary compression at the foramen magnum resulting from tonsillar herniation affected the venous drainage of the cervical cord, caused insufficient blood supply in the cervical cord and finally resulted in intramedullary cavitation.

From their autopsy studies and animal experiments of syringomyelia associated with the Chiari malformation, some investigators<sup>37</sup> also proposed that cervicomedullary compression at the foramen magnum resulting from tonsillar herniation was responsible for vascular impairment of the cervical cord at some distance caudal to that level, particularly a disturbance in venous drainage with resultant intramedullary cavitation.

Two types of syrinx in syringomyelia associated with the Chiari malformation—central canal dilation prominent at the thoracic level and cervical cord cavitation in the posterior column and posterior horn—were produced by the hydrodynamic force and by vascular impairment, respectively. Some intramedullary cavities located close to the central canal could easily communicate with it through enlarged parenchymal interspaces. Therefore, distending force could increase the size of the syrinx when the syrinx in the

cervical cord communicated with the central canal.<sup>37</sup> The enlargement of the other noncommunicating cavities can be explained by the theory, proposed by Ball and Dayan,<sup>44</sup> that CSF flows from the spinal subarachnoid space through the interstitial spaces of the posterior horn into the syrinx.

#### **1.6.4. Postinflammatory syringomyelia**

Postinflammatory syringomyelia, which may result from infections (e.g., tubercular, fungal, and parasitic) or from chemical meningitis, is commonly associated with arachnoiditis and arachnoidal scarring. Knowledge that spinal arachnoiditis produced spinal cord cavitation dates from 1861 when Vulpian reported the earliest case.<sup>29</sup>

There were 14 cases of syringomyelia resulting from arachnoiditis limited to the spinal cord in Barnett's review,<sup>29</sup> in which the diagnosis was confirmed by surgery or necropsy or myelography. Barnett considered syringomyelia associated with spinal arachnoiditis as one of the non-communicating types because there was no communication between the cyst and the fourth ventricle. Moreover, Barnett concluded in his review that ischemia of the central area of the spinal cord followed by subsequent cavity formation was an important factor in the production of the spinal syrinx. Caplan et al.<sup>8</sup> reported 5 patients with syringomyelia and chronic arachnoiditis and suggested that ischemia caused by meningeal scarring and disturbance of CSF circulation induced by focal scarring with spinal block were responsible for syrinx formation in the spinal cord. These hypotheses are consistent with the report of Cho et al.<sup>45</sup>, who produced an expanding syrinx in the spinal cord of their animal model when traumatic injury was either preceded or followed by the intradural injection of kaolin and they

demonstrated that the combined trauma and kaolin group was more prone to develop a syrinx. These results confirmed the conclusion by Barnett et al.<sup>29</sup> that tethering of the cord by focal scarring of the meninges, which limited mobility of the cord and created a subarachnoid block, was one of the pathogenic factors which were responsible for the formation and extension of the cavity.

#### **1.6.5. Syringomyelia associated with tumors**

The association of syringomyelia with spinal cord tumors had its origin in the discovery by Simon in 1875, who reported the simultaneous occurrence of syringomyelia and tumors.<sup>8</sup> There were numerous studies that proposed a variety of pathophysiologic mechanisms for the production of syrinx associated with neoplasms, such as edema, blockage of the perivascular spaces, disturbance in blood supply to the cord, spontaneous hemorrhage, and autolysis of the mass.<sup>8</sup>

#### **1.6.6. Posttraumatic syringomyelia**

There is no doubt regarding trauma as a cause of cavitory spinal cord lesions. However, the pathophysiology of posttraumatic syringomyelia is still controversial. Gardner hypothesized that CSF pulsations from a fourth ventricle outlet obstruction enlarged the central canal. However, clinically no communication between the fourth ventricle and the syrinx is demonstrated in most patients with posttraumatic syringomyelia.<sup>26</sup> Therefore, the mechanism proposed by Gardner is not tenable. Following this, many authors have proposed different theories to clarify the mechanism of posttraumatic syringomyelia, such as resorption of blood and necrotic tissue,<sup>46</sup> lysosomal autodigestion,<sup>46</sup> infarction,<sup>25</sup>

ischemia and edema caused by local arachnoiditis,<sup>22,45,47,48</sup> and CSF entry via enlarged perivascular spaces,<sup>44,49,50</sup> but the pathogenesis of posttraumatic syringomyelia is still poorly understood. Therefore, until now, there has been no effective therapeutic method to improve or restore the neurological function below the level of cavitory spinal cord lesions.

Allen first proposed the concept of secondary injury in 1911,<sup>22</sup> according to his finding in experimental acute spinal cord injury in dogs. The primary traumatic injury seldom produces total transection in patients with SCI. Additionally, it has been known that loss of neural function following acute traumatic injury to the spinal cord only in part results from direct or immediate damage to spinal gray or white matter. The concept that secondary injury leads to much of the tissue damage after traumatic SCI has been suggested by the slow progress of histopathological changes<sup>51</sup> and the continuing death of neurons in the spinal cord after primary trauma to the cord.<sup>52</sup> Strong evidence has been provided by the demonstration that neurological impairment can be reduced by numerous postinjury treatments. Bracken et al.<sup>53</sup> in 1991 reported a large-scale clinical trial in patients with SCI, showing that high dose of the steroid methylprednisolone can reduce functional deficits in patients with SCI and the secondary injury worsened biochemical and pathological changes in the cord after injury. Now it is well-established that damage to the spinal cord after SCI is produced by two distinct mechanisms: the primary mechanical injury and a secondary injury initiated by the primary injury.<sup>22</sup> Trauma to the spinal cord not only produces the primary mechanical damage but also causes progressive autodestruction of tissue at the trauma site, whose extent is dependent on the severity of the trauma.<sup>54</sup> Therefore, secondary injury processes play an important role in the overall

functional deficit.<sup>55,56</sup> In the last 20 years, various putative mechanisms of secondary injury have been proposed with the aim of finding methods to improve or restore neurological function. (Table 2) The mechanisms presented in Table 2 are adapted from the review article of Tator and Fehling.<sup>22</sup>

#### ***1.6.6.1 EAA mechanism***

The EAA glutamate is widely distributed within the CNS and serves as an excitatory neurotransmitter.<sup>57</sup> It has long been recognized that EAAs, such as glutamate and NMDA, can destroy neurons in the mammalian CNS<sup>58</sup> and that there are several types of EAA postsynaptic receptors, which mediate the neurotoxicity of EAAs.<sup>59</sup> It has been well-established that a significant elevation in the level of extracellular EAA occurs in brain ischemia<sup>60-65</sup> and that EAA antagonists can attenuate the damage of both ischemic<sup>66,67</sup> and traumatic injury to the brain.<sup>65,68,69</sup> A significantly increased extracellular EAA and associated enhanced entry of calcium<sup>70</sup> are believed to be one of the causal factors in the damage to certain neurons observed after cerebral ischemia or trauma.

Similarly, it has also been strongly suggested that EAAs are involved in secondary traumatic injury to the spinal cord. There have been numerous studies that demonstrate the local levels of EAAs, especially glutamate, rise to toxic levels following traumatic and ischemic spinal cord injury<sup>52,71-73</sup> and that support the involvement of EAAs in the pathologic changes after spinal cord injury. It was also observed that the extent of EAA increase was dependent on the severity of trauma.<sup>54,71</sup> By means of the microdialysis technique, Liu et al.<sup>52</sup> and other investigators<sup>72,73</sup> demonstrated that extracellular EAAs reached toxic levels

**Table 2. Secondary mechanisms of acute spinal cord injury**

---

1. Vascular changes
    - a. loss of autoregulation
    - b. systemic hypotension
    - c. hemorrhage
    - d. loss of microcirculation
    - e. reduction in blood flow
  2. Electrolyte changes
    - a. increased intracellular calcium
    - b. increased extracellular potassium
    - c. increased sodium permeability
  3. Biochemical changes
    - a. neurotransmitter accumulation
      - i) EAAs (e.g., glutamate)
      - ii) biogenic amines (e.g., dopamine)
    - b. arachidonic acid release
    - c. free-radical production
    - d. lipid peroxidation
    - e. endogenous opioids
    - f. lysosome
  4. Loss of energy metabolism  
(decreased adenosine triphosphate production)
  5. Inflammatory response
- 

upon impact injury to the spinal cord. Furthermore, Liu et al. found that the increases in EAAs (glutamate and aspartate) were much larger than the increases in glutamine and asparagine after impact injury. Neuronal discharge, breakdown of neurons and bleeding result in rises in amino acid concentrations and the last two are mainly responsible for the release of asparagine and glutamine. Therefore, they concluded that the EAAs specifically released in response to trauma and much of the increase in the levels of EAAs was from electrical activity of neurons instead of simple damage by trauma.<sup>52</sup> This conclusion is consistent with other studies, which have shown that the massive increases in extracellular levels of EAAs observed during ischemia or trauma are the results of ischemia-induced

shift of EAAs from intracellular to extracellular compartments<sup>54,63</sup> and the failure of uptake.<sup>64</sup> Their study provided strong evidence that EAAs, released in response to trauma, lead to secondary neuronal cell damage after traumatic spinal cord injury.

Further evidence was provided by reports of exacerbation of neuronal damage by EAA administration in the injured cord and attenuation of neuronal damage by some selective EAA antagonists (including antagonists of NMDA, KA and AMPA) following traumatic<sup>51,54,55,71,74-77</sup> or ischemic<sup>78,79</sup> injury to the spinal cord. These results also supported the hypothesis that EAA receptors at or near the injury site contributed to neuronal damage that results from contusive spinal cord injury.

To simulate a significant elevation of extracellular EAA level induced by spinal cord traumatic injury, many investigators infused EAA into the spinal subarachnoid space<sup>59,80</sup> or injected EAA<sup>81,82</sup> into the spinal cord of animals to produce dose-dependent pathological changes in the spinal cord neuronal systems. They found that the pathological changes after EAA injections, including cystic cavities, closely resembled those in clinical cases of posttraumatic syringomyelia. The report that the spinal microinjection of exogenous EAA promoted spinal endogenous glutamate release suggested a positive feedback system, which might induce and maintain increased NMDA and non-NMDA receptor activation.

Taken together, these results demonstrated that secondary damage to the spinal cord after traumatic injury can be partially attributed to the delayed neurochemical change within CNS tissue, which is a significant increase of extracellular EAAs.

Consequently the synapses are exposed to abnormally high concentrations of these neurotransmitters after traumatic injury to the spinal cord. Significantly increased EAAs are thought to damage neurons by excessive activation, which is mediated through specific membrane receptors mainly by two mechanisms: (a) an early chloride and sodium ion influx, leading to acute neuronal swelling and (b) a later calcium ion influx, leading to more delayed damage.<sup>52,73,83</sup> The later increased intracellular calcium is responsible for a cascade of cell events and further damage because the damage can occur in the absence of swelling.<sup>22,83</sup> Moreover, it has been suggested that the toxic effects of EAA on central neurons are mediated by an influx of extracellular  $\text{Ca}^{2+}$  rather than an influx of extracellular  $\text{Na}^+$  based on the observations that EAA neurotoxicity is largely preserved in sodium-free solution<sup>84</sup> and removal of extracellular calcium markedly reduced neuronal loss.<sup>85,86</sup> Additionally, histopathological and biochemical changes in trauma can be provoked by perfusion of a solution with high concentration of calcium ions around the spinal cord.<sup>22</sup> According to these hypotheses, excessive stimulation of membrane receptors by high extracellular concentration of EAAs may greatly increase  $\text{Ca}^{2+}$  influx to produce neuronal death in the CNS with accumulated intracellular  $\text{Ca}^{2+}$ .<sup>72,87,88</sup> The increased intracellular  $\text{Ca}^{2+}$  can activate a number of  $\text{Ca}^{2+}$ -stimulated enzymes, such as phospholipases, protein kinases, nitric oxide synthase, proteases and nucleases, which subsequently damage some organelles, including mitochondria and nucleus. All these eventually result in cell damage.<sup>73,83</sup> These hypotheses have been supported by the observations that a rapid decrease of extracellular calcium within the spinal cord following spinal injury and the restoration of neurological function after SCI in rat models by calcium-channel blockers.<sup>56,89</sup> Further evidence is provided by the report that  $\text{Ca}^{2+}$  accumulates at

the impact site in injured spinal cord and comes largely from the surrounding tissue.<sup>89</sup> Intracellular calcium influx and consequent accumulation is well-known as the final common pathway of toxic cell death in the nervous system.<sup>90</sup>

Recent studies in vitro have shown that the accumulation of intracellular  $\text{Ca}^{2+}$  can be divided into three distinct phases: (1) when the neuron is initially exposed to an increased concentration of glutamate, the intracellular  $\text{Ca}^{2+}$  increases to micromolar level; (2) the intracellular  $\text{Ca}^{2+}$  recovers to basal levels following the increase; (3) the intracellular  $\text{Ca}^{2+}$  gradually reaches a prolonged plateau. The terminal phase is significantly related to cell death.<sup>91</sup> By electron microscopy, Simon et al. found a sustained, excessive calcium entry and subsequent mitochondrial overload in vulnerable neurons during the terminal phase. However, transient or less marked calcium accumulation was observed in those neurons without such vulnerability. From these observations, they drew the conclusion that mitochondrial injury caused by intracellular calcium accumulation was a determining factor in irreversible neuronal injury.<sup>92</sup> In recent years, it has been known that neuronal damage following trauma mainly results from accumulation of intracellular  $\text{Ca}^{2+}$  which causes pathological changes in organelles and is potentiated by increases in osmotic pressure due to rises in intracellular sodium and chloride ion concentrations.<sup>52</sup>

Therefore, it can be concluded that traumatic CNS injury is followed by a sequence of cellular events. A secondary neuronal damage extending considerable distances from the primary lesion follows the primary mechanical damage to the neurons at the trauma site. Secondary neuronal damages start 2-3 h after the primary injury, producing more neuronal damage than the primary trauma. Initiated by the primary insult, a self-propelling cascade of cellular events is set in

motion in which many variables act concomitantly. Evidence has been provided that EAAs are involved in the secondary neuronal damage in traumatic SCI. The extracellular concentration of EAAs is significantly increased due to trauma. Several minutes is enough for a high concentration of free glutamate to kill the neurons.<sup>77</sup>

Neuronal degeneration produced by EAAs may be an important step leading to the formation of spinal cavities. One possible mechanism of cyst formation may be a cycle of events initiated by an increase of EAA levels following traumatic injury to the spinal cord. Prolonged depolarization of calcium channels and neurons due to excessive activation of EAA receptors by increased EAAs, destruction of cell membranes by trauma and EAA-mediated calcium channel activation results in intracellular calcium and sodium accumulation. This initiates a cascade of cell events, including impairment in mitochondrial function by accumulated calcium in mitochondria, calcium-activated neutral proteases to disrupt microtubular and neurofilament proteins, axonal degeneration, and the synthesis of toxic free radicals lead eventually to cell death. The necrosis of neurons stimulates the infiltration of macrophages and reactive astrocytes that wall off the necrotic area and finally a cavity is formed. The pressure inside the cavity and contraction of vascular smooth muscle by activation of calcium channels may result in local alteration in the microvascular perfusion of adjacent tissue and the resultant focal ischemia would then lead to increased EAA levels, thereby perpetuating the cycle of EAA-induced neurotoxicity.<sup>8,22</sup>

Additionally, the EAA mechanism may account for the more frequent location of syrinxes. Using quantitative autoradiography, Mitchell et al. found that EAA receptors were in highest concentrations in laminae I and II of the dorsal

horn in the cat spinal cord, whereas the sodium-dependent EAA transporter, the major route of inactivation of extracellular EAAs, was in its highest level in the ventral horn. Therefore, the ventral horn was more resistant to excitotoxic insults than the dorsal horn.<sup>93</sup>

#### ***1.6.6.2 Vascular mechanism***

There is often a substantial decline in spinal cord blood flow after trauma; such ischemia is believed to contribute to delayed tissue injury.<sup>75</sup> Several studies have shown a major reduction in the microcirculation and a lack of perfusion at the injury site after experimental cord trauma.<sup>22</sup> Further, Wallace et al.<sup>94</sup> demonstrated that there was a lack of perfusion of the arterioles, capillaries and venules at the injury site and the adjacent area, which was considerably cephalad and caudad distant from the injury site, while the large vessels of the cord (the anterior spinal artery and the anterior sulcal arteries) always remained patent even after severe cord injury. The ischemic areas included a large part of the gray matter and the surrounding white matter. Therefore, Tator et al.<sup>22</sup> postulated that secondary injury produced thrombosis or vasospasm of arterioles due to the accumulation of noradrenaline at the injury site. Additionally, a variety of investigations in different animal models showed major reduction of spinal cord blood flow after acute cord trauma.

The normal cord can autoregulate blood flow to maintain constant blood supply over a wide range of arterial pressure. However, autoregulation is markedly impaired after spinal cord trauma.<sup>95</sup> Moreover, neurogenic shock can be induced by acute cord trauma. It has been shown that posttraumatic hypotension and decreased cardiac output are caused after experimental acute spinal cord

injury in numerous studies. These declines result from a combination of decreased sympathetic tone and myocardial effects.<sup>96</sup>

These results have suggested that reduction of spinal cord microcirculation at and near the injury sites, impaired autoregulation of spinal cord blood flow, systemic hypotension, and diminished cardiac output contribute to ischemia after trauma in the spinal cord. Elevation of posttraumatic mean systemic arterial pressure to more than 160 mmHg failed to significantly improve spinal cord blood flow at the injury site and caused marked hyperemia at adjacent sites.<sup>95</sup> A linear relationship was found to exist between the severity of cord injury and the reduction in blood flow at the injury site. Further, both the severity of cord injury and the degree of posttraumatic ischemia were found to be significantly related to posttraumatic axonal dysfunction (motor and somatosensory tracts of the cord).<sup>22</sup>

It can be established that posttraumatic ischemia is a direct and damaging reaction to trauma due to its characteristics including the immediate onset, the dose-dependent severity of reduction, and the progressive and persistent time course. It is also strongly supported by the fact that treatment of the ischemia contributes to the restoration of cord function.<sup>97</sup>

However, the manner in which posttraumatic ischemia causes cyst formation in the spinal cord remains unknown. The deep microvasculature may be occluded by vasospasm resulting from mechanical damage or by the release of a vasoactive amine or other vasoconstrictor, direct endothelial damage or swelling due to acute cord injury, hemorrhage, and thrombosis or platelet aggregation. The targeted tissue is thus rendered ischemic and proceeds to degenerate. Macrophages and reactive astrocytes infiltrate and demarcate the necrotic area. Then a cavity is formed.<sup>98</sup>

### ***1.6.6.3 Inflammatory mechanism***

An inflammatory response to traumatic injury usually brings about wound healing. However, it has been suggested that this response in the spinal cord injury initiates and maintains progressive necrosis. Progressive necrosis precludes any meaningful tissue repair.<sup>47</sup> It has been well-established that a process of progressive necrosis results from ischemic changes occurring at the time of spinal cord injury.<sup>99</sup> It has been hypothesized that reperfusion injury of the endothelial cell after ischemic changes is responsible for the uncoordinated inflammatory responses. The ischemia can transform the xanthine dehydrogenase in the endothelial cell into a xanthine oxidase. Then, during reperfusion, oxygen activates the xanthine oxidase to oxidated xanthine, transferring its electrons to molecular oxygen to generate superoxide radicals. These radicals, which are toxic to the endothelial cell, damage the capillary wall. This vascular injury is exacerbated by neutrophils, which aggregate at sites of vascular damage, secreting additional reactive oxygen species. In this way, the inflammatory response causes damage to the endothelial cell, disruption of vascular integrity, edema, extravasation of erythrocytes, migration of neutrophils and monocytes into the injured region, and the subsequent release of cytotoxic substances. The sustained release of cytotoxic substances in this uncoordinated inflammatory response is believed to play a key role in progressive necrosis in spinal cord injury.<sup>47</sup>

Progressive necrosis denotes the process in which spinal cord lesions increase gradually in size and undergo liquefaction necrosis; as a result, the normal tissue fabric of the spinal cord is gradually replaced by fluid-filled, glia-lined cavities. This hypothesis has been confirmed by numerous reports that the tissue necrosis

can be significantly reduced by treatment with anti-inflammatory agents and that wound healing is adversely affected by the presence of tissue necrosis.<sup>22,47</sup>

#### ***1.6.6.4 Other mechanisms***

Biogenic amines (dopamine, noradrenaline, serotonin and histamine) act as neurotransmitters in the brain and in the spinal cord. Some investigators<sup>100-103</sup> focused considerable attention on biogenic amines as possible mediators contributing to the formation of the cystic cavity in posttraumatic syringomyelia. They reported that elevated levels of biogenic amines were observed within the spinal cord after trauma and paralleled a marked reduction in spinal cord blood flow in experimental trauma. However, conflicting results have been reported.<sup>104</sup> These results failed to confirm previous reports of amine alteration in head and spinal cord trauma. Neurological deficits were not observed after intracerebral injections of serotonin and an impact injury to the thoracic cord did not lead to changes in noradrenaline, dopamine or serotonin despite the presence of severe hemorrhage and necrosis. Additionally,  $\alpha$ -methyl-p-tyrosine, which reduces the levels of central dopamine and noradrenaline, did not demonstrate a protective effect after spinal cord trauma. Therefore, the role of biogenic amines in spinal cord trauma remains to be determined.

The lysosome mechanism was proposed by several authors.<sup>46</sup> Their studies produced spinal cord cavitation in dogs by transecting the spinal cord. They found that transection of the spinal cord was followed by massive accumulation of lysosomes and release of lysosomal hydrolases within spinal cord stumps. They suggested that release of lysosomal hydrolases resulted in autolysis of the cord stumps and subsequent cord cavitation.

The endogenous opioid mechanism was advanced by Faden et al.<sup>105</sup>, who described the therapeutic effects of the opiate receptor antagonist naloxone in experimental models. They suggested that endogenous opioids might play a pathophysiological role in the spinal cord following traumatic injury.

Clinically, the mechanism of cyst expansion is more important. A prospective study of 449 traumatic paraplegic and tetraplegic patients with spinal cord injury demonstrated that neurological worsening or improvement was attributed to the enlargement or collapse of the cystic cavity in the spinal cord.<sup>10</sup> It was also found that complete collapse of the cyst resulted from surgical realignment of the spine which restored a normal free circulation of CSF while enlargement of the syrinx was always closely related to cord impression, tense syrinx and kyphosis which disturbed the CSF flow within the subarachnoid space. This latter finding supported the hypothesis that disturbances of the normal CSF circulation within the subarachnoid space could result in enlargement of the cyst. This finding is consistent with other hypotheses that CSF enters the syrinx through the perivascular spaces and the interstitial spaces from the spinal subarachnoid space.<sup>(12,61,188)</sup>

The spinal canal is subject to continuous pressure swings which are mainly mediated by the epidural veins, which are in free, valveless communication with the vertebral venous plexuses. Every time a Valsalva maneuver takes place (for example, coughing or straining), the intrathoracic and intraabdominal pressure is transmitted inside the spinal canal via the valveless vertebral venous plexus. Normally pressure is readily equalized between the top and bottom of the spine. In the presence of a partial subarachnoid block, fluid can be forced upward past the block more efficiently than it can run down again.<sup>106</sup> Williams et al.<sup>107</sup>

proposed that this may lead to a collapsed theca below the block, thus creating a suction effect that promotes entry of CSF into the syrinx. This is the “suck” mechanism. Syrinx fluid may move more readily than the CSF in the subarachnoid space, because the latter fluid finds some resistance from the arachnoid strands, the dentate ligaments, the vessels, and the nerve roots that connect the cord to the dura. The movement of the syrinx fluid can be violent enough to extend the cavity both cranially and caudally. The pressures involved in a cough often exceed 100 mmHg and the total energy therefore provides a potentially destructive force. This is the “slosh” mechanism. These two mechanisms explain the propagation of the syrinx, but are not universally accepted as yet. Some studies also showed that neurological deterioration resulted from lifting heavy weights, straining, and even transmission of shock waves during lithotripsy.<sup>10</sup> All of these observations suggested that intraspinal hydrodynamic factors may play a major role in expansion of the syrinx in posttraumatic syringomyelia. Therefore, entry of CSF,<sup>44,49,50</sup> spinal tethering by local arachnoiditis<sup>20</sup> and craniospinal pressure difference<sup>8</sup> have been suggested as the main causes of expansion of syrinxes, but their relative contributions are still unknown.

### ***1.7 Animal Models***

A laboratory model of syringomyelia that simulates the pathophysiology occurring in humans is needed, which would allow for accumulation of data on syrinx formation and the identification of factors that contribute to and aggravate the syrinx. At the same time, studies could determine the effectiveness of various treatments. Although the laboratory model would not be a replacement for studies

of human subjects, a wealth of information would be obtained to provide additional insights.

### **1.7.1 Animal models of communicating syringomyelia**

The reports of animal models of congenital communicating syringomyelia are few. Kuwamura et al.<sup>8</sup> reported the dilated central canal in congenitally hydrocephalic mice. This study confirmed Gardner's hydrodynamic theory of dilation of the central canal by the demonstration that blockage of the communication between the obex and the central canal prevented the formation of syringomyelia.

An experimental model of acquired communicating syringomyelia can be produced in animals by injecting kaolin into the cisterna magna.<sup>43</sup> Chakraborty et al.<sup>108</sup> performed intracisternal injection of kaolin to produce communicating syringomyelia in rabbits. MRI demonstrated the communication between the fourth ventricle and the syrinx in most animals. The ultrastructural changes included demyelination of varying degrees and slight edematous change in the peri-syringeal white matter, abundant astrocytic proliferation with a large number of glial filaments at the margin of the syrinx, and the enlarged perivascular spaces in both the gray and white matter. In this model, continuing axonal degeneration and demyelination were observed to be accompanied by an abortive attempt at regeneration and remyelination. They suggested that these observations might be the cellular basis for the refractoriness of communicating syringomyelia even after surgical treatment. However, occurrence of postinflammatory hydrocephalus /syringomyelia in humans is rare and the validity of extrapolating these findings from the kaolin-induced model to the human condition is quite limited.

The pathology of human syringomyelia including tonsillar herniation demonstrated less extensive arachnoiditis and the lack of hydrocephalus, while the development of syringomyelia in the animal model was closely related to extensive arachnoiditis and hydrocephalus.<sup>8</sup> Therefore, Yamazaki et al.<sup>109</sup>, by transplanting an extradural neoplasm, produced a new experimental model of chronic tonsillar herniation in rats, whose central canals in the spinal cord were enlarged from the C<sub>5</sub> to the T<sub>8</sub> segments. They found that the histological changes in the spinal cord in this new model reflected an early stage of communicating syringomyelia.

#### **1.7.2 Animal models of non-communicating syringomyelia**

Based on previous pathological investigations, syringomyelia associated with the Chiari I malformation is characterized by dilation of the central canal (hydromyelia) and/or paracentral intramedullary cavitation (syringomyelia) located in the posterior horn and/or the posterior column of the cervical cord. Yamada et al.<sup>37</sup> reported that two types of syrinx — central canal dilation in the thoracic cord and intramedullary cavities in the posterior column and posterior horn in the cervical cord — were produced by a percutaneous injection of kaolin solution into the cisterna magna in a canine model. Hydrocephalus was also observed in almost 90% of dogs treated with kaolin and half of the intramedullary cavities did not communicate with the central canal. The pathological features of cervical cavitation in this kaolin model resembled those in human subjects and vascular impairment of the cervical cord may provide a reasonable explanation for the initial process of non-communicating syringomyelia associated with the Chiari I malformation. However, there are several limitations with respect to correlating

it with the human condition, including leptomeningeal granulomata induced by kaolin, hydrocephalus, hydromyelia and the age of the syrinx.

Another experimental model of acquired non-communicating syringomyelia can be produced in animals by injecting kaolin into the spinal cord. An inflammatory response with ependymitis and occlusion of the central canal outflow pathway resulted. Subsequently, cavitation and dilation of the central canal occurred with the histopathologic features of syringomyelia.

Milhorat et al.<sup>110</sup> produced this model of non-communicating syringomyelia by injecting kaolin into the dorsal columns of the spinal cord at C-6 in rats. They found that kaolin crystals and polymorphonuclear leucocytes entered the central canal within 24 hours and drained rostrally. The rostral drainage resulted in a proliferation of ependymal cells and periependymal astrocytes, which produced the synechiae and obstruction in the central canal at the level of the injection and above it. After 72 hours, the upper end of the central canal (the obstructed segments) became acutely dilated and produced an ependyma-lined syrinx in 22/30 animals. The syrinxes did not communicate with the fourth ventricle rostrally and there was no evidence of basilar arachnoiditis, ventricular ependymitis or hydrocephalus in the histology. These authors believed that the central canal of the spinal cord acted like a 'sink' draining CSF rostrally into the fourth ventricle. They provided further evidence that the central canal can remove substances as large as cellular elements from the parenchyma of the spinal cord. Further, they hypothesized that the obstruction of this outflow pathway might play a role in the pathogenesis of non-communicating syringomyelia.

### **1.7.3 Animal models of posttraumatic syringomyelia**

Posttraumatic syringomyelia is characterized by a variety of histopathological changes resulting from mechanical trauma and vascular compromise of the cord parenchyma.<sup>22,30</sup> Three experimental models of posttraumatic syringomyelia have been produced. The mechanical model is the best characterized and most widely used model of posttraumatic syringomyelia and is produced by the contusion or weight drop method first described by Allen.<sup>111</sup> The other two experimental models have been produced recently. Syringes in the parenchyma of the spinal cord in the ischemic model<sup>98</sup> resulted from vascular compromise including ischemia produced by a photochemical method, while marked elevation of EAAs, occurring in both traumatic and ischemic injury, was produced by injecting the potent exogenous EAA (QA) into the spinal cord in the excitotoxic model.<sup>81</sup> All these experimental approaches share the distinction of producing one or more of the pathological changes commonly associated with human injuries and each has provided valuable insights into the putative mechanisms of posttraumatic syringomyelia.

#### ***1.7.3.1 Mechanical model***

In 1890, Schmasus first reported that degeneration and cavitation of the spinal cord were produced in an experimental rabbit model as the result of a direct blunt trauma to the backs of rabbits.<sup>8</sup> Soon, Allen<sup>111</sup> in 1911 designed a weight-drop technique to deliver a quantifiable impact to the spinal cord of animals. The weight-drop technique, which was refined by later researchers,<sup>112</sup> was used to demonstrate the formation of posttraumatic syrinx and to elucidate the pathophysiologic mechanism of posttraumatic syringomyelia. Balentine et al.<sup>113</sup> and other investigators<sup>27,114</sup> utilized a weight-drop technique to produce severe

traumatic injuries to the spinal cord in animals, which caused stepwise sequentially pathological changes in the cord. A fusiform zone of spinal cord necrosis developed, which was similar to the configuration found in human spinal cord injuries. They found that spinal cord pathology did not parallel the clinical neurological condition; spinal cord pathological changes, which were initially prominent in the center of the cord, started as small hemorrhages and edema in the gray matter and progressed through central necrosis, adjacent white matter edema, and demyelination, to finally involve the entire cord. Traumatically induced spinal cord necrosis was the result of vascular injury occurring immediately at the time of impact and was characterized by fibrinoid necrosis and disruption of major arteries as well as veins. In addition, ultrastructural observation in these studies showed that the necrotic process of cellular constituents was piecemeal, and was characterized by intracellular calcification and heterophagocytosis in the traumatized tissue.

The weight drop method is the most widely used experimental model of posttraumatic syringomyelia. However, there are two problems with this model. One is that the impact is so overwhelming that other factors contributing to necrosis may not be demonstrated.<sup>113</sup> The other is that this model can not produce consistent SCI especially when contusion injuries are of moderate severity, resulting in non-reproducible anatomical and behavioral outcomes.<sup>98</sup>

To study the role of spinal blockage or arachnoiditis in posttraumatic syringomyelia, kaolin was injected into the subarachnoid space in the spinal cord, resulting in tethering due to adhesions between the spinal cord and the dura. The animal group which received traumatic injury only was compared with the animal group which received traumatic injury following injection of kaolin.<sup>45</sup> It was

found that there was a tendency for the combined trauma/kaolin injection group to be more prone to develop a syrinx. They concluded that fixation of the spinal cord and obstruction of the CSF pathway by adhesive arachnoiditis at the site of injury may play an important role in initiating the expansion of the syringomyelia cavity. It has also been assumed that tethering of the spinal cord may lead to a reduction in spinal cord blood flow, triggering a release of EAAs, which in turn causes tissue damage and leads to excitotoxic cascades, eventually contributing to the formation and expansion of cavities within the spinal cord.<sup>4</sup>

#### ***1.7.3.2 Ischemic model***

Traumatic spinal cord injury results in degeneration of neural tissue by a number of pathophysiological mechanisms. Local spinal cord ischemia is one of these mechanisms. It has been known that spinal cord blood flow is considerably reduced after traumatic injury.<sup>79</sup>

Bunge et al.<sup>98</sup> and other researchers<sup>79</sup> use the photochemical technique to induce local spinal cord ischemic injury in the rat, developing the photochemical lesion model with minimal variability to better understand mechanisms of posttraumatic syringomyelia. Usually rostral and caudal to this photochemical lesion in the spinal cord, smoothly contoured and secondary empty cavities appeared from 28 days to 17 months after lesioning. They did not, however, increase in size with time. Pathological changes after lesioning were studied by light and electron microscopy. The photochemical lesions resulted in extensive necrotic regions bordered by swollen axons, a massive influx of macrophages, an increase in the perivascular space in surrounding spared tissue, demyelination in the early stage and later myelination, by both oligodendrocytes and Schwann

cells, in the tissue surrounding the necrotic lesion. These changes resembled those observed after SCI caused by contusion or compression.

### *1.7.3.3 Excitotoxic model*

In recent years there have been numerous studies that demonstrate the involvement of glutamate in the posttraumatic syringomyelia<sup>52,73</sup> and significantly increased levels of EAAs caused by spinal ischemia as well as spinal cord trauma.<sup>4,79</sup> Additionally, glutamate has been thought as one of several putative chemical mediators contributing to the central cascade of secondary pathological changes following spinal cord traumatic injury.<sup>22</sup> Recently, the role of different glutamate receptor subtypes in the pathophysiology of SCI was evaluated in a series of studies in which NMDA and non-NMDA receptor agonists were microinjected into the rat spinal cord.<sup>81,115-119</sup> In these studies the intraspinal injection of QA, NMDA and AMPA resulted in pathological changes, including cell death and the formation of spinal cavities, which closely resembled those found after traumatic SCI.<sup>111</sup> This is also in line with the repeated findings that blockade of NMDA and non-NMDA receptors can limit neuronal damage in spinal ischemia and mechanical spinal trauma.<sup>79,116-120</sup> Yezierski et al.<sup>81,82</sup> injected QA into the spinal cord, producing selective elimination of different populations of neurons. After a long period of time, cavities were formed in the spinal cord. These cavities were generally unilateral and varied in size and number. In some cases there was a slight dilation of the central canal. The mechanism of cavity formation following QA injection is not understood. As a potent agonist of two subtypes of EAA receptors, QA may produce neuronal degeneration by prolonged activation of both ionotropic and metabotropic receptors. Prolonged

depolarization of calcium channels and neurons due to excessive activation of EAA receptors by increased EAAs, destruction of cell membranes by trauma and EAA-mediated calcium channel activation results in intracellular calcium and sodium accumulation. This initiates a cascade of cell events, including impairment in mitochondrial function by accumulated calcium in mitochondria, calcium-activated neutral proteases to disrupt microtubular and neurofilament proteins, axonal degeneration, and the synthesis of toxic free radicals, leading eventually to cell death. The necrosis of neurons stimulates the infiltration of macrophages and reactive astrocytes, which wall off the necrotic area and finally an initial focal cyst is formed.

In conclusion, the results of the experimental models described above support the general hypothesis that spinal traumatic injury causes neurochemical, anatomical and pathophysiological changes that collectively constitute a central injury cascade responsible for the formation of focal cysts.<sup>111</sup> However, the mechanism of subsequent syrinx formation remains unclear.

## **2. Excitatory amino acids**

The last 40 years have witnessed considerable progress in the understanding of excitatory amino acids (EAAs). Hayashi and his colleagues<sup>121</sup> were the first to demonstrate the convulsive effects of L-glutamate and L-aspartate in mammalian brain in 1954. Later the depolarizing and excitatory actions of the EAAs on single central neurons were demonstrated.<sup>122</sup> Today it is widely accepted that the EAAs, such as glutamate and aspartate which are widely distributed in the CNS, play an essential role in normal synaptic transmission, synaptic plasticity, and various

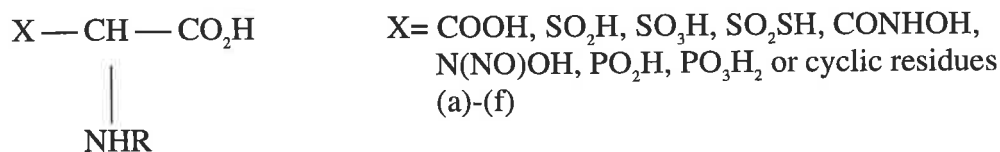
neurodegenerative diseases including posttraumatic syringomyelia, Huntington's disease, Alzheimer's disease and stroke.<sup>57,74,122-124</sup>

## 2.1 Structure and classification

### 2.1.1 Structure

The number of EAAs that are now known runs to well over a hundred. Most have an  $\alpha$ -aminomethylcarboxylic acid terminal, with a second ( $\omega$ ) acidic group located at the end of a chain of one to three atoms from the carboxyl group. The  $\omega$ -acidic group shows wide structural variation (Fig. 1). It is common that the enantiomer varies in potency. The highest activity usually resides in the L isomer, except N-alkyl-D-aspartic acids.<sup>122,125</sup>

The structures of some representative EAAs are shown in Fig 2..<sup>83,126-129</sup>



General formula

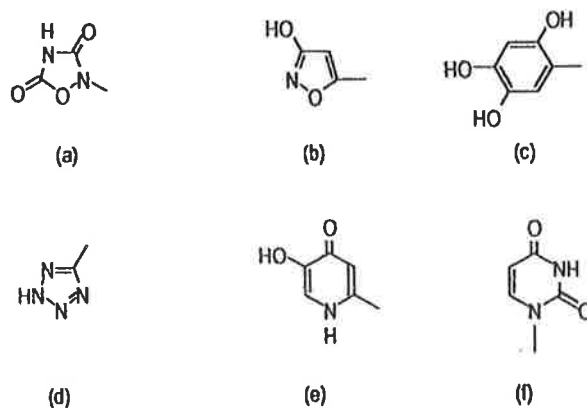


**Figure. 1** General structure of excitatory amino acids, showing the diversity of the  $\omega$ -acidic group. (Adapted from Watkins JC: *The NMDA receptor concept: origins and development*, in Collingridge GL, Watkins JC(eds): *The NMDA receptor*. Oxford, New York, Tokyo, Oxford University Press: 1-30, 1994)

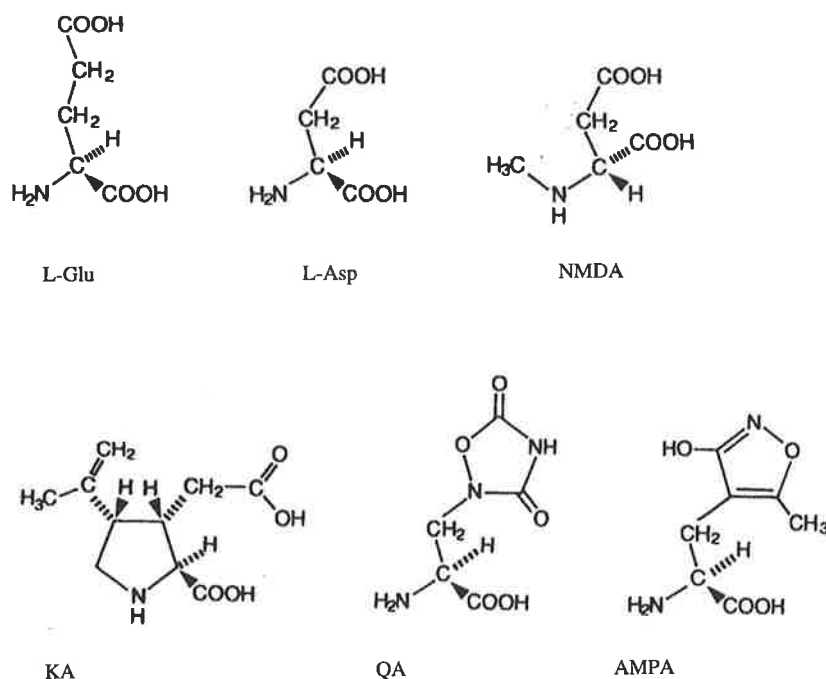


**Figure 2.** The structures of L-glutamic acid, L-aspartic acid, NMDA, KA, QA, and AMPA. (Adapted from Watkins JC: *The NMDA receptor concept: origins and development*, in Collingridge GL, Watkins JC (eds): *The NMDA receptor*. Oxford, New York, Tokyo, Oxford University Press: 1-30, 1994)

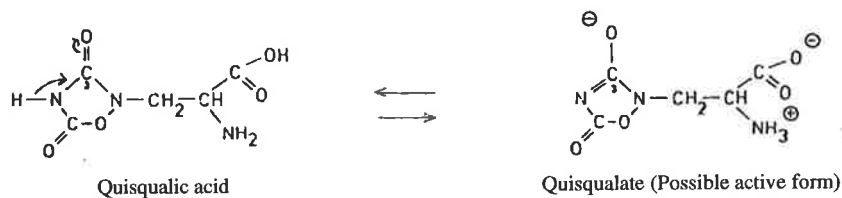


**Figure 3.** Ionic structure of Quisqualic acid. (Adapted from Watkins JC: *Excitatory amino acids*, in McGeer EG, Olney JW, McGeer PL (eds): *Kainic acid as a tool in neurobiology*. New York, Raven Press: 37-69, 1978)

Quisqualic acid, one of the most potent EAAs, is a natural heterocyclic  $\alpha$ -amino acid obtained from seeds of *Quisqualis fructus* and *Q. indica*.<sup>127,130-133</sup> Its full chemical name is  $\alpha$ -Amino-3,5-dioxo-1,2,4-oxadiazolidine-2-propanoic acid, whose molecular formula is  $C_5H_7N_3O_5$  and molecular weight is 189.127.<sup>132-134</sup> The ionic structure of quisqualic acid, which may be the active form, is shown in Fig 3.. Its unusual oxadiazolidinedione system is strongly acidic with a pKa of 4.15.<sup>135</sup>

Quisqualic acid depolarizes the crayfish neuromuscular junction and is a very potent excitant of spinal neurones in the frog, rat and cat,<sup>136,137</sup> with an activity 22-90 times that of L-glutamate. It is synaptically released and removed from the extracellular environment by low-affinity uptake systems, which also transport L-glutamate in high affinity and other acidic amino acids. The relative potencies of EAAs are mainly determined by their removal rate from the extracellular space.<sup>138,139</sup>

### 2.1.2 Classification

It has been well established that EAAs act on specific receptors to excite the mammalian central neurones<sup>121,140</sup> and multiple receptors for EAAs exist in the mammalian CNS.<sup>141</sup> Multiple receptors are involved in EAA synaptic transmission.<sup>142</sup> This is supported by the observations that a range of selective antagonists block the actions of some excitants but not others.<sup>143,144</sup> Therefore, more than 100 EAAs are classified by their receptors. Ultrastructurally, post-synaptic excitatory receptors, which are involved in the mediation of both the excitatory and toxic action of EAAs, are located on dendritic and somal membranes.<sup>145</sup>

The EAA receptors comprise two major types: the ionotropic receptors, which operate ion channels and are subdivided into AMPA, kainate and NMDA receptors, and the metabotropic receptors falling roughly into two groups, those that stimulate phosphoinositide hydrolysis and those that inhibit cyclic AMP production.<sup>122,146-148</sup> The former group includes mGlu1 and mGlu5, while the latter group includes mGlu2, mGlu3, mGlu4, mGlu6, mGlu7, and mGlu8.<sup>149</sup> Table 3 shows a summary of functional features and general distribution of EAA receptors

in the mammalian CNS.<sup>122,150</sup> Thus, NMDA, AMPA and KA are selective agonists for particular receptor types, while a variety of other EAAs, including L-glutamate have mixed actions on more than one type of receptor.<sup>144</sup>

Quisqualic acid is able to function as an agonist at multiple excitatory amino acid receptor substrates in the CNS. It has weak affinity for NMDA receptors<sup>151</sup> and high affinity for the AMPA, kainate, and the metabotropic receptors. The first three EAA receptor types operate the gate ion channel directly, while the metabotropic receptors operate via second-messenger systems, including the stimulation of membrane inositol phospholipid metabolism.<sup>130,152-154</sup> This is consistent with the observation that quisqualate toxic effects can not be prevented by antagonists of NMDA or reducing  $Ca^{2+}$ .<sup>155</sup>

Glutamate is an endogenous amino acid which can activate all of the receptor classes and has the highest affinity for the NMDA receptor, whereas NMDA, QA and KA are exogenous amino acids, which do not exist in the CNS.<sup>156,157</sup>

EAA receptors not only mediate normal synaptic transmission along excitatory pathways, but also participate in the modification of synaptic connections during development and changes in the efficacy of synaptic transmission throughout life. However, over-activation of select receptors can also mediate neuronal degeneration and even cell death.<sup>142,158</sup>

## ***2.2 Synaptic transmission and neurotoxicity***

### **2.2.1 Synaptic transmission**

**Table 3.** Summary of functional characteristics and general distribution of excitatory amino acid receptors in the mammalian CNS (adapted from Watkins JC: *The NMDA receptor concept: origins and development*, in Collingridge GL, Watkins JC, ed: *The NMDA receptor*, 2<sup>nd</sup> edition. Oxford, New York, Tokyo, Oxford University Press:1-17,1994)

---

NMDA	Widely distributed in mammalian CNS and especially enriched in hippocampus and cerebral cortex. The conductance activated by NMDA receptor agonists is voltage-dependent, voltage sensitivity depending on extracellular Mg <sup>2+</sup> . Important in the induction of long-term potentiation, a form of neuronal plasticity, and diseases including clinical epilepsy and neurodegeneration. Antagonized selectively by D-2-amino-5-phosphonovalerate (D-APV) and inhibited non-competitively by phencyclidine-like (PCP) compounds. Potentiated by glycine.
AMPA	Widespread in CNS; parallel distribution to NMDA receptors. The conductance activated by AMPA receptor agonists is voltage-independent, involving Na <sup>+</sup> and K <sup>+</sup> . Blocked by selective antagonists.
Kainate	Concentrated in a few specific areas of CNS, complementary to NMDA/AMPA receptor distribution, such as stratum lucidum region of hippocampus. The conductance activated by kainate receptor agonists is voltage-independent, involving Na <sup>+</sup> and K <sup>+</sup> .
Metabotropic	A group of receptors stimulating the production of inositol triphosphate and inhibiting cyclic AMP formation. Subtypes differentially activated by L-glutamate, quisqualate, ibotenate and so on, but not by AMPA, NMDA, or kainate. Not antagonized by NMDA or non-NMDA antagonists. Maybe involved in developmental plasticity.

---

It has been well established that glutamate, aspartate and possibly other EAAs act as neurotransmitters at the majority of excitatory synapses in the vertebrate CNS.<sup>57,146,150,159</sup> Additionally, EAAs are thought to play an essential role in the induction of the plastic changes in synapses.<sup>123</sup>

Many studies have demonstrated that receptors for EAAs are involved in mediating synaptic transmission in the mammalian spinal cord.<sup>150,160,161</sup> A number of electrophysiological experiments have suggested that EAA receptors are

involved in spinal sensory pathways. EAA receptor agonists can increase the firing rate in 75% of spinal neurons, while D- $\alpha$ -aminoadipate, an antagonist of all three EAA receptor subclasses, can inhibit Renshaw cell response evoked by electrical stimulation of large myelinated primary afferent fibers. The existence of functional NMDA receptors on intrinsic spinal neurons is suggested by the reduction of polysynaptic excitation in the spinal cord by NMDA antagonists. More recently, it has been demonstrated that NMDA receptors predominantly mediate glutamate-induced depolarization of primary sensory neurons.<sup>150,161</sup>

Some other experiments suggest a transmitter role of EAAs in spinal nociceptive inputs. NMDA and AMPA can activate primarily nociceptive neurons, 60% of which were projection neurons. Spinal neurons sensitive to aspartate or glutamate were found to be primarily located in the superficial dorsal horn. PCP was reported to inhibit responses of identified spinothalamic tract cells to iontophoretically applied glutamate and to noxious mechanical stimuli, whereas neuronal responses to peripheral noxious mechanical stimulation can be significantly increased by either NMDA or AMPA at subthreshold doses. By means of spinal microdialysis technique, increased extracellular levels of glutamate and aspartate in the dorsal spinal cord of freely moving rats were observed following peripheral nociceptive stimulation.<sup>150,160,162</sup>

Taken together, glutamate and aspartate are excitatory neurotransmitters in several kinds of primary afferent fibers and in many interneurons of the spinal cord dorsal horn. Many, but not all, dorsal horn neurons can be excited by these EAAs through specific receptors. Administration of EAAs was found to facilitate the responses of primate dorsal horn cells to mechanical stimulation of their peripheral receptive fields while EAA antagonists can reduce the response.

Further these results are supported by anatomical evidence that some synapses on primate spinothalamic tract neurons contain EAAs.<sup>160</sup> Therefore, EAAs may play a key role in sensory transmission in the spinal cord.

Glutamate functions as an excitatory transmitter in the CNS, but it is also a powerful neurotoxin when its extracellular concentration is sufficiently high. This is supported by the observation that the sensitivity of central neurons to hypoxia and ischemia (hypoxic-ischemic brain damage) can be greatly diminished by either blockade of synaptic transmission or the antagonism of postsynaptic glutamate receptors.<sup>159</sup>

## **2.2.2 Neurotoxicity**

### **2.2.2.1 Background**

In the EAA field, Hayashi first discovered the convulsive effects of glutamate and aspartate in mammalian brain in 1954.<sup>122,148</sup> Soon, Lucas and Newhouse<sup>163</sup> in 1957 established the toxicity of systemically administered glutamate in the mouse retina and later other researchers demonstrated that Glu and structural analogs of Glu exerted their depolarization action on postsynaptic dendritic and somal receptor sites of the neuron to produce neuroexcitatory activities or neurotoxic activities without damaging axons of passage. Afterwards, Olney et al.<sup>78</sup> in 1969 proposed the concept of “excitotoxic” amino acids to explain the neurotoxicity of those structural analogs of Glu, i.e. EAA, which have both neuroexcitatory and neurotoxic activity mediated through the actions of glutamatergic transmission.<sup>164</sup> More recently mounting evidence includes confirmation of the depolarizing effects and neurotoxic effects of EAAs *in vitro*;<sup>165,166</sup> and the demonstration that brief exposure to glutamate was found to

produce morphological changes in mature cortical cell culture beginning as early as 90 seconds after exposure, followed by widespread neuronal loss over the next hours;<sup>167</sup> and that NMDA or non-NMDA agonists can produce local neuronal degeneration in vitro and in vivo.<sup>168-171</sup> Furthermore, some studies suggested that amino acid neurotoxicity was a consequence of an intracellular  $\text{Ca}^{2+}$  overload brought about by excessive  $\text{Ca}^{2+}$  influx.<sup>125,172,173</sup> It is now accepted that selective neuronal death can be produced by excessive release of endogenous EAAs in the CNS in some pathological conditions, including spinal or cerebral ischemia and trauma, seizure-mediated brain damage, and hypoglycemic brain.<sup>157</sup> Glia and other non-neuronal cell types are spared due to their lack of excitatory receptors, which function in synaptic transmission. Therefore, this phenomenon that only neurons die and non-neuronal cells are spared is termed selective neuronal necrosis.<sup>164</sup>

#### **2.2.2.2 Mechanisms**

A powerful plasma uptake carrier located in both neurons and glia can lower the extracellular glutamate concentration to about 1  $\mu\text{M}$  while a specific transporter can package glutamate into synaptic vesicles for subsequent exocytosis (Fig 4). These two transport pathways maintain the extracellular glutamate concentration in normal conditions.<sup>159,174</sup>

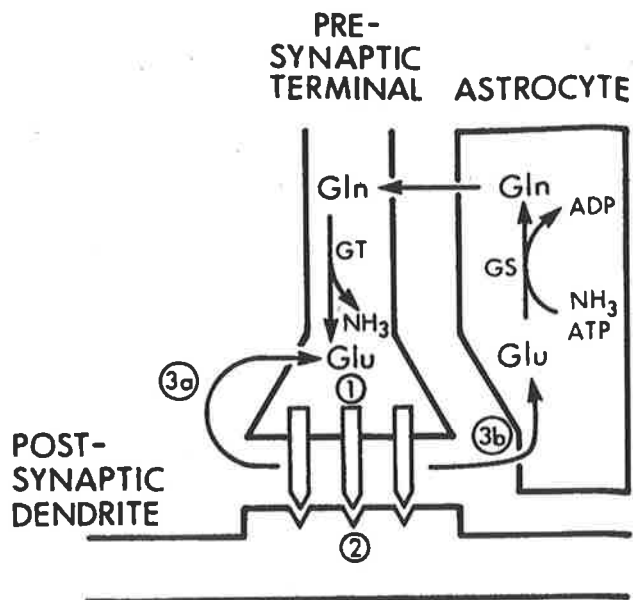


**Figure 4.** A schematic glutamergic synapse with presynaptic nerve terminal and postsynaptic dendrite containing glutamate receptors. An astrocyte is next to the synapse. The numbers correspond to glutamate release from synaptic vesicles (1), glutamate binding to postsynaptic EAA receptors (2), and glutamate reuptake into nerve terminal (3a) and astrocyte (3b). (ATP= adenosine triphosphate; ADP= adenosine diphosphate; Gln= glutamine; GS= glutamine synthase; GT= glutaminase) ( Adapted from Rothman SM, Olney JW: *Glutamate and the pathophysiology of hypoxic-ischemic brain damage. Ann neurol* 19:105-111,1986.)

However, in some pathological conditions such as anoxia/ischemia and trauma in the CNS, the regulation is lost. The excessive rise of extracellular  $K^+$  induced by anoxia/ischemia or trauma in CNS will depolarize neurons, increasing vesicular release of glutamate ( if ATP levels are sufficient), will promote the release of glutamate by reversal of the plasma uptake carrier (if the extracellular glutamate concentration is low) and will inhibit uptake directly. In addition, the powerful plasma uptake carriers are inhibited by decreased extracellular  $Na^+$  as a result of inhibition of  $Na^+$  pump or a large  $Na^+$  influx, depolarization of the neuron by the increased  $K^+$ , and arachidonic acid released by the high glutamate concentration. The resulting rise in glutamate concentration will depolarize neurons further and thus release more  $K^+$ . This is a positive feedback system

which causes a large rise in extracellular glutamate concentration. If neurons are exposed to 100  $\mu\text{M}$  glutamate for more than 5 minutes, they will die due to an excessive  $\text{Ca}^{2+}$  influx.<sup>174</sup>

A significant rise in extracellular glutamate concentration causes excessive activation of all postsynaptic EAA receptors, leading to a lethal influx of extracellular  $\text{Ca}^{2+}$  through cell membrane channels (Fig. 5).<sup>146,175-178</sup> Ionotropic NMDA, kainate and AMPA receptors trigger  $\text{Ca}^{2+}$  influx from the extracellular fluid via two pathways. One is the NMDA receptor-gated ion channel, which is highly permeable to  $\text{Ca}^{2+}$  to allow a significant influx of  $\text{Ca}^{2+}$ . The other is the voltage-dependent  $\text{Ca}^{2+}$  channel, which is activated by the depolarization. Strong depolarization can be produced by activation of KA, AMPA and NMDA receptors and facilitates the opening of the NMDA ionophore, increasing  $\text{Ca}^{2+}$  directly via the NMDA channel. Additionally, the AMPA, KA, and NMDA receptor activation also produces other ionic changes, including  $\text{Na}^+$  influxes and  $\text{K}^+$  effluxes. The metabotropic receptor, which is linked via G proteins to phospholipase C (the enzyme responsible for diacylglycerol and  $\text{IP}_3$  formation), activates protein kinase C via diacylglycerol and releases  $\text{Ca}^{2+}$  from internal stores to increase intracellular  $\text{Ca}^{2+}$  via  $\text{IP}_3$  while the activation of AMPA/KA and metabotropic receptors results in an increase of arachidonic acid formation.<sup>179-181</sup>

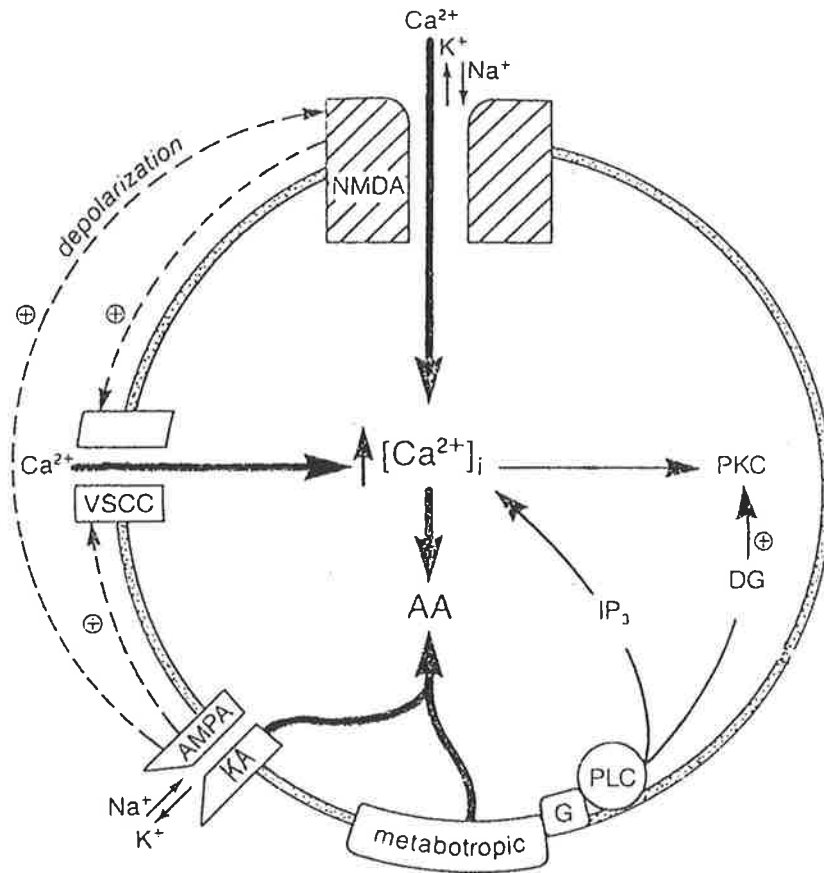


**Figure. 5** Schematic diagram showing a sustained influx of  $\text{Ca}^{2+}$  following activation EAA receptors: AMPA, KA, NMDA, and metabotropic receptors. (VSCC= voltage-sensitive  $\text{Ca}^{2+}$  channels; AA= arachidonic acid; PKC= protein kinase C; G= GTP-binding protein; PLC= phospholipase C; DG= diacylglycerol;  $\text{IP}_3$ = inositol-1,4,5-triphosphate.) (Adapted from Schoepp D, Bockaert J, Sladeczek F: Pharmacological and functional characteristics of metabotropic excitatory amino acid receptors. *Trends Pharmacol Sci* 11:508-515,1990.)

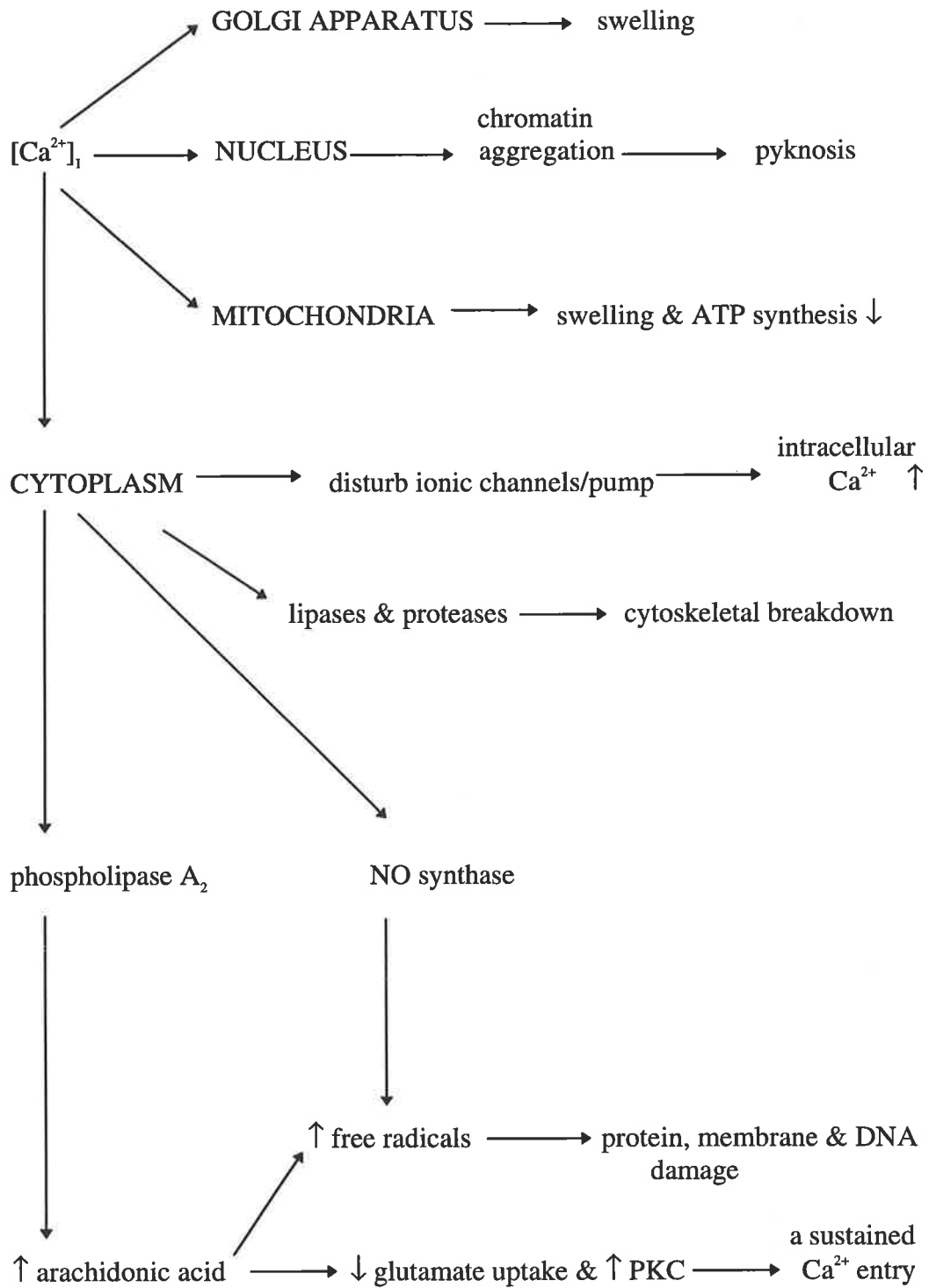


**Figure. 6** Irreversible neuronal damage as a result of sustained influx of Ca<sup>2+</sup> (NO= nitric oxide, PKC= protein kinase C, DNA= deoxyribonucleic acid)

Intracellular  $\text{Ca}^{2+}$  accumulation produces prominent cytopathological changes, leading to irreversible neuronal damage (Fig. 6).<sup>125,173</sup> One of the earliest changes is a swelling of the cisternae of the Golgi apparatus, which are the early site of  $\text{Ca}^{2+}$  uptake. Chromatin in the nuclei starts to aggregate and, coincidentally,  $\text{Ca}^{2+}$  accumulation in the nuclei can be detected. As  $\text{Ca}^{2+}$  in the nuclei increases, the chromatin becomes progressively more clumped and eventually nuclei progress to frank pyknosis, a characteristic feature of dead cells. A population of mitochondria also undergo swelling, in proportion to the amount of  $\text{Ca}^{2+}$  inside them. As a result, the oxidative phosphorylation is impaired and ATP synthesis significantly decreases. As well as causing pathological changes in organelles, sustained increase in  $\text{Ca}^{2+}$  also influences ionic channels or pumps and activates a variety of  $\text{Ca}^{2+}$  sensitive enzymes, leading up to the following destructive cascade.

1. Elevated  $\text{Ca}^{2+}$  is able to inhibit  $\text{K}^+$  currents, depress responses to GABA mediated through  $\text{GABA}_A$  receptors, augment responses to NMDA, and inhibit the activity of the  $\text{Na}^+$ - $\text{K}^+$  pump. All these contribute to a feed-forward effect, further increasing intracellular  $\text{Ca}^{2+}$  as well as promoting other ionic disturbances.

2. Phospholipase  $\text{A}_2$ , activated by excess  $\text{Ca}^{2+}$ , leads to the production of arachidonic acid. Arachidonic acid itself is potentially dangerous as it can induce a lasting inhibition of glutamate uptake and activate protein kinase C (PKC). PKC activation and its translocation into membranes contributes to a sustained  $\text{Ca}^{2+}$  entry pathway leading to cell death. Moreover, during its metabolism, arachidonic acid can give rise to free radicals, which will damage proteins, membranes, and DNA.

3. The activated proteases and lipases can cause cytoskeletal breakdown due to degradation of spectrin, microtubules, and neurofilaments.

4. Nitric oxide (NO) is a diffusible, free radical species that is synthesized by the enzyme NO synthase. A major stimulus for NO synthase activation is excess  $\text{Ca}^{2+}$  in cytoplasm. NO is potentially toxic through its ability to inactivate key iron/sulphur-containing enzymes and react with superoxide ions to generate peroxynitrite, a precursor of more toxic free radicals, including the hydroxyl radical.

It is concluded that excessive activation of EAA receptors on vulnerable neurons leads to a sustained  $\text{Ca}^{2+}$  influx and a failure of homeostatic mechanisms serving to maintain intracellular  $\text{Ca}^{2+}$  at low levels, contributing directly or indirectly to cell death, and that  $\text{Ca}^{2+}$  influx through receptor-activated channels may be a required condition (factor) for EAA toxicity in addition to the passive and voltage-sensitive ionic movements caused by the depolarization.<sup>165</sup>

It has been well-documented that quisqualic acid-induced neurotoxicity is attributed to the excessive activation of KA, AMPA and metabotropic receptors.<sup>182</sup> However, autoradiographic studies have shown that quisqualic acid has weak affinity for NMDA receptors and electrophysiological studies have also demonstrated that quisqualic acid activates NMDA receptor channels. Furthermore, Pai et al.<sup>151</sup> demonstrated in their study that quisqualic acid-induced neurotoxicity in vitro is reduced by either NMDA or non-NMDA receptor antagonists. The activation at the AMPA and KA receptors by quisqualic acid might produce enhanced release of glutamate from the terminal, which could then act on the NMDA receptor. Additionally, the depolarization at the AMPA and KA receptors by quisqualic acid facilitates the opening of the NMDA ionophore. So it has been proposed that both NMDA and non-NMDA receptors are involved in neuronal damage produced by quisqualic acid. A role for metabotropic receptors

in quisqualate-induced neuronal degeneration has also been demonstrated in vivo studies. Although activation of the metabotropic receptor alone can not induce cell death due to impotence of a selective agonist for metabotropic receptor in producing neurotoxicity, release of intracellular  $\text{Ca}^{2+}$  from internal stores after metabotropic receptor activation can potentiate  $\text{Ca}^{2+}$ -mediated degenerative effects of glutamate agonists acting concomitantly at ionotropic receptors.<sup>178</sup>

### ***2.3 Neurodegenerative diseases***

EAAAs, major excitatory neurotransmitters, participate in normal synaptic transmission throughout the CNS and produce neurotoxicity by excessive activation of excitatory amino acid receptors.<sup>183</sup> The toxicity resulting in the degeneration of receptive neurons plays an important role in acute and chronic neurodegenerative disorders, such as seizure-mediated brain damage,<sup>184,185</sup> hypoglycemic brain damage, cerebral ischemia and trauma, Huntington's disease,<sup>186,187</sup> olivo-pontocerebellar atrophy,<sup>188</sup> senile dementia of the Alzheimer type, parkinsonism and amyotrophic lateral sclerosis. In vivo and in vitro studies have shown that the pathological changes closely resemble those induced by EAAAs and antagonists of EAA receptors can significantly attenuate the tissue damage.<sup>83,95,189</sup>

## **AIMS AND HYPOTHESES**

### **Hypotheses**

1. Quisqualic acid will produce parenchymal syrinxes in the spinal cord of rats, comparable to human posttraumatic syrinxes.
2. Enlargement of the syrinx will be enhanced by local arachnoiditis induced by subarachnoid kaolin injection.

### **Aims**

1. To produce cystic cavitation in the parenchyma of the spinal cord in the rat using intramedullary injection of quisqualic acid.
2. To elucidate the role of adhesive arachnoiditis in syrinx formation by comparing the effects of intramedullary quisqualic acid alone with that of intramedullary quisqualic acid and subarachnoid kaolin injection.
3. To study the response of the axon, astrocyte and macrophage in the spinal cord to the intramedullary injection of quisqualic acid.

## METHODOLOGY

### 1. Animals used and ethics approval

All the experimental procedures were approved by the Animal Ethics Committees of the Institute of Medical and Veterinary Science (Project numbers 30/98 and 64/98) and the University of Adelaide. Male Sprague-Dawley rats were used in the experiments and were supplied by and housed in the Institute of Medical and Veterinary Science. Prior to surgery, rats were kept in cages in groups of up to six. Postoperatively, they were housed in individual cages and given food and water ad libidum. Neurological examinations were made daily and analgesia administered as required.

Forty-two male Sprague-Dawley rats, weighing 300g to 450 g, were used in this study. The animals were divided into six groups (Table 4). Group A comprised one normal un-operated rat used as an anatomical control. Group B consisted of three control rats that received a unilateral injection of 2  $\mu$ l mixed solution (1.6  $\mu$ l normal saline and 0.4  $\mu$ l 1% Evans Blue) into the spinal cord. Group C consisted of five rats that received an injection of 5  $\mu$ l 250 mg/ml kaolin into the subarachnoid space. Group D consisted of ten rats that received a unilateral injection of 2  $\mu$ l 8.3 mM (1.6 mg/ml) quisqualic acid solution, the EAA receptor agonist, into the spinal cord. Group E comprised ten rats that received a unilateral injection of 2  $\mu$ l 23.7 mg/ml quisqualic acid suspension into the spinal cord. Group F consisted of thirteen rats that received a unilateral injection of 2  $\mu$ l 23.7 mg/ml quisqualic acid suspension into the spinal cord following injection of 5  $\mu$ l 250 mg/ml kaolin into the subarachnoid space.

**Table 4.** Rats used to study post-traumatic syringomyelia.

<b>Group</b>	<b>Injection</b>	<b>Survival following injection</b>	<b>Number of rats</b>	<b>Average weight <math>\pm</math> SD</b>
A (normal)	-	-	1	350 g
B (control)	Normal saline & Evans Blue	4 weeks	3	350 $\pm$ 18 g
C	Kaolin (subarachnoid)	4 weeks	5	320 $\pm$ 20 g
D	8.3 mM QA (1.6 mg/ml)	1 week	1	330 g
		2 weeks	4	387 $\pm$ 20 g
		3 weeks	3	325 $\pm$ 5 g
		4 weeks	2	382 $\pm$ 8 g
E	23.7 mg/ml QA	died	1	346 g
		1 week	1	335 g
		2 weeks	2	385 $\pm$ 10 g
		3 weeks	5	336 $\pm$ 5 g
		4 weeks	1	408 g
F	23.7 mg/ml QA & Kaolin (subarachnoid)	died	1	355 g
		1 day	1	350 g
		1 week	1	350 $\pm$ 10 g
		2 weeks	4	380 $\pm$ 11 g
		3 weeks	5	410 $\pm$ 20 g
		4 weeks	1	450 g

## **2. Preparation of quisqualic acid solutions and suspensions**

Two different preparations of quisqualic acid were used for intramedullary injection. A solution of 8.3 mM (1.6 mg/ml) quisqualic acid was made by adding 0.537 ml of 0.9% sterile saline and 0.1 ml of 1% sterile Evans Blue to 1 mg of quisqualic acid (Sigma Chemical Corporation, US). A suspension of 23.7 mg/ml quisqualic acid was created by adding 0.170 ml of 0.9% sterile saline and 0.041 ml of 1% sterile Evans Blue to 5 mg of quisqualic acid (Sigma Chemical Corporation, US). The 8.3 mM quisqualic acid preparation was aliquoted into

sterile vials of 0.02 ml samples and stored at -20°C. The 23.7 mg/ml quisqualic acid suspension was sonicated for 1 hour, before being aliquoted (0.02 ml) and stored at -20°C. Aliquots of 23.7 mg/ml quisqualic acid suspension were sonicated for 30 minutes prior to injection.

### **3. Preparation of kaolin suspensions**

Freshly prepared non-sterile kaolin was used for each subarachnoid injection. A suspension of 250 mg/ml of kaolin (Sigma Chemical Corporation, US) was prepared by diluting 2.5 mg kaolin into 10 ml 0.9% sterile saline.

### **4. Anesthesia**

Anesthesia was induced in each rat with 4% isoflurane in oxygen (1.5 L/min) in an anesthetic chamber. Rats were positioned prone on a heat insulating pad. Anesthesia was maintained with the animal self ventilating 2.5% isoflurane in oxygen (1.5 L/min) through a nose cone. A heat lamp was used to maintain body temperature. Following the surgical procedure, anesthesia was withdrawn and the rat supplied with 100% oxygen for 1-2 minutes before placing the rat in the postoperative recovery cage.

### **5. Surgical procedure**

#### ***5.1 Quisqualic acid injection***

A 3 cm midline incision was made in the skin, followed by blunt dissection to expose the lower cervical spine. Paraspinal muscles were stripped from the spinous processes of C5 to C7 under a dissecting microscope. A laminectomy of C6 was performed to expose the dura and the spinal cord. A single puncture was

made through the meninges 0.5 mm to the right of the midline at the C6 segmental level, using a C-1 taper needle (Ethicon 8706, Johnson&Johnson Medical Pty. Ltd., Sydney). The QA syringe (5 µl, SGE Pty. Ltd., Victoria) fitted with a modified bevel needle (0.19 mm outer diameter No. 036701<sup>Pk12</sup>) was advanced through the meningeal puncture to a depth of approximately 0.5 mm, such that the needle orifice lay within the dorsal horn of the spinal cord, with the bevel facing medially. Two microliters of QA preparation was slowly injected over a 1 minute period. The needle was left in place for a further minute, before being slowly withdrawn. The wound was closed in layers using 3-0 synthetic absorbable sutures.

### ***5.2 Kaolin injection***

For subarachnoid kaolin injection a more extensive (C5-7) laminectomy was performed. The dura and arachnoid membrane were punctured using a C-1 taper needle at the level of C6. The fixed curved needle (0.47 mm outer diameter) of the kaolin syringe (10 µl, SGE Pty. Ltd., Victoria) was introduced into the subarachnoid space and the tip advanced to the level of C5. Five microlitres of kaolin suspension was slowly injected. The curved needle was left in position for 1 minute, before being slowly withdrawn.

### ***5.3 Combined injection of quisqualic acid and kaolin***

In animals that received both subarachnoid kaolin and intraspinal QA injection, laminectomies of C5-7 were performed. Kaolin injection as described in section 5.2, was followed by intraspinal QA injection as described in section 5.1.

#### **5.4 Saline injection**

Dissection and exposure of the cord was made as previously described with a laminectomy of C5-7. Two microliters of sterile normal saline was injected into the dorsal horn at C6 level, using the same procedure as described for QA injection.

#### **6. Perfusion-fixation**

Following a survival period of 1-4 weeks, rats were induced and anesthetized with isoflurane. The rat was positioned supine and the thoracic cage opened to expose the heart and aorta. A blunt 19 gauge needle was introduced through the apex of the heart into the ascending aorta. Two milliliters of 1000 IU/ml heparin was injected into the aorta. The heart was clamped transversely at the apex to secure the needle in place. The right atrium was opened. The rat was then perfused with freshly prepared 4% paraformaldehyde in 0.1 M phosphate buffer (pH 7.4, at room temperature) for 15 minutes at a pressure of 120 mmHg. Perfusion pressures were generated with compressed air in a closed system and monitored with a sphygmomanometer.<sup>190</sup>

#### **7. Tissue processing**

##### **7.1 Removal of spinal columns from rats**

The entire spinal column was removed from each rat immediately after perfusion-fixation and postfixed in 4% paraformaldehyde in 0.1 M phosphate buffer (pH 7.4) overnight. The spinal cord was then dissected out and divided into nine 1-cm segments. Each segment was marked at the rostral end on the right side with a small vertical incision to allow orientation.

## ***7.2 Paraffin sections***

Tissue blocks were dehydrated in graded alcohol baths and cleared with chloroform, prior to processing into paraffin wax. Five micrometer serial sections were cut at (150 µm) levels with a microtome and mounted onto slides coated with APT (Sigma Chemical Corporation, US). The sections were dried at 37°C for at least 12 hours prior to use. Sections from each level were stained with hematoxylin and eosin and immunohistochemically as described below.

## ***7.3 Immunohistochemical techniques***

### **7.3.1 Immunoperoxidase staining method for GFAP**

Immunostaining for GFAP, an astrocyte marker, was carried out on 5-µm paraffin sections using standard immunoperoxidase staining protocols.<sup>191,192</sup> The sections were deparaffinized in xylene and cleared in graded ethanol baths. Endogenous peroxidase activity in the tissue was blocked by incubation with 3% H<sub>2</sub>O<sub>2</sub> in PBS and non-specific binding was suppressed by incubation with blocking serum (15% NHS in PBS). The slides were then incubated overnight with the primary anti-GFAP polyclonal antibody (DAKO Corporation, 6392 via Real Carpinteria, C.A.), diluted 1:1500 in 4% NHS/PBS. The following day, a 1:300 dilution of swine anti-rabbit biotinylated secondary antibody followed by the streptavidin/HRP (DAKO Corporation, 6392 via Real Carpinteria, C.A.) was added to the sections. DAB (Pierce, Rockford, I.L.) in H<sub>2</sub>O<sub>2</sub> and NiCl was used as the chromogen for visualisation. The tissue sections were then counterstained with eosin and mounted for light microscopy ( For details of the GFAP immunostaining technique, see Appendix 2, GFAP immunostaining, page 131 ).

### **7.3.2 Immunoperoxidase staining method for ED1**

Immunostaining for ED1, a pan rat macrophage marker, was carried out on 5- $\mu$ m paraffin sections using standard immunoperoxidase staining protocols.<sup>191,193</sup> The sections were deparaffinized in xylene and dehydrated in graded ethanol baths and hydrated in PBS. After endogenous peroxidase activity in the tissue was blocked with 3% H<sub>2</sub>O<sub>2</sub> in PBS and nonspecific binding blocked with 15% NHS/PBS, the sections were incubated for one hour with mouse anti-rat primary ED1 monoclonal antibody (Serotec Ltd., Oxford, UK), diluted 1:400. After washing in 0.01 M PBS, sections were incubated with a 1:20 dilution of sheep anti-mouse secondary antibody conjugated by peroxidase (Amersham Pharmacia Biotech, UK) for 60 minutes. After washing in PBS, the slides were stained for peroxidase activity with DAB in H<sub>2</sub>O<sub>2</sub> and NiCl. The tissue sections were then counterstained with eosin and mounted for light microscopy (For details of the ED1 immunostaining technique, see Appendix 3, ED1 immunostaining, page 132).

### **7.3.3 Immunoperoxidase staining method for $\beta$ -APP**

Immunostaining for  $\beta$ -APP, a marker for axonal injury, was carried out on 5- $\mu$ m paraffin sections using standard immunoperoxidase staining protocols.<sup>191,194</sup> <sup>196</sup> APP immunostaining was performed using the same protocol as for GFAP, with the following exception of primary antibody diluted in 1:10000 (Mouse  $\alpha$  APP, Zymed Laboratories INC, USA) and secondary biotinylated antibody diluted 1:200 (Rabbit  $\alpha$  Mouse, DAKO Corporation, 6392 via Real Carpinteria, C.A.) (For details of the  $\beta$ -APP immunostaining technique, see Appendix 4,  $\beta$ -APP immunostaining, page 133).

## **8. Photography**

Photomicrographs were taken with an Olympus PM20 camera system and an Olympus BX50 microscope. Film used for microscopic photography was Kodak EPY-36 Tungsten 64T Ektachrome.

## **RESULTS**

Two rats (one in Group E and the other in Group F) died due to anaesthetic complications. Additionally, there were bilateral upper limb paralyses in one rat of Group F that was sacrificed 24 hours after operation. These three rats were excluded from this study. The presentation of histological appearance in the normal rat will be followed by the results for saline, kaolin, QA and QA plus kaolin injection.

### **1. Normal control rats (Group A)**

Normal histological appearances were demonstrated in the transverse sections at the C6 segmental level of spinal cord in the normal rat (uninjected) (Figure 7). The substance of the cord was divided into outer white matter and inner gray matter. The inner gray matter had the shape of an H. No pathological changes were shown in the H&E stained transverse section and in the transverse sections, stained for GFAP, ED1 and APP, at the same level (Figure 7).

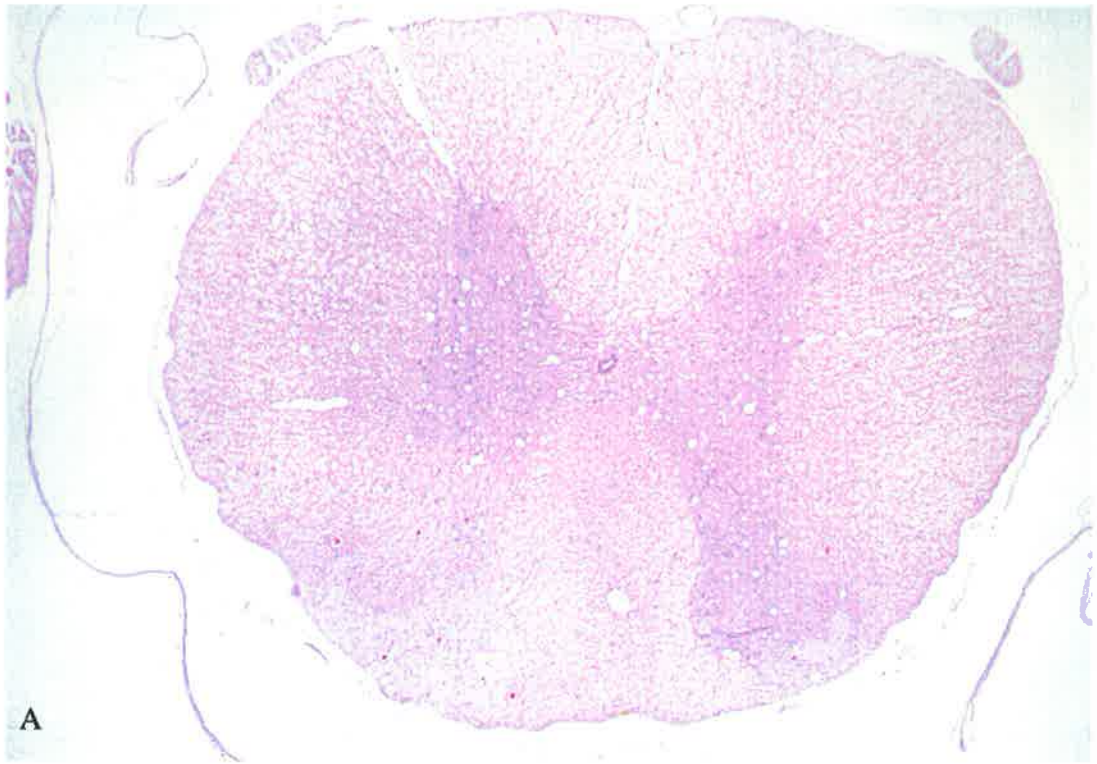


**Figure 7.** *Photomicrographs of transverse sections at C6 segmental level from a normal rat, showing normal histological appearance. A: H&E, x10. B: GFAP, x10. Figure 7 continued on next page.*

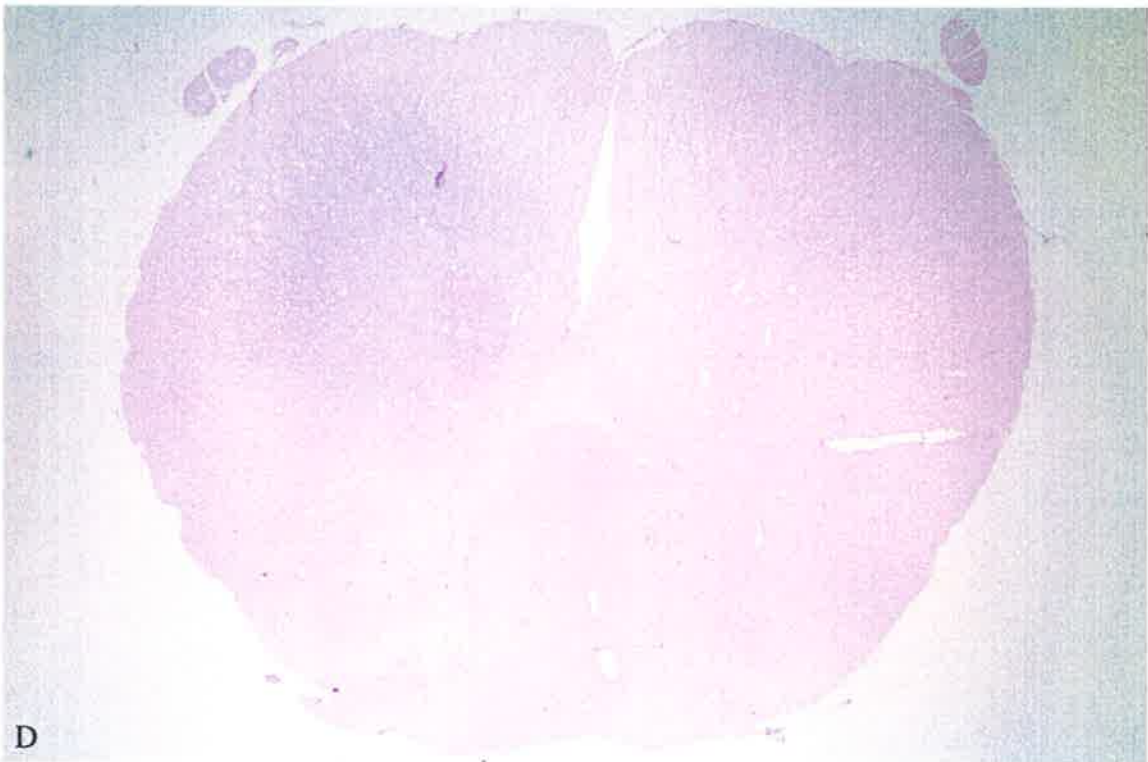
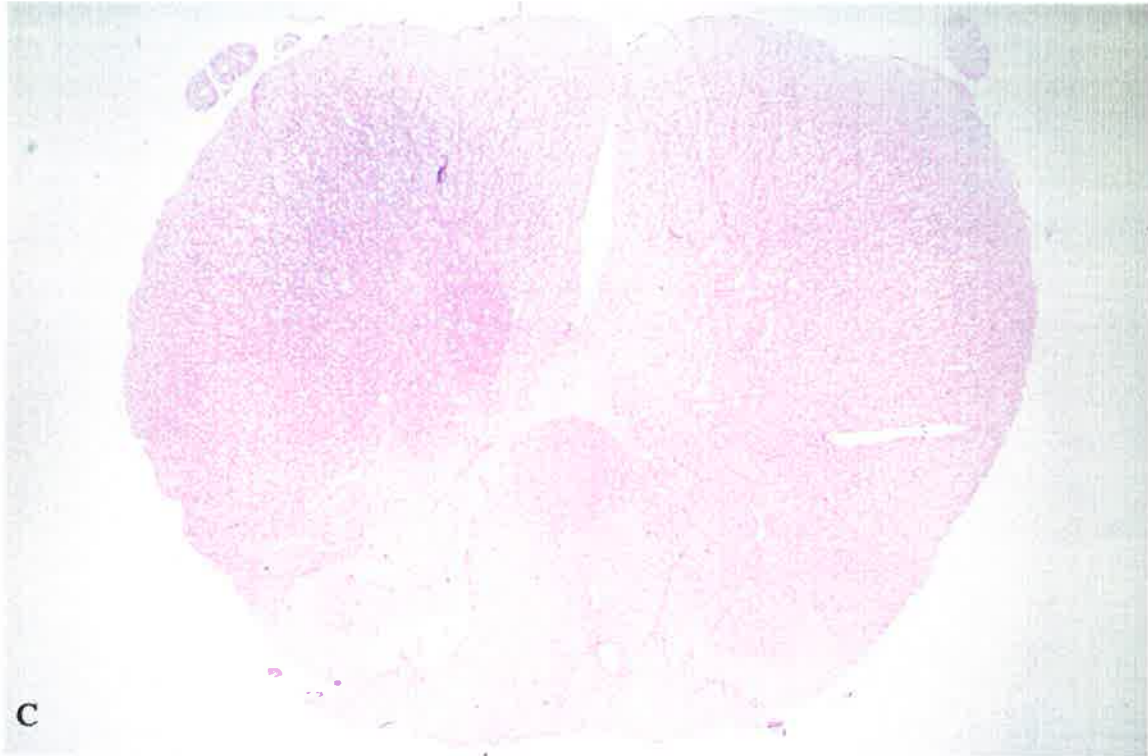


**Figure 7 (cont).** C: *ED1*, *x10*. D: *APP*, *x10*.

## **2. Saline control rats (Group B)**

Transient right upper limb weakness was observed in all three Group B rats after operation. All recovered within 1 day following operation. No rat in Group B developed spinal cord cysts. Transverse sections at the level of injection are shown in Figure 8. No cavitation in the gray or white matter was observed. The resulting mild inflammatory response was confined to the side of injection (right). The right side was indicated by the knife mark made at processing (Figure 8A). Intense GFAP staining was observed on the side of injection (right) compared to the uninjected (left) side (Figure 8B).

At higher magnification, the histological appearances of the same sections are shown in Figure 9. The normal central canal, deposition of yellow hemosiderin pigment and mild inflammatory response were seen in the H&E stained section. In addition, the healthy neurons in the gray matter on the side of injection were observed and the gray matter in the dorsal horn on the side of injection did not shrink (Figure 9A). A small number of ED1-positive macrophages in response to injection injury were seen in the transverse section at the same level (Figure 9C) and no APP staining was demonstrated in the transverse section at the same level (Figure 9D).

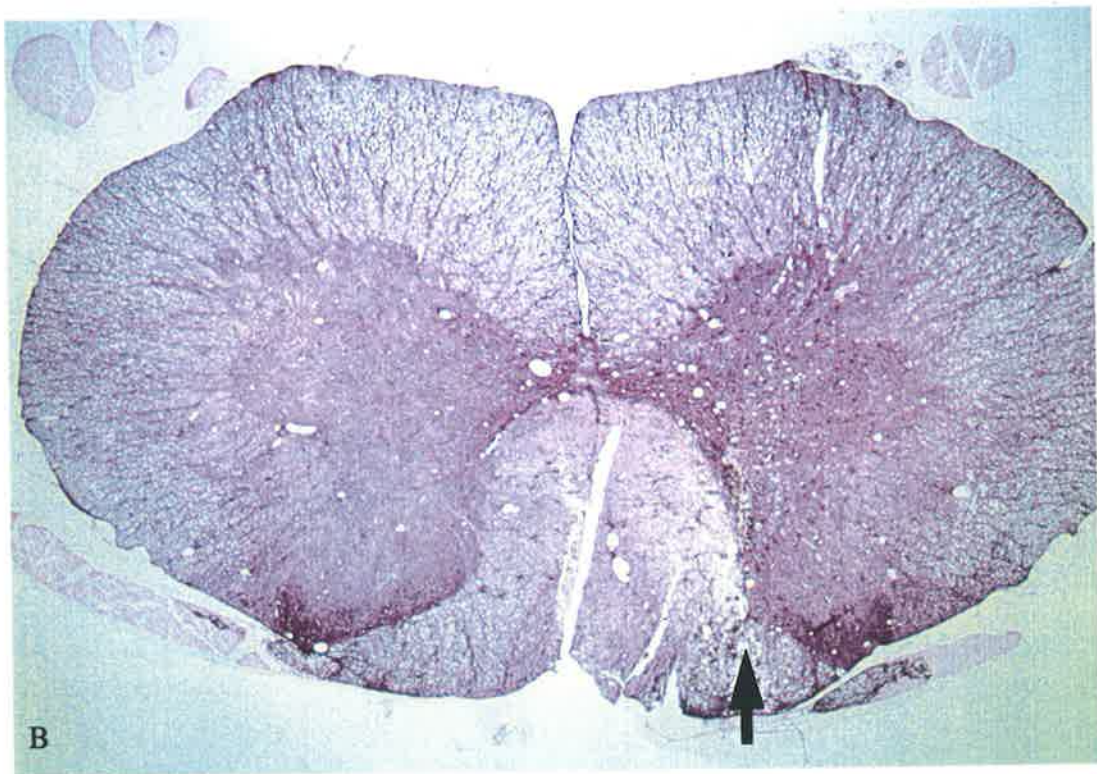
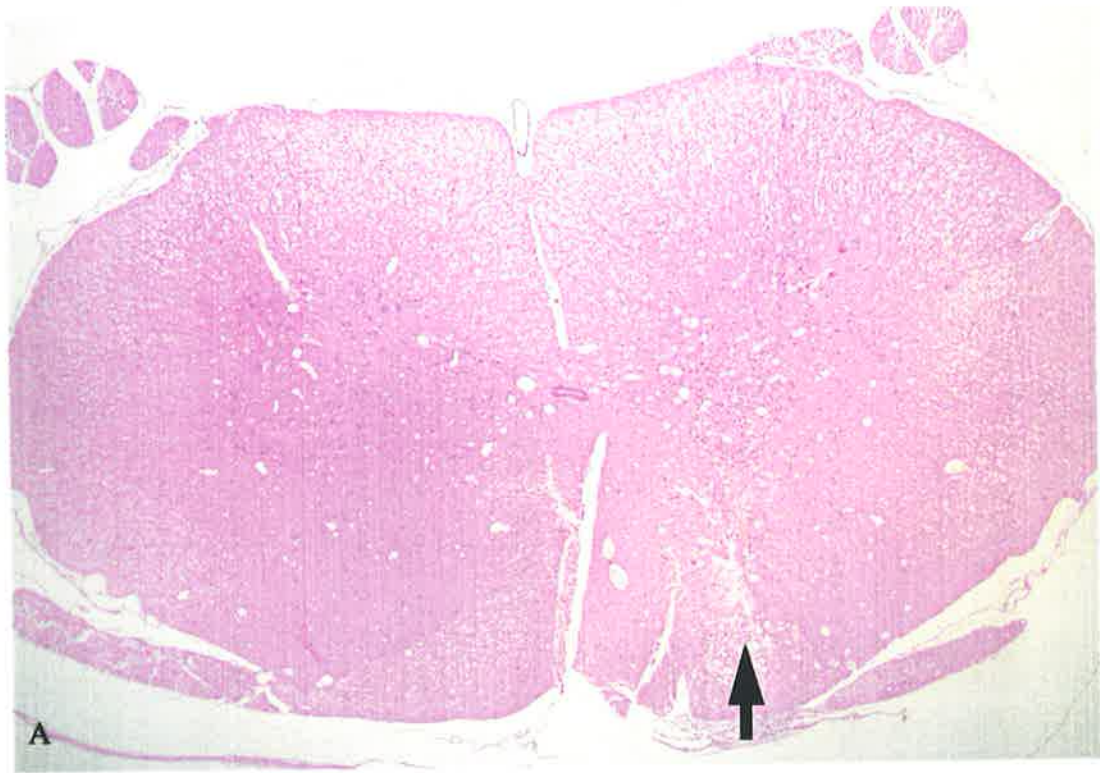


**Figure 8.** Photomicrographs of transverse spinal cord sections at C6 segmental level from a control rat sacrificed four weeks after sterile 0.9% saline injection, demonstrating mild inflammatory response to saline injection at the point marked with an arrow. A: H&E, x10. B: GFAP, x10.

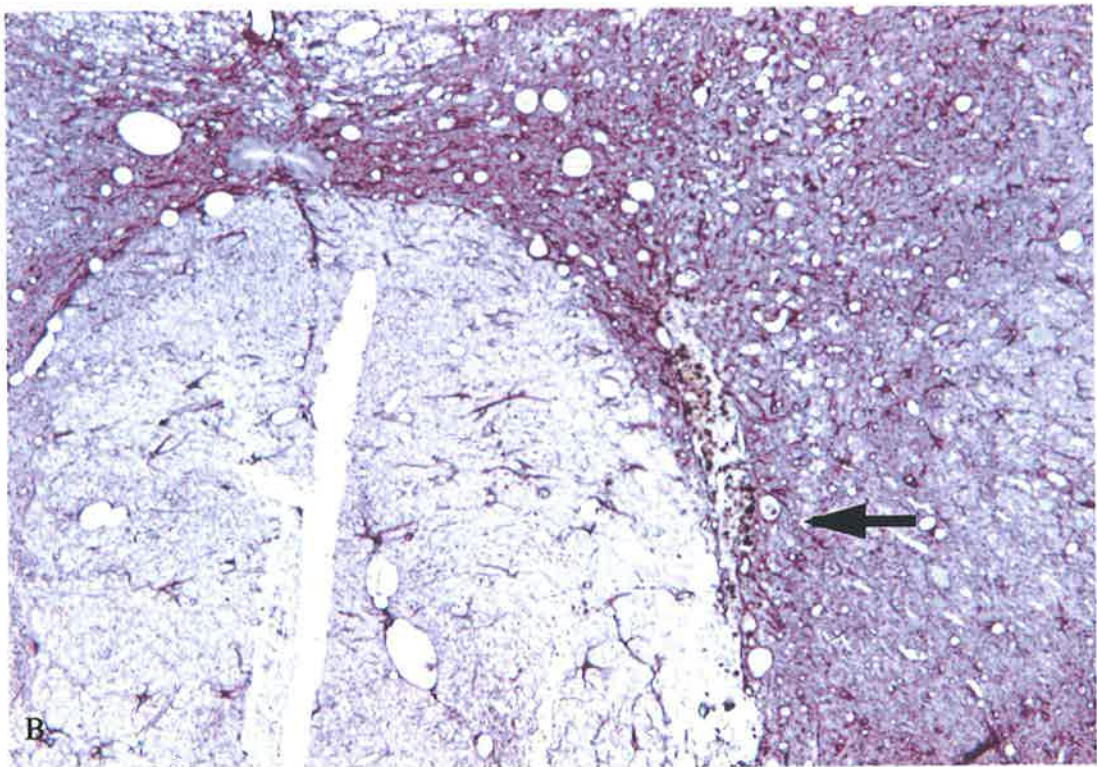
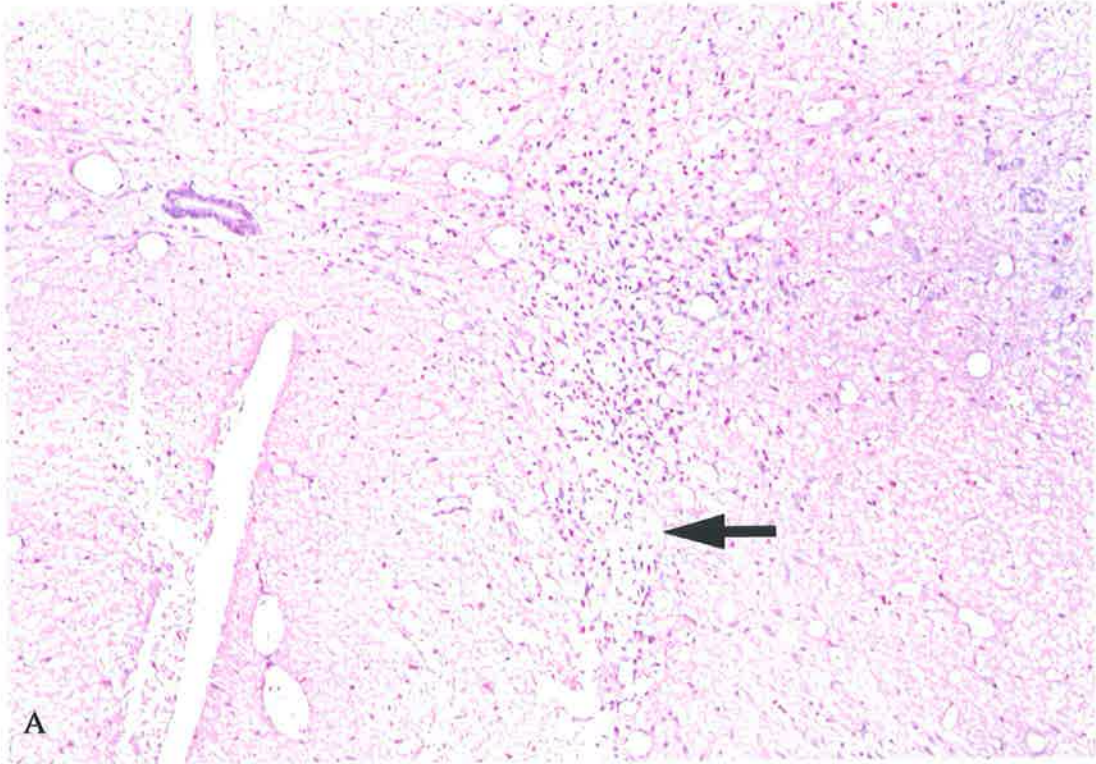


**Figure 9.** High-power view of same slides as in Fig. 8. The pictures showed the mild inflammatory response to normal saline injection (arrows). A: H&E, x25. B: GFAP, x25. Figure 9 continued on next page.

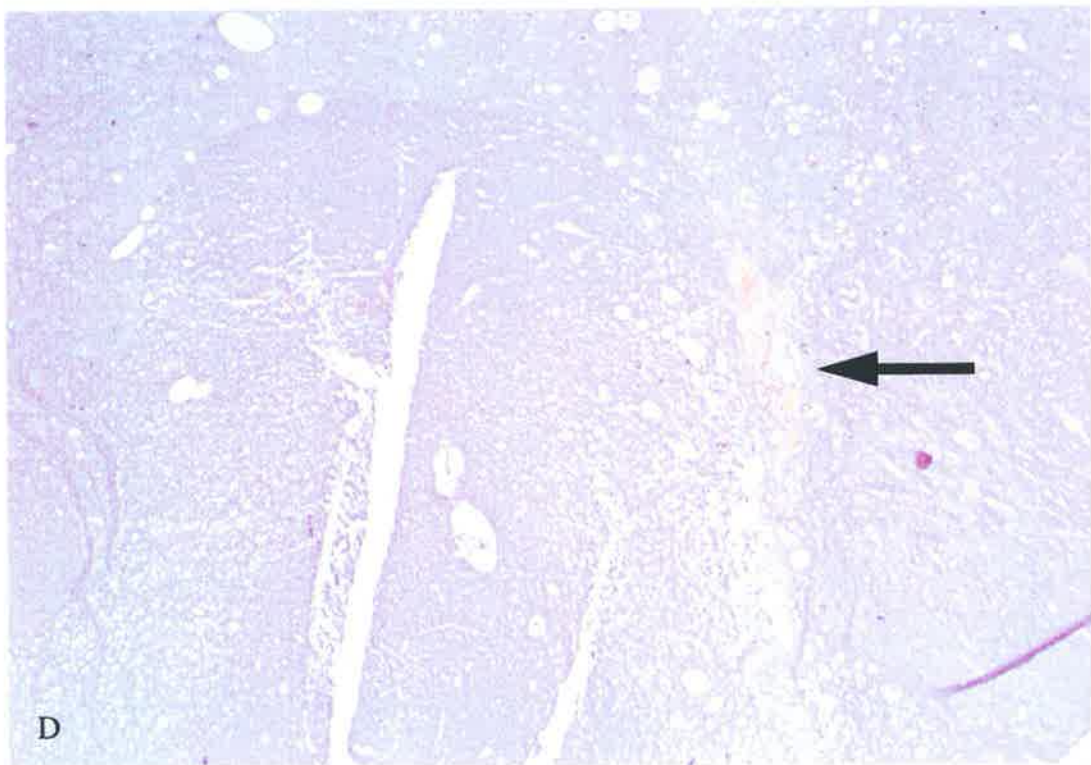
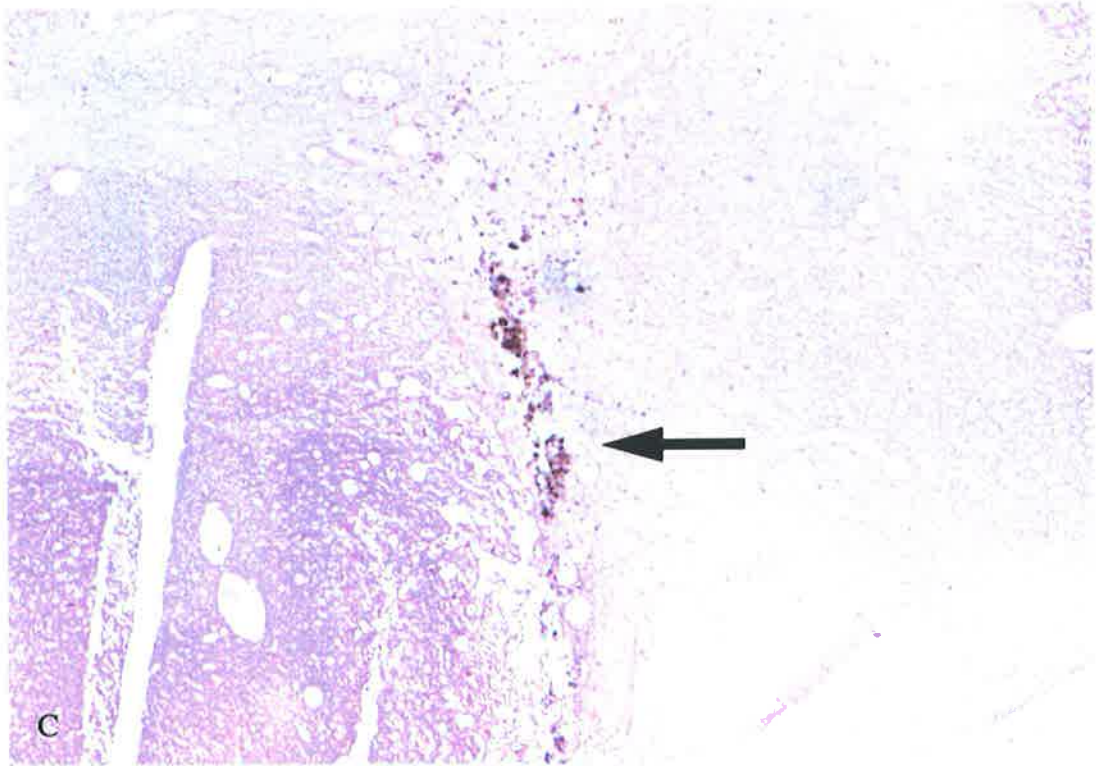


**Figure 9 (cont).** C: A small number of ED1-positive macrophages in response to saline injection injury were shown (arrow). ED1, x25. D: Deposit of yellow hemosiderin pigment (arrow) was seen without APP accumulation. APP, x25.

### **3. Subarachnoid kaolin injection (Group C)**

No obvious neurological deficit was observed in the Group C rats following operation. None of the five animals developed spinal cord cysts. A subarachnoid block was achieved by adhesive arachnoiditis in the subarachnoid space, which was infiltrated with kaolin crystals and inflammatory cells (Figure 10). The predominant inflammatory cell type was the macrophage and kaolin-laden macrophages were present within the subarachnoid space. It was observed that some kaolin leaked from the subarachnoid space into the subdural space. No cell loss, cavitation, or other noticeable changes in the gray or white matter were observed in the transverse sections. The central canal was normal and no kaolin crystals were observed in the central canal.

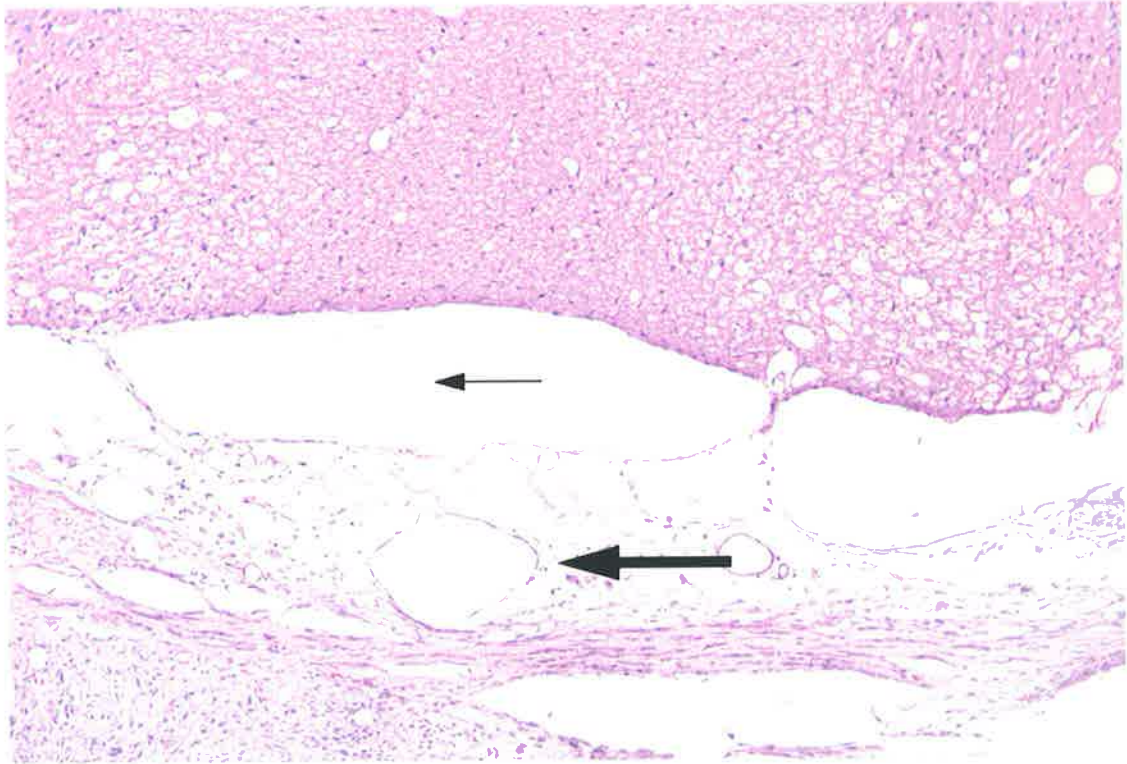


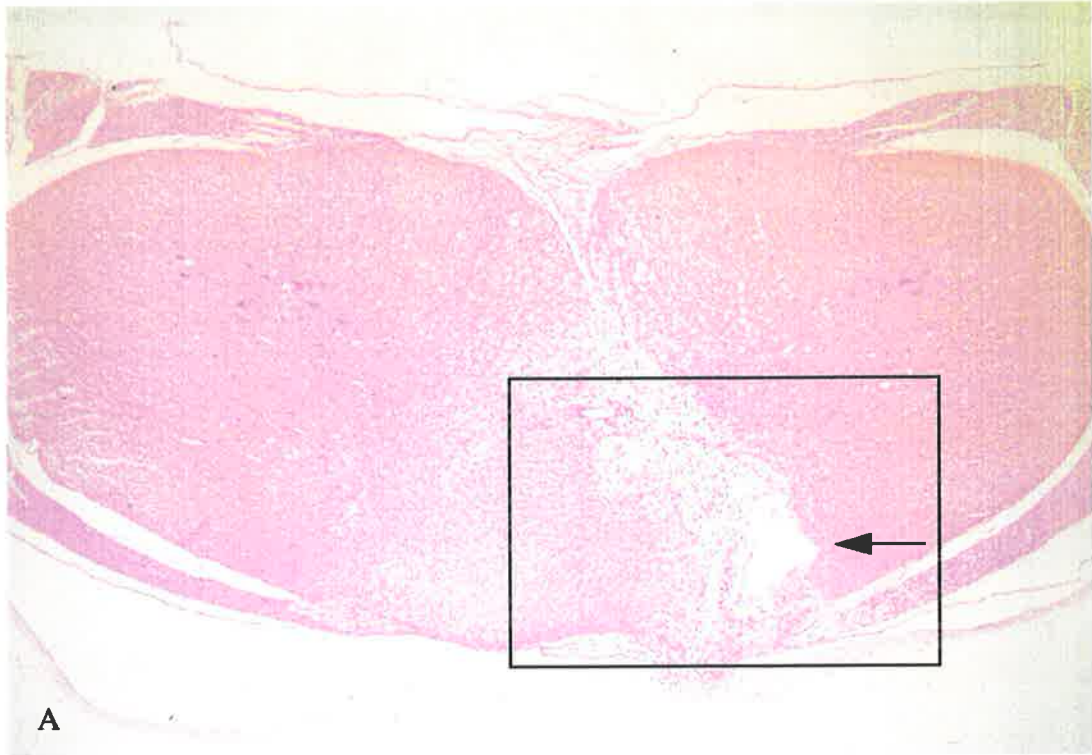
**Figure 10.** *Transverse sections at C6 segmental level of the spinal cord from a rat sacrificed four weeks after subarachnoid kaolin injection, showing spinal arachnoiditis and subarachnoid block. Subpial space (small arrow) was expanded during the sectioning due to different density of the tissue. Kaolin-laden macrophages and blood vessels were seen in the blocked subarachnoid space (large arrow). H&E, x25.*

#### **4. Intramedullary QA injection (Group D and E)**

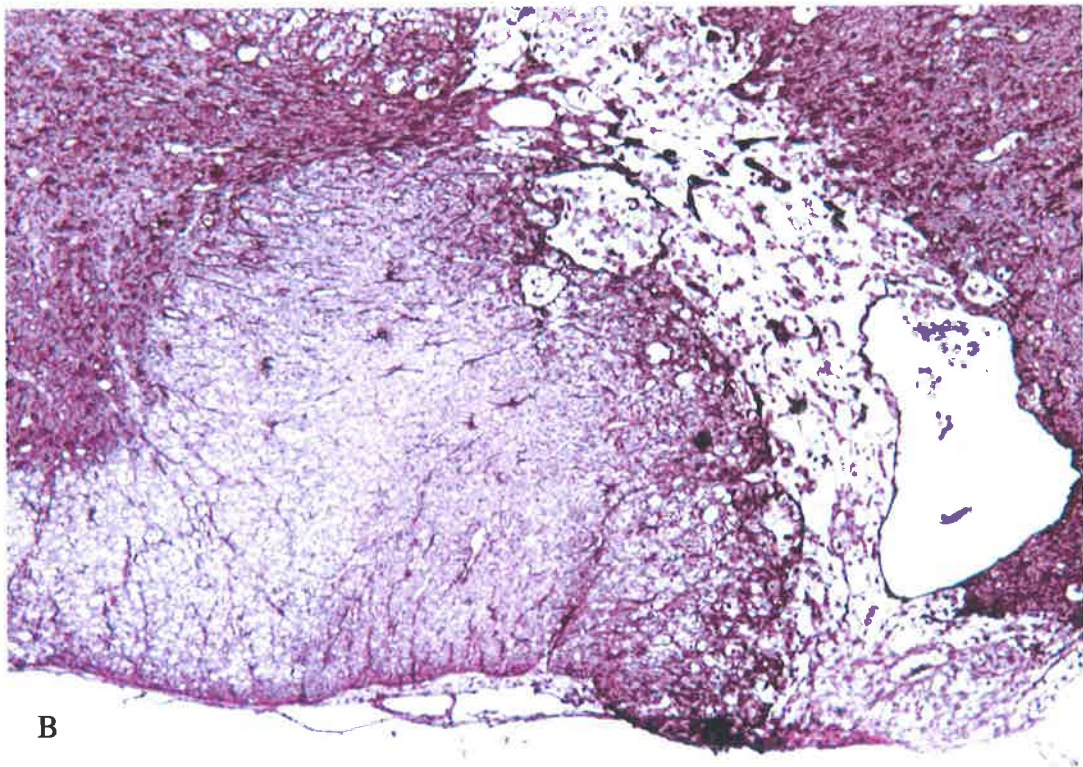
Transient right upper limb weakness was observed in all QA-injected rats of Group D and E. All recovered within 3 days following operation. There was non-selective neuron loss in all QA-injected animals. Intraspinous injections of different concentrations of 2  $\mu$ l QA resulted in a dose-dependent loss of neurons in the spinal gray matter. Additionally, the longitudinal extent of fluid-filled cysts or cystic spaces was confined to the segment of injection (C6). Based on the QA concentration, animals were divided into two groups: low concentration QA solution (8.3 mM or 1.6 mg/ml) and high concentration QA suspension (23.7 mg/ml).

##### ***4.1 Low concentration QA injection (Group D)***

Eight of 10 rats injected with low concentration QA (8.3mM) developed a spinal cord cyst or cystic spaces. An example of inflammatory response, neuron loss and a small cyst is shown in Figure 11 (animal # 19). The small well-defined cyst did not communicate with the normal central canal (Figure 11A). Compared to mild GFAP staining in the normal tissue (Figure 7B) and in the Group B saline control rats (Figure 8B), intense GFAP staining was observed in the transverse sections, stained for GFAP, at the equivalent level (Figure 11B). Additionally, numerous GFAP-positive hypertrophic astrocytes were observed near the cyst (Figure 11B). A number of ED1-positive macrophages were scattered throughout the parenchyma in the transverse section, stained for ED1, at the same level (Figure 11C). The APP immunostaining at the same level, however, showed only sparse accumulation of APP (Figure 11D).



A



B

**Figure 11.** Transverse sections, at C6 segmental level, of spinal cord from a rat sacrificed four weeks after low concentration QA injection (8.3 mM). A: A small well-defined cyst was shown (arrow). H&E, x10. B: The cyst from the outlined region in Figure 11A is magnified. GFAP, x25. Figure 11 continued on next page.

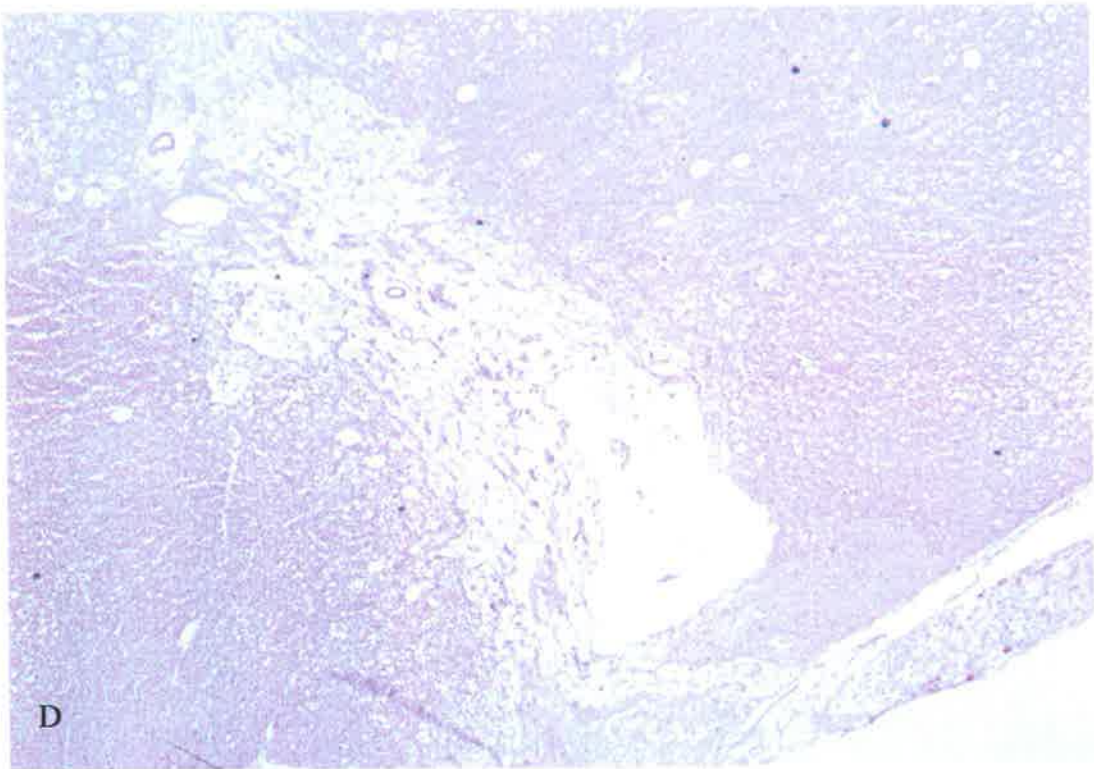
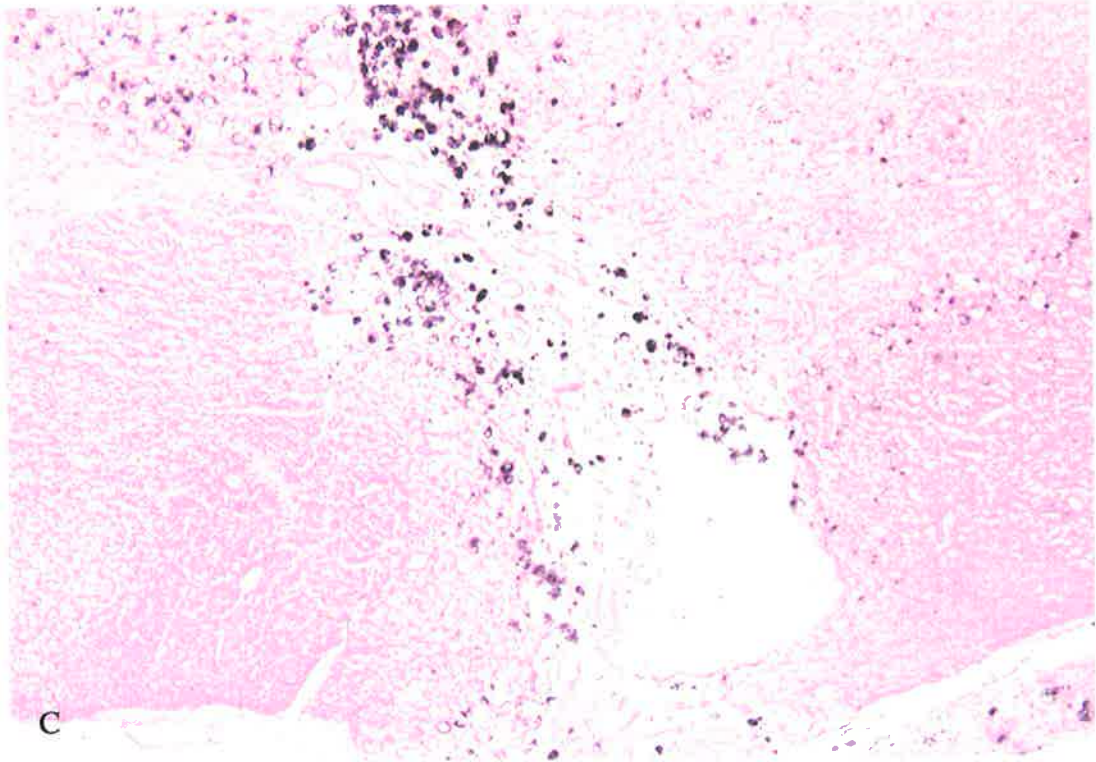


**Figure 11 (cont).** *The cyst from the outlined region in Figure 11A is magnified. C: ED1, x25. D: APP, x25.*

#### **4.2 High concentration QA injection(Group E)**

Compared to the pathological changes in the tissue with low concentration QA, a larger cyst or larger cystic spaces were seen in 8 of 9 rats injected with high concentration (23.7 mg/ml) QA suspension. Figure 12 shows extensive inflammatory response and neuron loss bilaterally in the H&E stained transverse section from a rat sacrificed four weeks after an injection of high concentration of 2  $\mu$ l QA suspension (animal # 28). Larger fluid-filled cystic spaces were found in the gray matter on the side of injection. These larger fluid-filled cystic spaces were separate from the central canal which was normal (Figure 12A). Moreover, three phases of pathological progress were found in the tissue: early inflammatory reaction in the gray matter contralateral to the injection site, intermediate consolidated necrosis in the middle and late fluid-filled cystic spaces ipsilateral to the injection (Figure 12A). Intense GFAP staining and some intensely staining hypertrophic astrocytes were observed in the transverse section, stained for GFAP, at the same level (Figure 12B). There were many more ED1-positive macrophages than those observed in the tissue with low concentration QA injection (Figure 11C) throughout the parenchyma, especially in the immediate vicinity of cystic spaces (Figure 12C). APP immunostaining showed minor APP accumulation localised to the immediate vicinity of cystic spaces at the same level (Figure 12D).

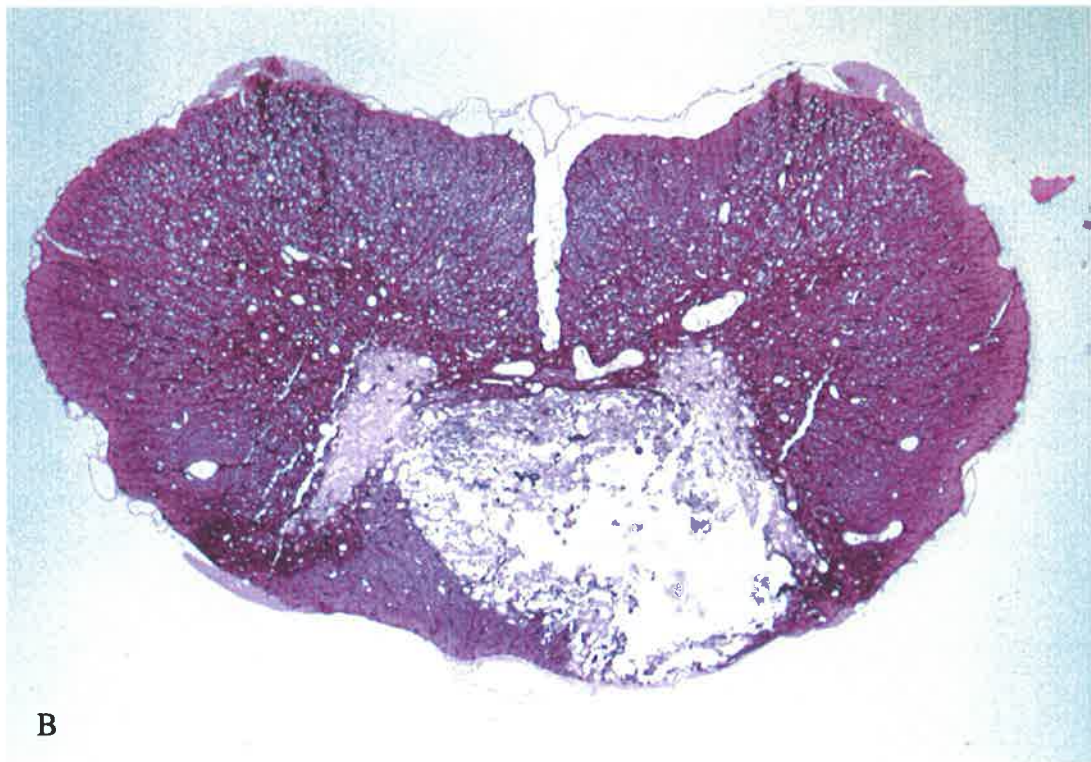


**Figure 12.** *Photomicrographs of transverse sections at C6 segmental level from a rat sacrificed four weeks after an injection of high concentration of QA (23.7mg/ml), showing bigger cystic spaces. A:H&E, x10. B: GFAP, x10. Figure 12 continued on next page.*

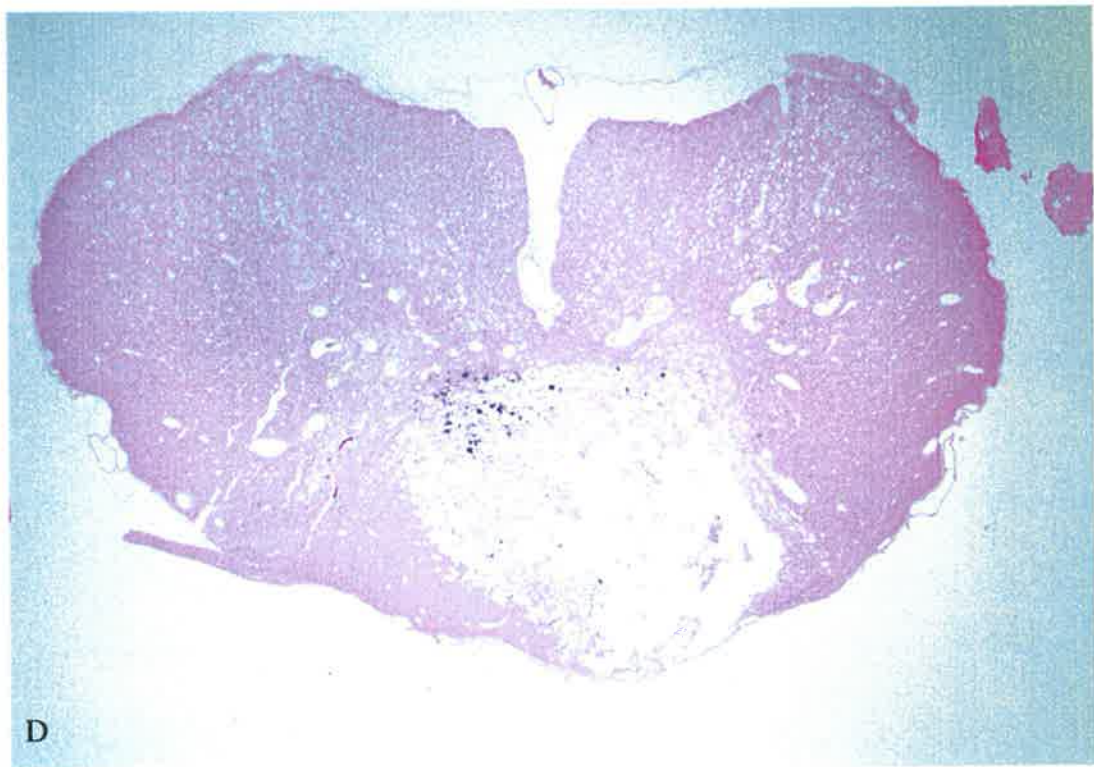
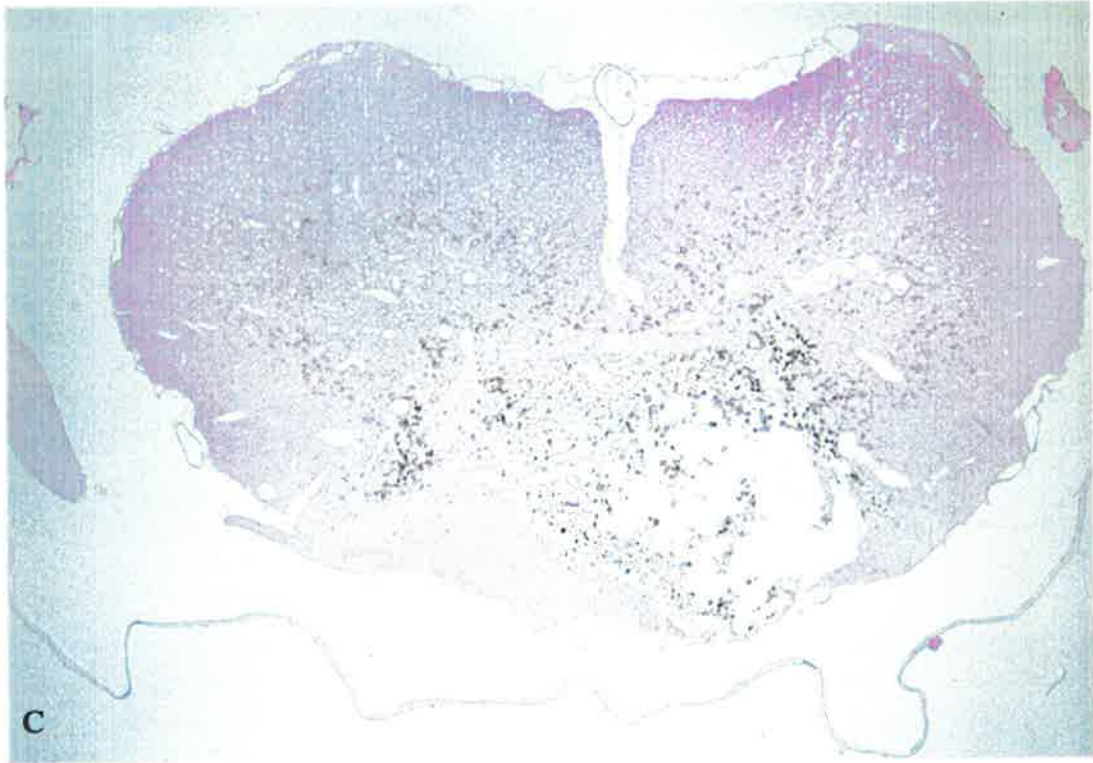


**Figure 12 (cont).** C: ED1, x10. D: APP, x10.

## **5. Intramedullary QA injection with subarachnoid kaolin injection (Group F)**

Transient right upper limb weakness was observed in all rats of Group F following operation. All recovered within 3-5 days after operation. Syring formation was seen in 9 out of 11 animals. The longitudinal extension of neuronal degeneration, syrinx and inflammatory response exceeded two segments. An example sacrificed three weeks after a combination of intraspinal QA injection and intrathecal kaolin injection is shown in Figure 13 (animal # 35). There were three well-defined separate syringes in the dorsal part of the spinal cord, which were clearly separate from the normal central canal. The subarachnoid space obstructed by the arachnoiditis and islands of cells floating in the syrinx were demonstrated. Additionally, an extensive inflammatory responses and neuron loss bilaterally were seen in the parenchyma, especially near the syringes (Figure 13A). In the immediate vicinity of spinal cavities there were also numerous GFAP-positive hypertrophic astrocytes embedded in a dense network of GFAP stained fibers (Figure 13B). Two regions near the syringes unstained for GFAP (Figure 13B) were infiltrated with ED1-positive macrophages and large numbers of macrophages were scattered throughout the parenchyma (Figure 13C). The limited APP accumulation was confined to the immediate vicinity of spinal cavities at the same level as injection (Figure 13D).

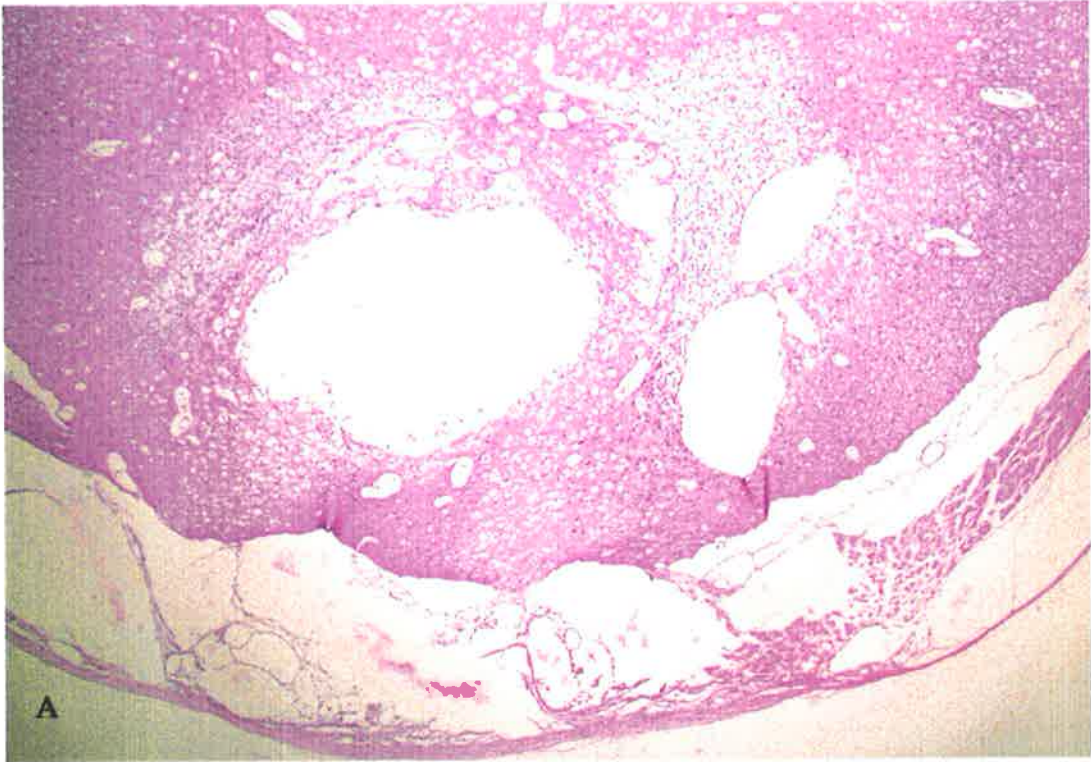


**Figure 13.** *Transverse sections at C6 segmental level after a combination injection of 23.7 mg/ml QA into the dorsal horn and 250 mg/ml kaolin into the subarachnoid space, showing three separate syrinxes. A: H&E, x10 . B: GFAP, x10. Figure 13 continued on next page.*

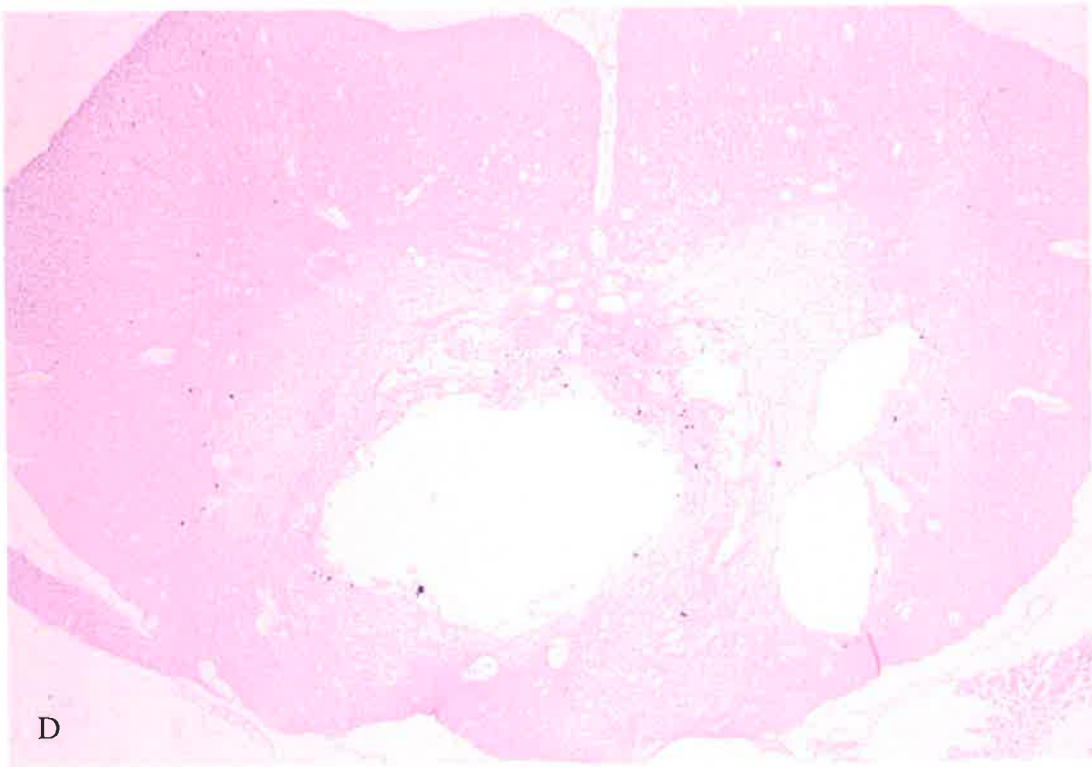
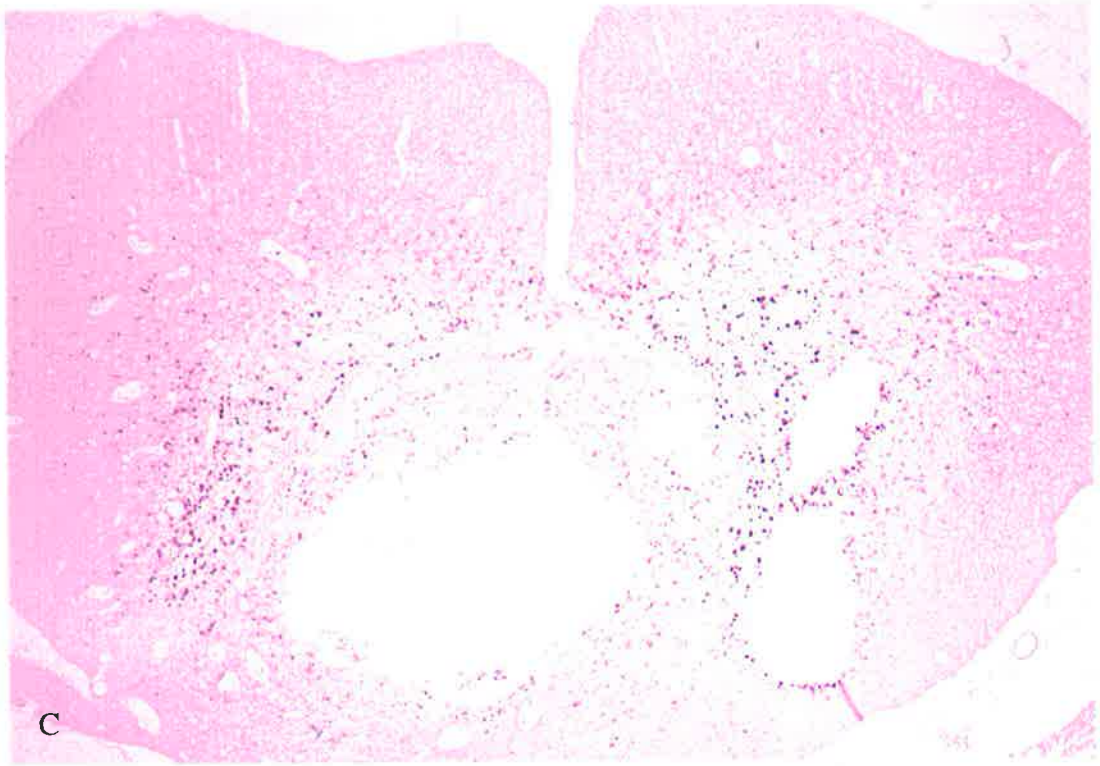


**Figure 13 (cont).** C: ED1, x10. D: APP, x10.

Photomicrographs, at higher magnification, in Figure 14 showed the largest of three separate syrinxes seen in Figure 13. The large well-demarcated syrinx was surrounded by an extensive inflammatory response and some islands of cells floated in the syrinx (Figure 14A). The lining of the cavity consisted of GFAP-positive astrocytes and some of islands of cells floating in the cavity were composed of GFAP-positive astrocytes (Figure 14B). The region surrounding the cavitation was infiltrated with ED1-positive macrophages and some cells floating in the cavity were ED1-positive macrophages (Figure 14C). APP accumulation was confined to the vicinity of spinal cavitation (Figure 14D).

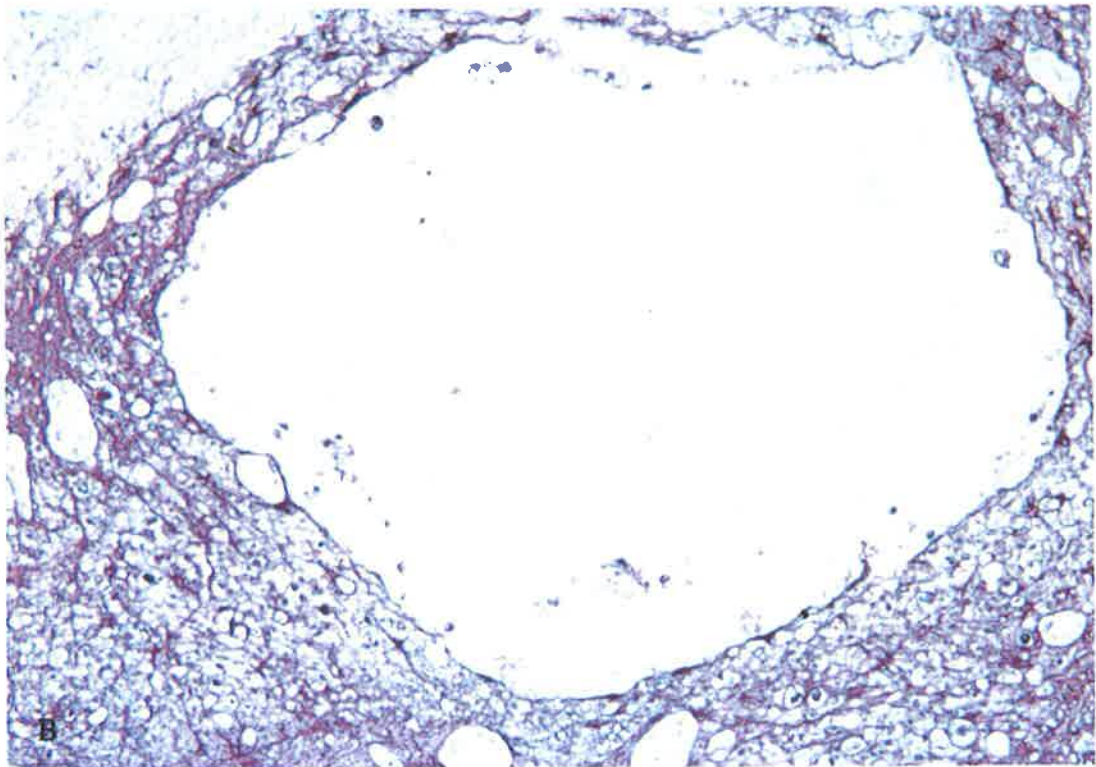
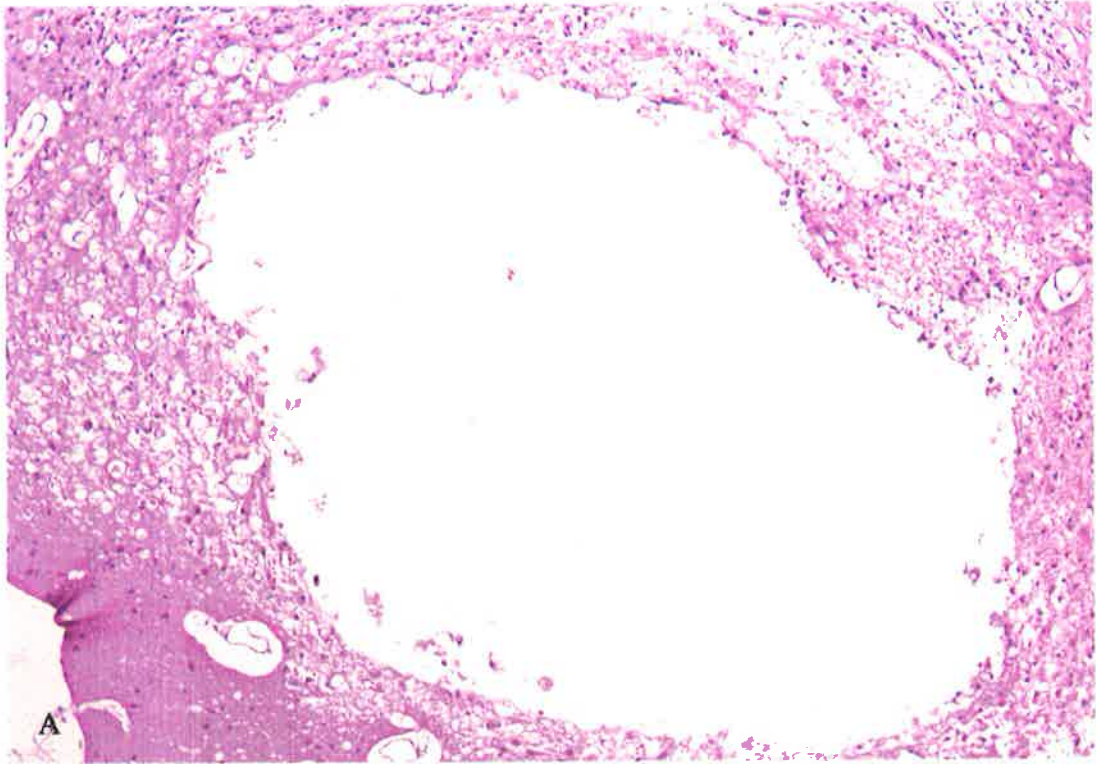


**Figure 14.** *High-power photomicrographs of same slides as Figure 13. The lining of spinal cavitation consisted of GFAP-positive astrocytes. A: H&E, x25. B: GFAP, x25. Figure 14 continued on next page.*

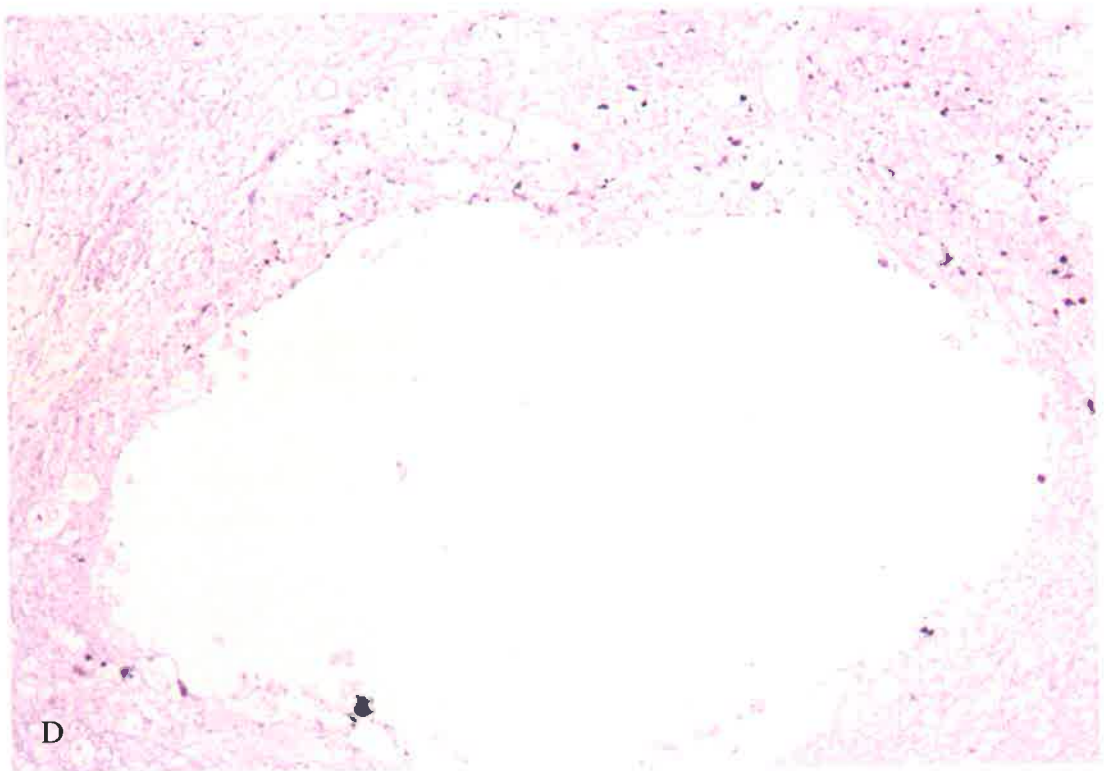


**Figure 14 (cont).** C: *ED1*, x25. D: *APP*, x25.

Photomicrographs, at higher magnification, in Figure 15 show the other two small syrinxes from the case seen in Figure 13. These two small syrinxes were separated by a thin septum and were surrounded by an extensive inflammatory response (Figure 15A). The lining of the two syrinxes was composed of GFAP-positive astrocytes and numerous intensely staining hypertrophic astrocytes were found in the vicinity of the cavitation (Figure 15B). The region surrounding the cavitation was infiltrated with ED1-positive macrophages (Figure 15C). The sparse APP accumulation was confined to the vicinity of spinal cavitation (Figure 15D).

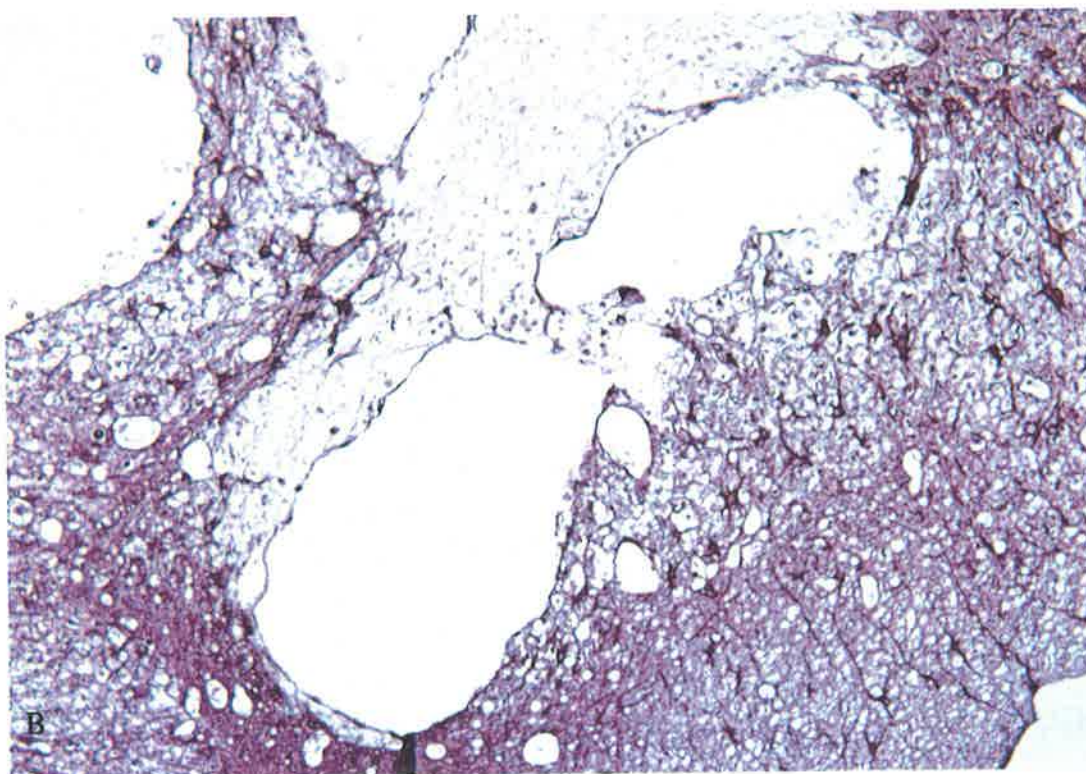
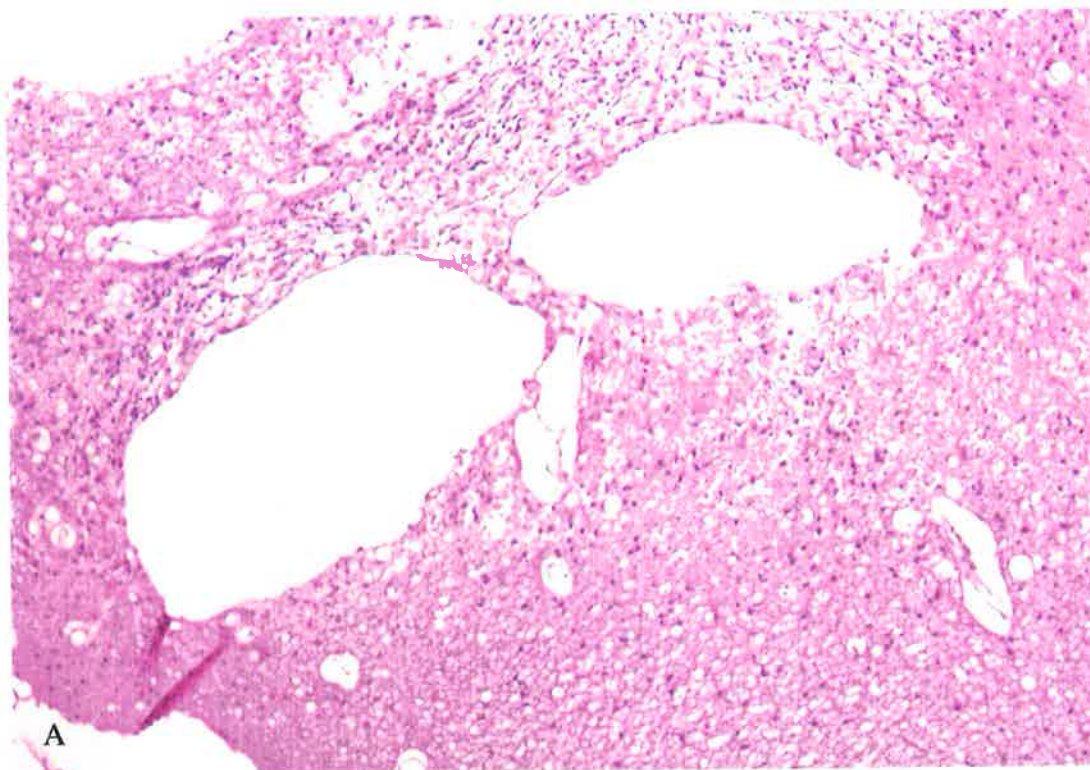


**Figure 15.** *High-power photomicrographs of same slides as Figure 13, showing two well-defined small syrinxes separated by a thin septum in the dorsal part of spinal cord. A: H&E, x25. B: GFAP, x25. Figure 15 continued on next page.*

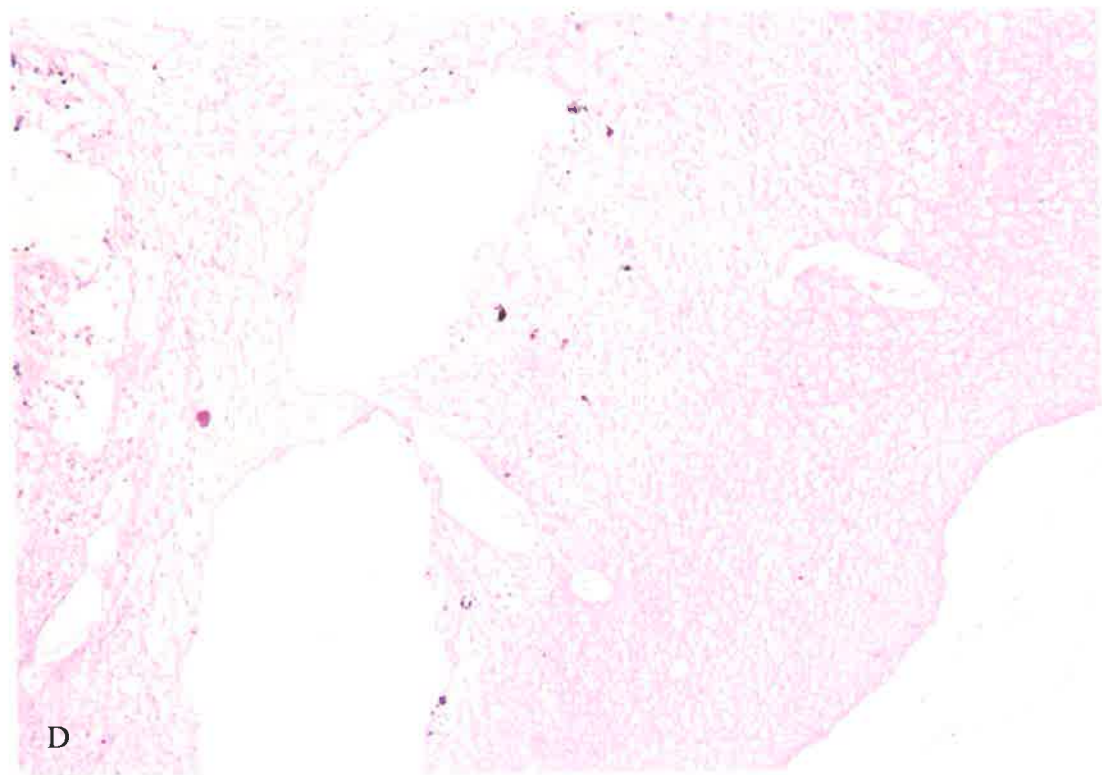
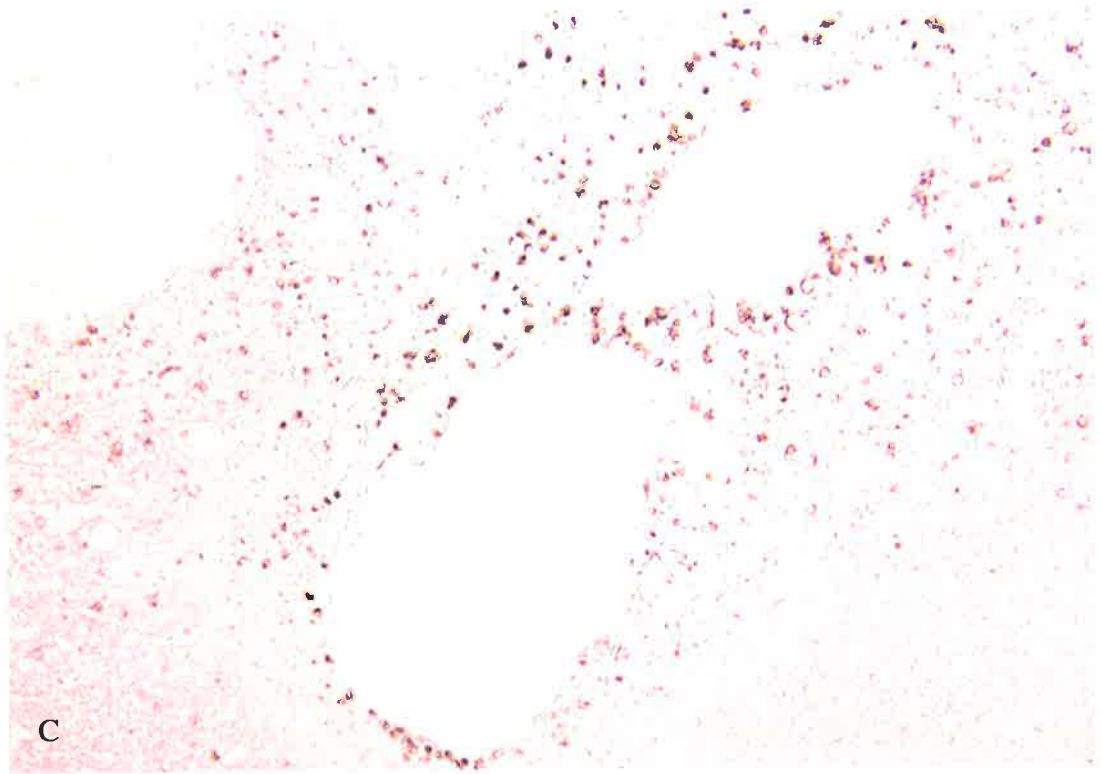
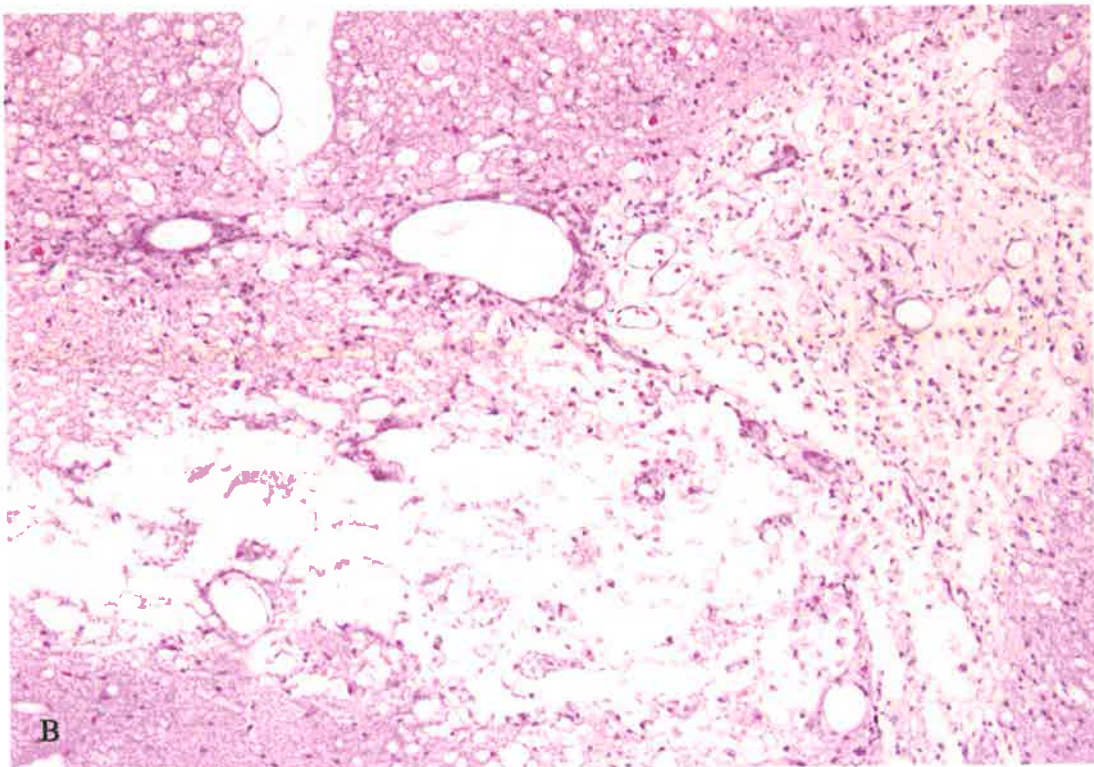
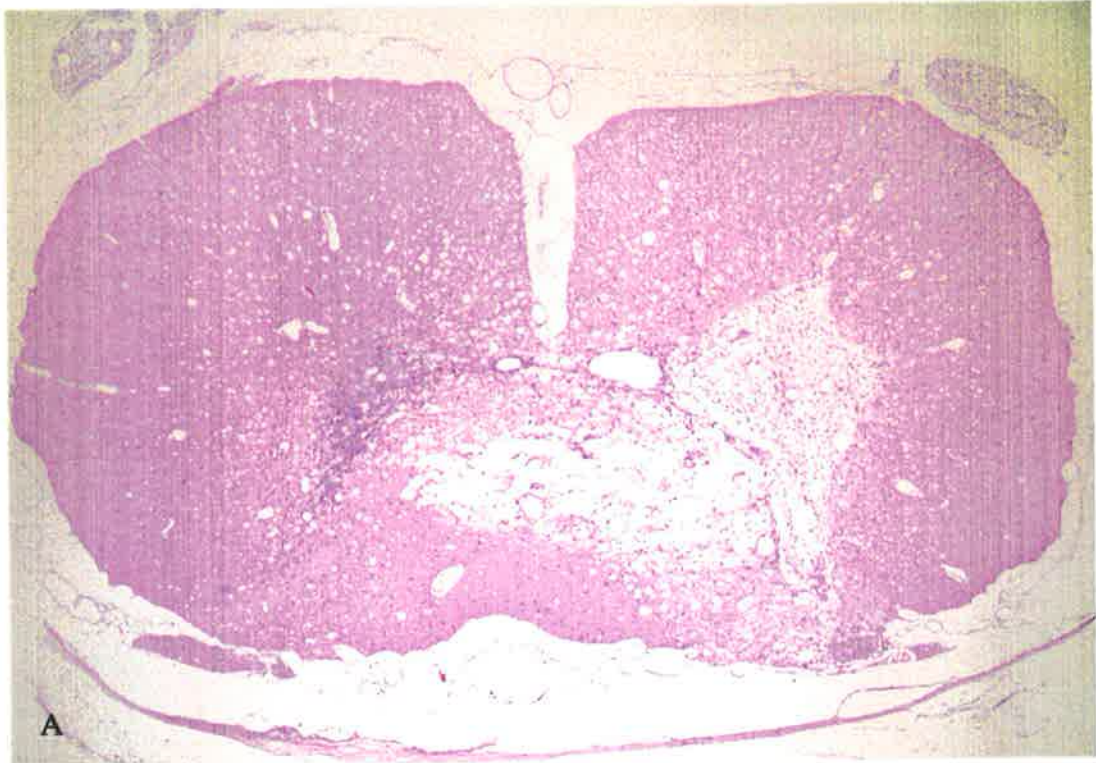


**Figure 15 (cont).** C: *ED1*, x25. D: *APP*, x25.

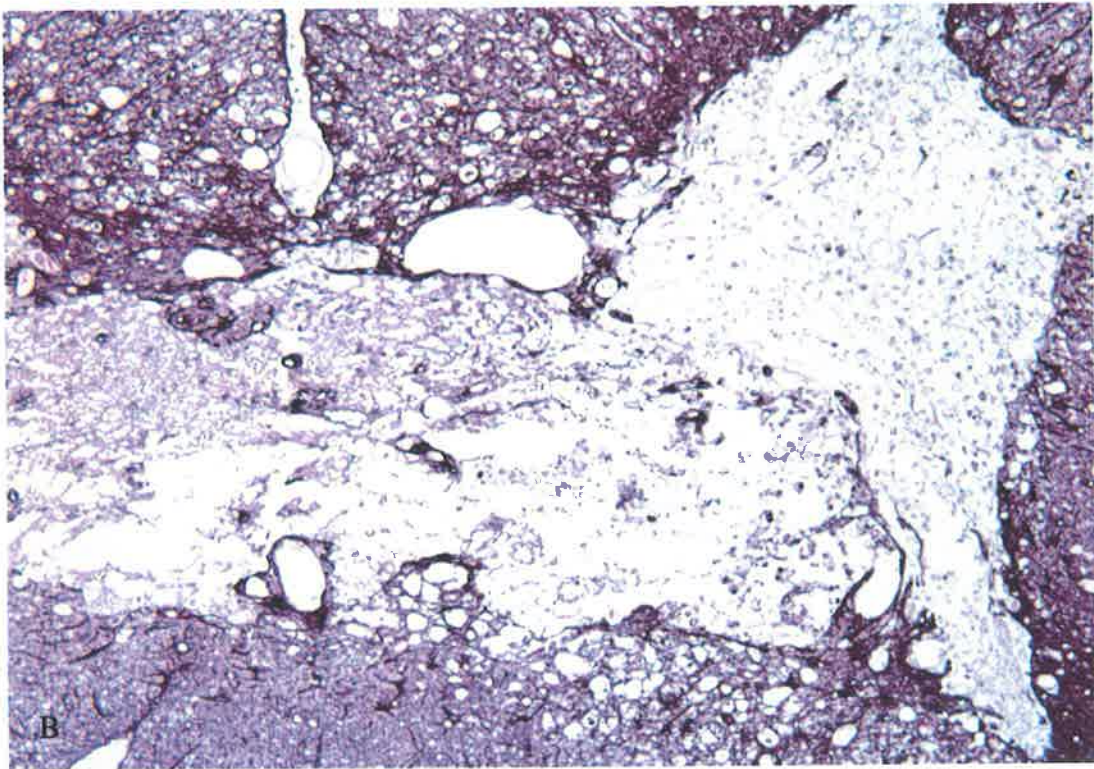
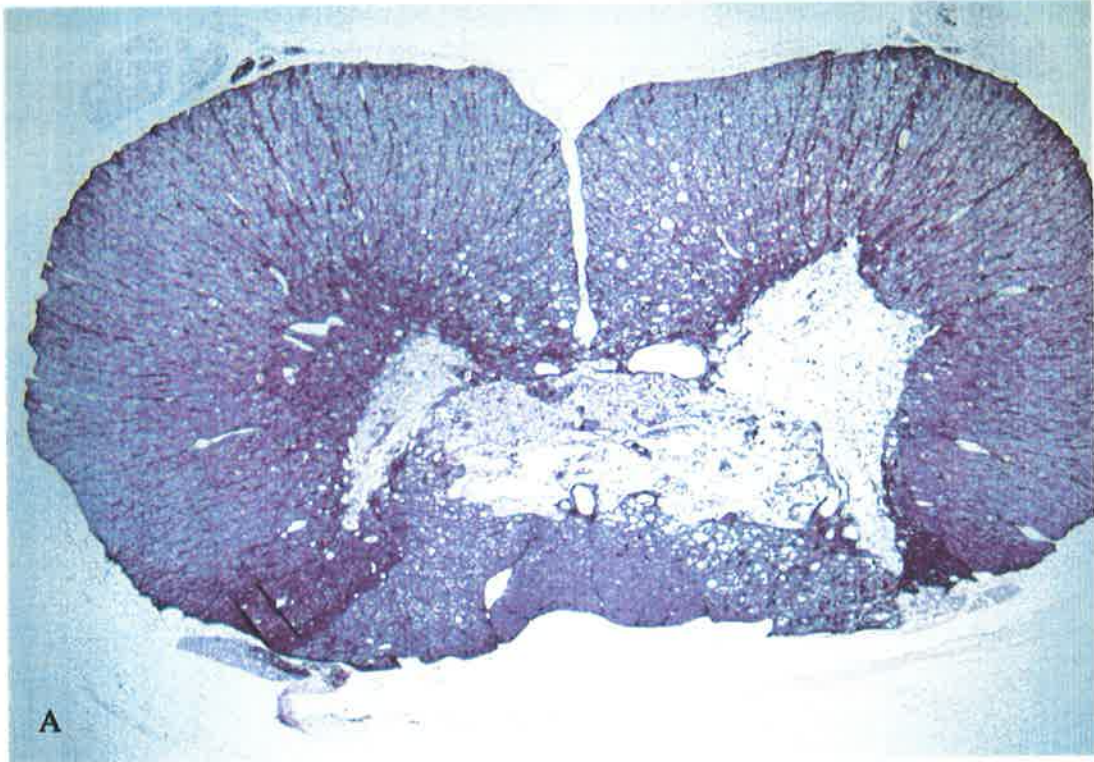
Figure 16 shows the H&E stained section 0.8 mm rostral to the lesioned level seen in Figure 13. Figure 17 is the same section as Figure 16 immunostained for GFAP. Three phases of pathological progression can be observed in the H&E stained section: (1) early phase of inflammatory mononuclear response in the gray matter contralateral to the injection side; (2) intermediate phase of consolidated necrosis in the gray matter ipsilateral to the injection region infiltrated with macrophages; (3) late phase of fluid-filled cystic spaces separated by islands of cells and blood vessels (Figure 16). Additionally, the central canal was normal and it did not communicate with the fluid-filled cystic spaces.

In the region with inflammatory response and neuron degeneration there were also some GFAP-positive hypertrophic astrocytes embedded in a dense network of GFAP stained fibers. In addition, islands of GFAP stained astrocytes were found in the fluid-filled cystic spaces (Figure 17).

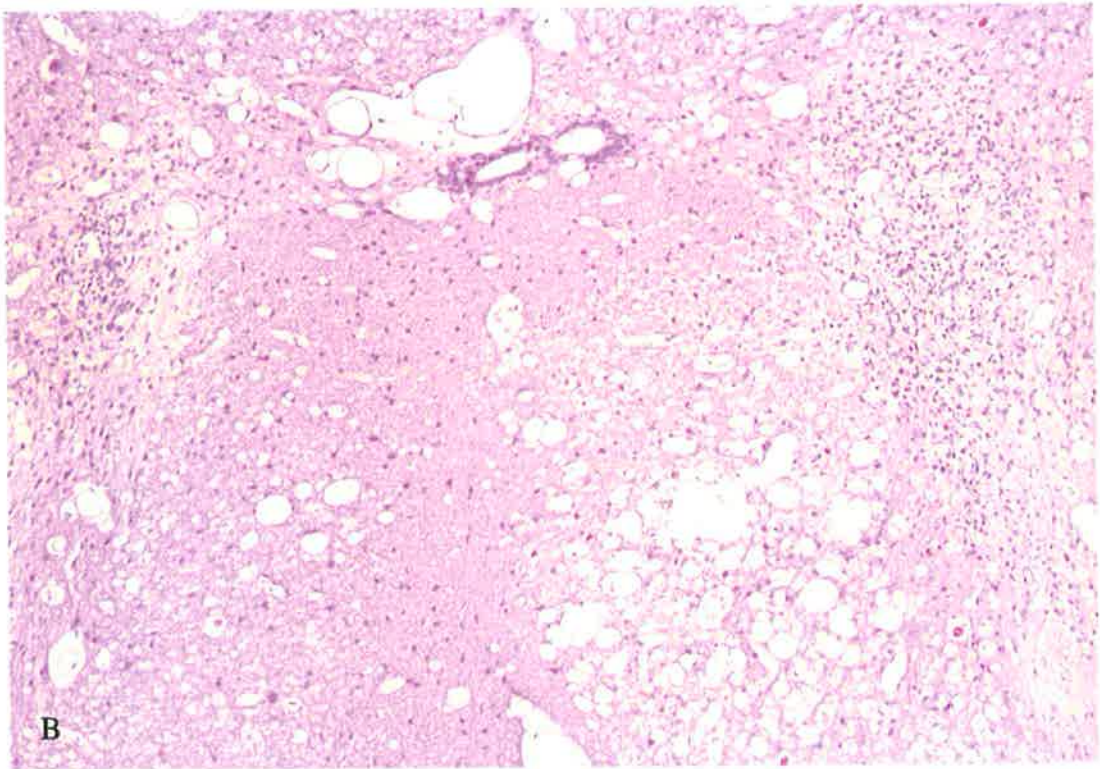
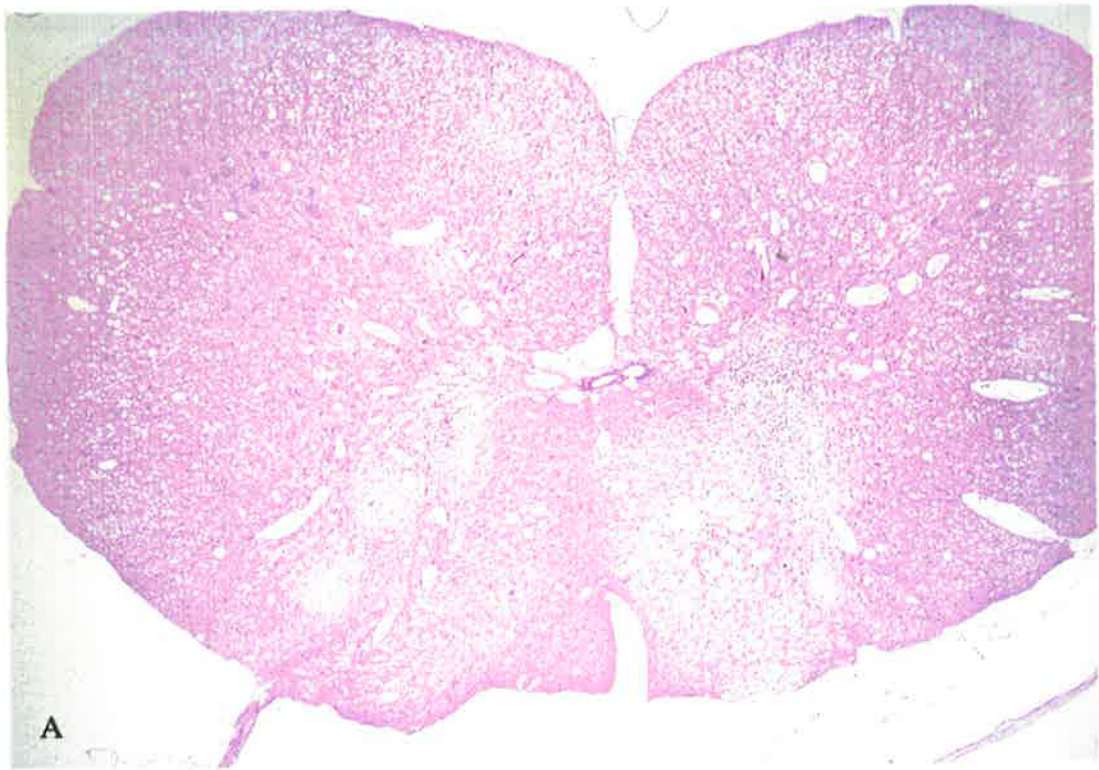
Figure 18 shows the transverse section 1.0 cm rostral to the lesioned level seen in Figure 13. Bilateral inflammatory mononuclear response and extensive neuron loss were found in the parenchyma and unilateral spongy degeneration was found in the posterior white column on the side of injection. The central canal had no apparent pathological changes.



**Figure 16.** *Transverse section, at the level 0.8 cm rostral to lesioned level, of spinal cord from the case seen in Figure 13. A: Inflammatory response, consolidated necrosis and cystic spaces separate from the central canal. H&E, x10. B: High-power view. H&E, x25.*



**Figure 17.** *Photomicrographs of transverse section, stained for GFAP, at the same level as in Figure 16. A: Some GFAP-positive astrocytes embedded in a dense network of GFAP stained fibers. GFAP, x10. B: High-power view as in Figure 17A. GFAP, x25.*



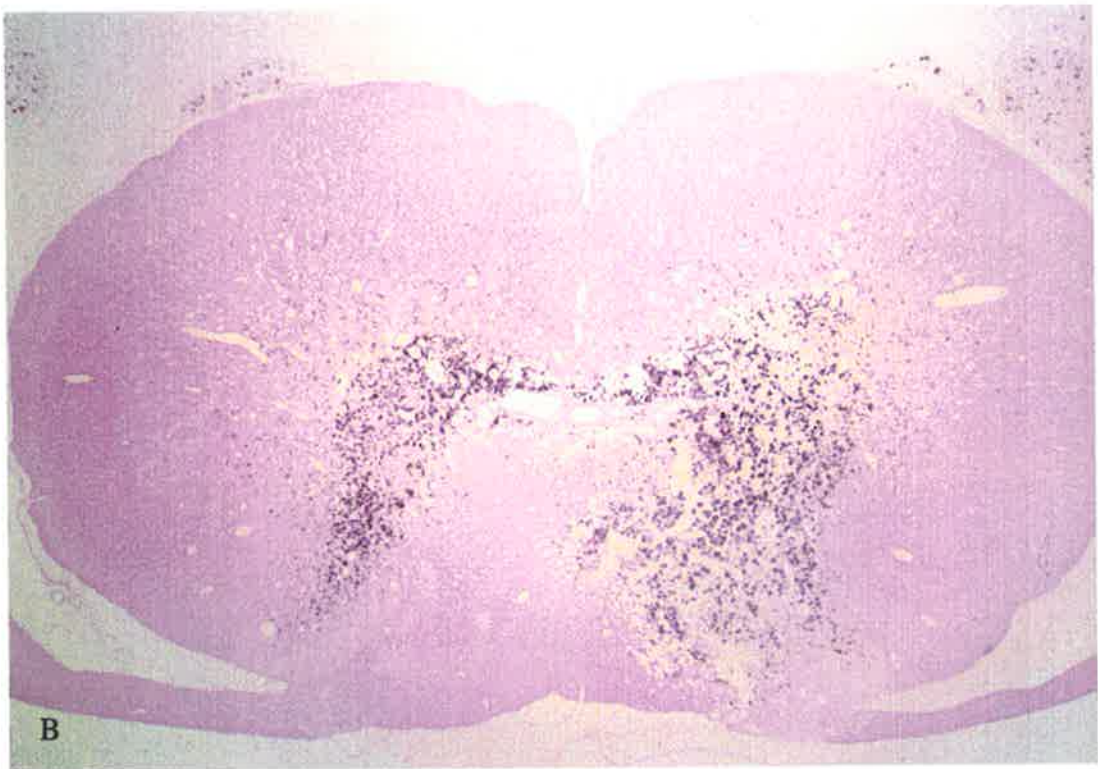
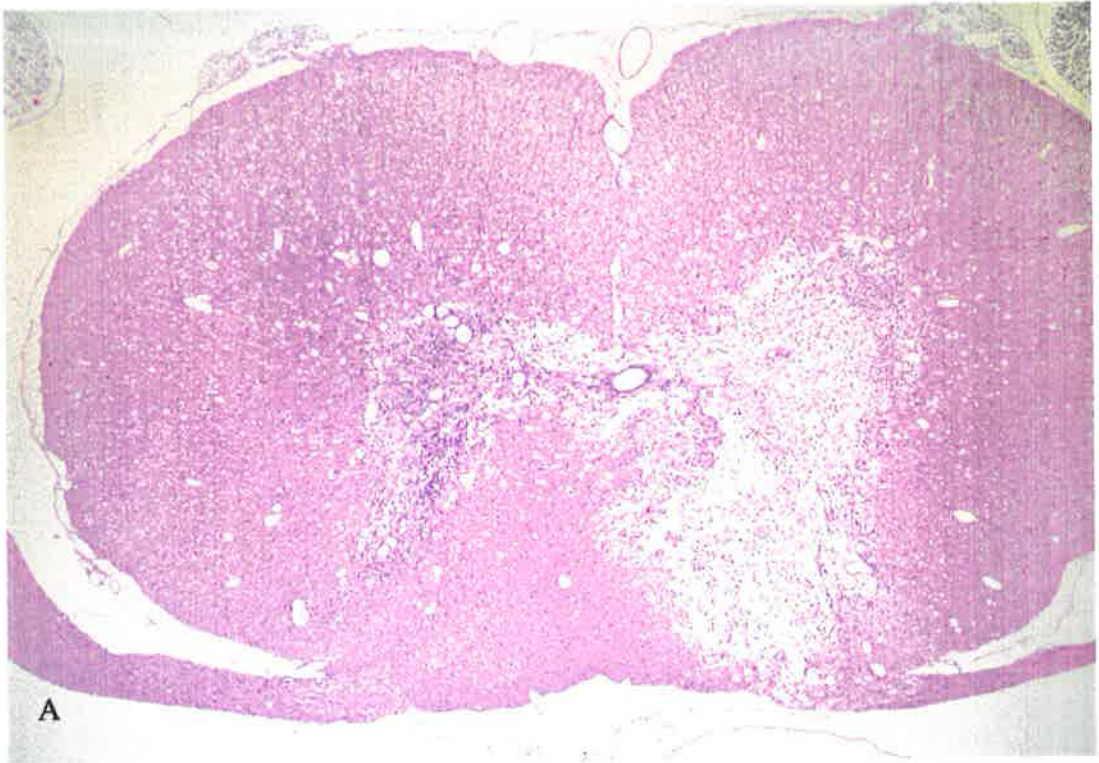
**Figure 18.** *Photomicrograph of transverse section at the level 1.0 cm rostral to injection seen in Figure 13. A: Bilateral inflammatory response. H&E, x10. B: High-power view of the case seen in Figure 18A. H&E, x25.*

Figure 19 is taken from 0.5 cm caudal to the lesioned level seen in Figure 13. Inflammatory reaction, necrosis and extensive neuron loss were found on both sides, especially on the side of injection. The central canal was a little enlarged (Figure 19A). Numerous ED1-positive macrophages on both sides were linked by a track of macrophages in the gray commissure around the central canal (Figure 19B).

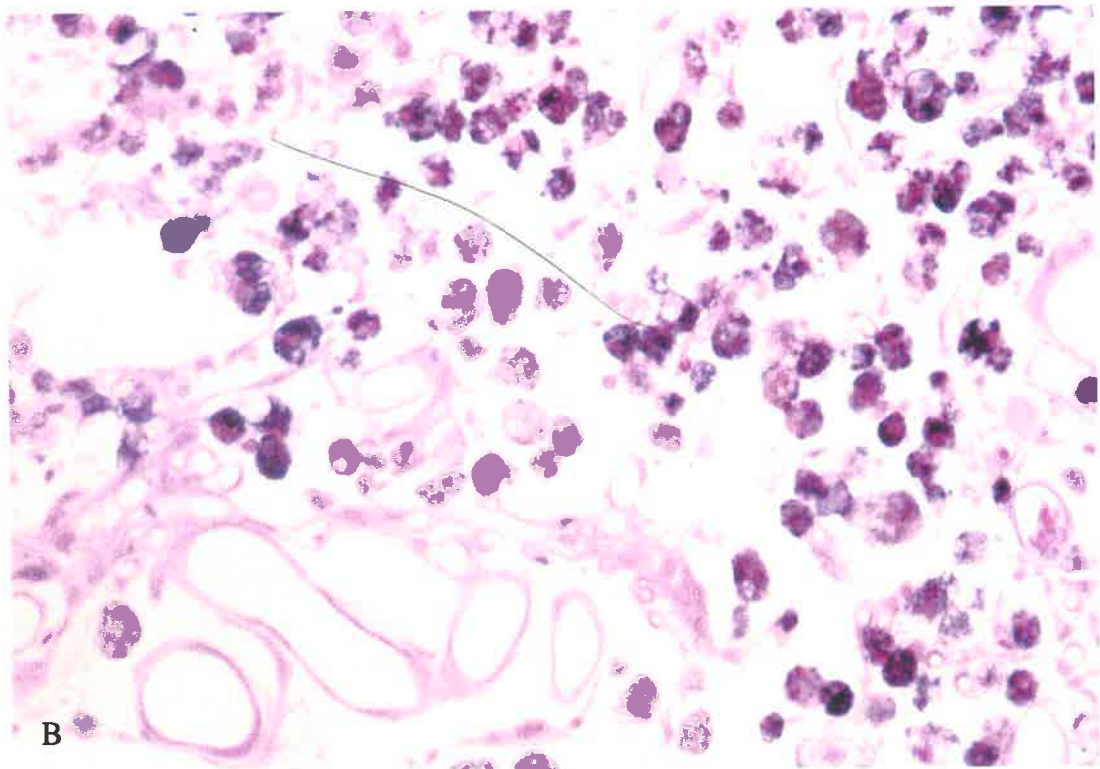
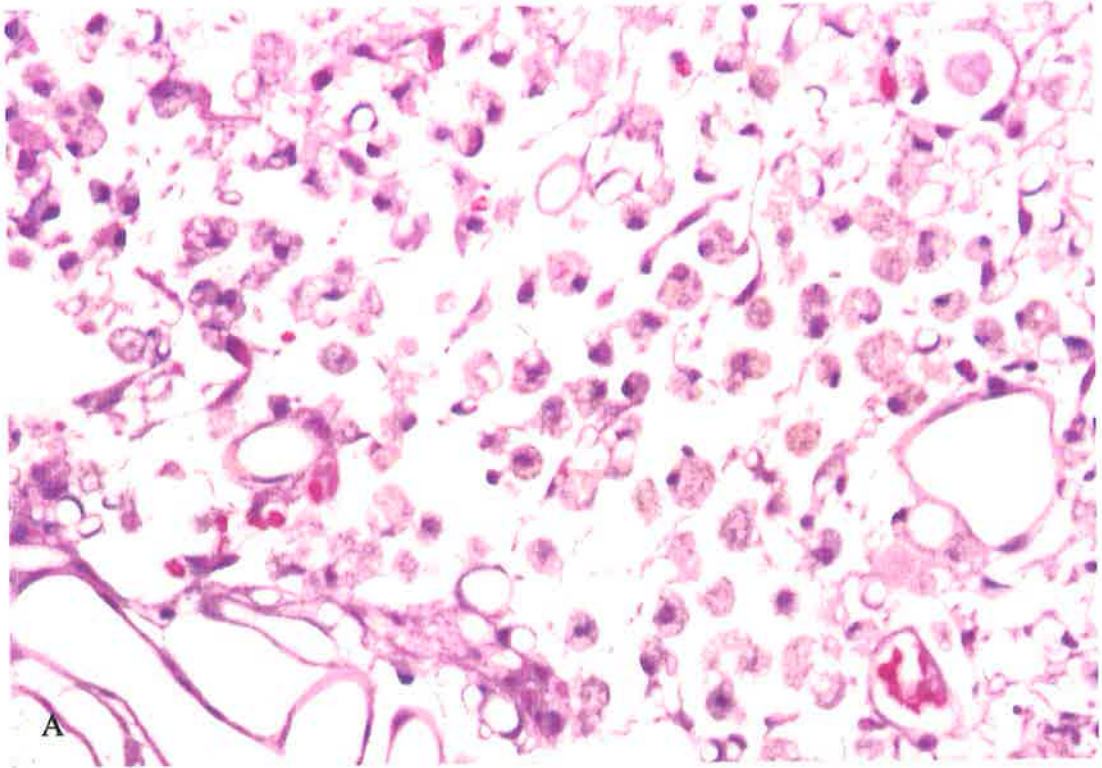
High-power views of the same slides as in Figure 19 demonstrated numerous ED1-positive foamy macrophages and some blood vessels in the necrotic region (Figure 20).

Figure 21 is taken from 0.8 cm caudal to the lesioned level seen in Figure 13. There were bilateral inflammatory responses and neuron loss in the parenchyma (Figure 21A). In the transverse section stained for macrophages at the same level as in Figure 21A, there were numerous ED1-positive macrophages in the gray matter on both sides, linked by a track of macrophages in the gray commissure around the central canal (Figure 21B).

The summary of injection parameters, survival time and pathological findings in six groups of rats are shown in Table 5. The sizes of the cysts shown in Table 5 are the biggest. The longitudinal extent and size of cavities are generally related to injection concentration and to duration of survival though there is variability in the size and extent of spinal cavities with the same different injection concentration and at the same survival times.



**Figure 19.** *Photomicrographs of the transverse section at the level 0.5 cm caudal to the lesioned level seen in Figure 13. A: Bilateral inflammatory responses. H&E, x10. B: Numerous ED1-positive macrophages in the gray matter. Macrophage, x10.*



**Figure 20.** High-power view of same slides as in Figure 19. A: Foamy macrophages and blood vessels in the necrotic region. H&E, x100. B: ED1-positive macrophages. Macrophages, x100.

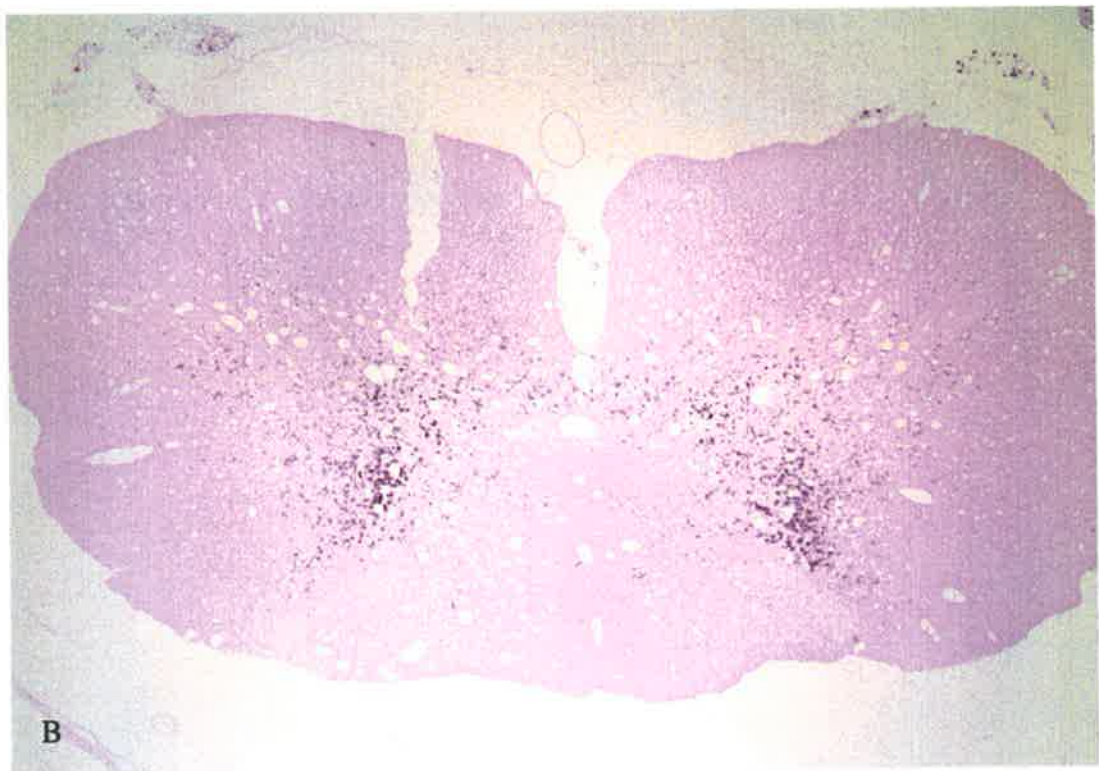
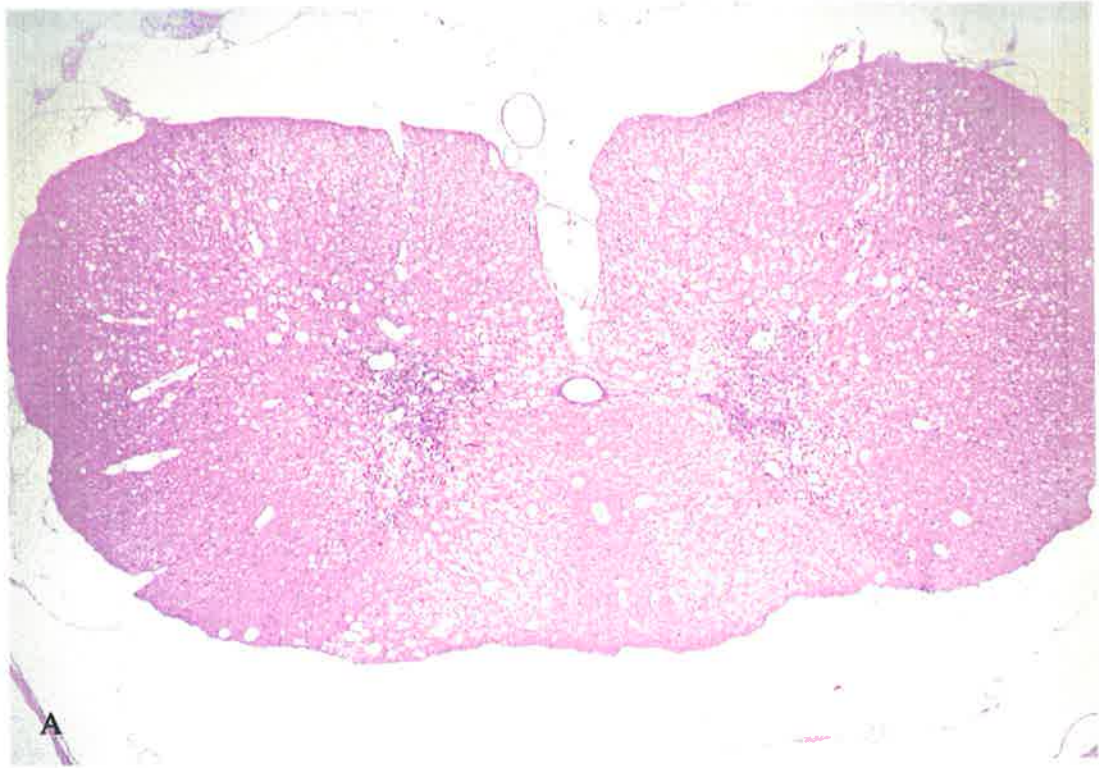


**Figure 21.** *Photomicrographs of transverse sections at the level 0.8 cm caudal to the lesioned level seen in Figure 13. A: Bilateral inflammatory responses and neuron loss. H&E, x10. B: Numerous ED1-positive macrophages. Macrophage, x10.*

**Table 5.** *Injection parameters, survival time, and pathological findings in six groups of experimental rats.*

Group	Injection	Animal #	Survival	Extent and size of the cysts (mm)
A	-	1	-	-
B	Normal saline & Evans Blue	2-4	4 weeks	-
C	Kaolin	5-9	4 weeks	-
D	8.3 mM QA (1.6 mg/ml)	10	1 week	None
		11	2 weeks	0.30 & 0.5
		12	2 weeks	0.30 & 0.6
		13	2 weeks	0.30 & 0.5
		14	2 weeks	None
		15	3 weeks	0.30 & 0.4
		16	3 weeks	0.45 & 0.7
		17	3 weeks	0.30 & 0.5
		18	4 weeks	0.30 & 0.4
		19	4 weeks	0.30 & 0.5
E	23.7 mg/ml QA	20	1 week	3.00 & 1.0
		21	2 weeks	3.30 & 1.0
		22	2 weeks	3.00 & 1.0
		23	3 weeks	3.00 & 0.9
		24	3 weeks	None
		25	3 weeks	2.70 & 0.8
		26	3 weeks	3.60 & 0.9
		27	3 weeks	3.00 & 1.0
		28	4 weeks	3.00 & 1.0
		F	23.7 mg/ml QA & Kaolin	29
30	2 weeks			8.70 & 0.9
31	2 weeks			9.00 & 1.0
32	2 weeks			9.30 & 1.0
33	2 weeks			None
34	3 weeks			10.20 & 1.0
35	3 weeks			10.50 & 1.2
36	3 weeks			10.35 & 0.9
37	3 weeks			9.90 & 1.1
38	3 weeks			9.60 & 1.0
39	4 weeks			None

## DISCUSSION

### 1. QA as a tool in a rat model for traumatic SCI

QA is a potent agonist of multiple EAA receptors and can be used as a tool in the rat model of traumatic spinal cord injury to reproduce in rats many of the pathological and clinical features of traumatic SCI.

The pathological findings in this animal model parallel the sequelae of human traumatic SCI. Direct intraspinal microinjection of nanomole amounts of QA resulted in fluid-filled cysts or cystic spaces and neuronal loss (Figure 11, 12 and 13). Correspondingly, cavities in human SCI are present in a substantial glial fiber network with intense astrocytic fibrous gliosis that replaces the damaged nerve fibers and neuron cell bodies.<sup>197</sup> GFAP-positive hypertrophic astrocytes embedded in a dense network of GFAP stained fibers were also observed in these experiments (Figure 11, 14 and 15). Immunoperoxidase staining for GFAP was used to investigate this astrocytic response. GFAP is an intermediate filament protein specifically localized in astrocytes. GFAP has a molecular weight of 47,000 and antibodies to this protein localize specifically in astrocytes. Other glial cells and neurons are unstained.<sup>191</sup>

Inflammatory mononuclear response and consolidated necrosis in the gray matter infiltrated with ED-1 immuno-stained large foamy macrophages was also seen in this animal model (Figure 19, 20 and 21), corresponding to the most striking pathological change in human SCI: the accumulation of large foamy macrophages in response to necrosis of nerve fibers and neurons.<sup>197</sup> ED1, a rat macrophage marker, was used to elucidate the inflammatory response. ED1 monoclonal antibody recognizes a cytoplasmic antigen in rat macrophages and cells of the mononuclear phagocyte system.<sup>193</sup> High concentration QA caused a

bilateral inflammatory response which may be related to spread of QA from the injection site via the gray commissure around the central canal. This assumption is supported by the track of macrophages in the gray commissure shown in Figure 19 and 21.

Unexpectedly, only sparse APP accumulation was observed in the tissue in this animal model. This most likely results from the severe damage to neurone cell bodies caused by QA, resulting in rapid neuronal death and disintegration of axonic material.  $\beta$ -APP, transported by fast axoplasmic flow, is an integral transmembrane nerve cell surface glycoprotein originating from a gene on chromosome 21.<sup>194</sup>  $\beta$ -APP can be used as a marker of axonal injury because inhibition of axoplasmic flow in damaged axons leads to accumulation of  $\beta$ -APP in the axon.<sup>195,196</sup> Accumulation of APP follows sublethal-injury to the neurons but cell death results in cessation of axoplasmic flow and therefore no further buildup of APP.

Intraspinal injection of low concentration QA (8.3 mM) produced a single small cyst, local inflammatory response and unilateral neuron loss (Figure 11), while high concentration QA (23.7 mg/ml) resulted in a large cysts, extensive inflammatory response and bilateral neuron loss in the transverse spinal cord sections (Figure 12). These findings demonstrate the marked effect of QA concentration on the extent of neuron loss and the size of the cyst in the spinal cord. Furthermore, at the site of cavitation there was increased staining for GFAP and large numbers of macrophages, which are consistent with the possible mechanism of initial cyst formation in excitotoxic injury described in section 1.7.3.3. These experiments also confirmed the neurotoxicity of QA. Additionally, the areas of necrosis involved both gray and white matter. This contradicts the

traditional concept that excitotoxic injury usually induces selective neuronal necrosis, but a recent study has shown glutamate receptors in the two major glial cell types (astrocytes and oligodendrocytes) and activated glutamate receptors in glial cells during neuronal activity.<sup>198</sup> The combined effect on neuron and glia may explain why a cyst forms rather than an area of gliosis following spinal injections of QA. Another possibility would be trauma produced by the injection needle, however control animals injected with saline and Evans blue showed small areas of necrosis but did not develop cysts.

Except for these pathological changes, a noteworthy clinical feature of this excitotoxic model was the absence of permanent motor deficits in QA-injected rats with massive neuronal loss in the spinal cord, which was similar to those described in many cases of traumatic SCI. Preservation of function despite profound neuronal loss is often observed in many patients with traumatic SCI and those suffering posttraumatic syringomyelia. The question is raised: how is function preserved despite massive neuronal loss? This is conventionally explained by the location of many syrinxes in the gray matter.<sup>19</sup> Because the syrinx usually begins as an intramedullary cavity within the gray matter at the base of the posterior column, the first fibers to be affected are those subserving pain and temperature as they cross from the dorsal horn to the contralateral side of the cord via the anterior white commissure.<sup>19</sup> Therefore, these syrinxes do not directly affect motoneurons or ascending and descending tracts, at least in the early stage. Recently, Goldstein et al.<sup>19</sup> added the explanation that as interneurons became necrotic over time, spared descending motor axons changed their usual pathways through the interneurons and connected with denervated motoneurons in new ways. The significant axonal sprouting of descending pathways and

synaptogenesis may be implicated in these changes. This hypothesis is supported by the recent findings in animals that new neuronal circuitry can be formed to replace that which is lost within the adult animal central nervous system following trauma.<sup>19</sup>

Close simulation of the pathological changes described following traumatic SCI and the pathogenesis of cavities in the clinical condition of posttraumatic syringomyelia in this excitotoxic (QA) model suggests that QA can produce syrinxes, which are comparable to human posttraumatic syrinxes.

The fluid-filled cysts or cystic spaces produced by QA without kaolin are simple and nonexpansible, corresponding to the small fluid-filled cysts that are common after traumatic SCI in the human. On MRI almost 50% of injured spinal cords have one or several small cysts that can be called the primary cyst.<sup>199</sup>

Primary cysts occur in a proportion of cases following traumatic SCI. The “primary cyst” at the injury site, which usually does not extend more than one vertebra beyond the level of the injury and does not require surgical treatment, is distinct from true posttraumatic syringomyelia that extends over more than two segments. The primary cyst represents established spinal cord damage resulting from traumatic injury, which can be simulated by the intraspinal QA injection in the animal model. The occurrence of posttraumatic syringomyelia in patients with primary cysts is significantly correlated with spinal subarachnoid block and the resulting alteration of CSF flow.<sup>200</sup>

## **2. The role of subarachnoid block in posttraumatic syringomyelia**

To study the effect of subarachnoid block resulting from arachnoiditis, subarachnoid injection of kaolin was performed to produce inflammation in the

subarachnoid space in Group B and E. It was found that the combination of subarachnoid kaolin and intraspinal QA injection (Group E) produced multiple cavities (Figure 13) that were much larger and more extensive than those found in rats injected with QA alone. This suggests that enlargement of syrinxes is enhanced by the block of the subarachnoid space (arachnoiditis) and the ideal excitotoxic model of posttraumatic syringomyelia in the rat was achieved in Group E. Additionally, subarachnoid kaolin injection alone (Group B) did not produce a syrinx in the parenchyma and did not cause enlargement of the central canal even though blockage of the subarachnoid space was achieved (Figure 10), demonstrating that subarachnoid block is a necessary but not sufficient cause of large and expansible cavitation in the spinal cord. The results of Group B and E are consistent with the report of Cho<sup>45</sup> that there was a tendency for the combined mechanical trauma/kaolin injection group to be more prone to develop a syrinx and there was no spinal cavitation in the kaolin injection alone group.

This study demonstrated that alteration of CSF flow may be an important mechanism leading to the enlargement of the syrinx. The correlation between the spinal subarachnoid block and the development of a syrinx supports the pathogenic theory of Williams<sup>106</sup> (theory of 'slosh' and 'suck'). The primary cyst is believed to result from liquefaction of hematomyelia, myelomalacic necrosis, or drastic release of EAAs. The secondary enlargement of the cavity occurs as a consequence of the intracordal fluid movement due to an increase in epidural venous pressure. It has been reported that CSF tracks along the perivascular spaces to gain access to the center of the cord.<sup>44</sup> Every time a Valsalva maneuver takes place (for example, coughing or lifting), the intrathoracic and intraabdominal pressure is transmitted inside the spinal subarachnoid space via the

valveless venous plexus around the vertebral bodies. When compressed in the spine, the CSF has nowhere else to go but the head. Normally the pressures are readily equalized by movement of the CSF up into the head followed by return to the normal resting distribution of that fluid. In the presence of a subarachnoid block, fluid can be forced upward or downward past the block, which results in a collapsed syrinx above or below the block and a suction effect that promotes entry of CSF into the syrinx cavity. This is the “suck” mechanism (Figure 35).<sup>106</sup> Syrinx fluid may move in preference to the CSF in the subarachnoid space because the CSF fluid finds some resistance from the arachnoid strands, dentate ligaments, the vessels, and the nerve roots that connect the cord to the dura. The pressure involved in a cough often exceeds 100 mmHg so that the movement of the syrinx fluid can be violent enough to extend the cavity both rostrally and caudally. Such movement of syrinx fluid is called “slosh” (Figure 22).<sup>106</sup>

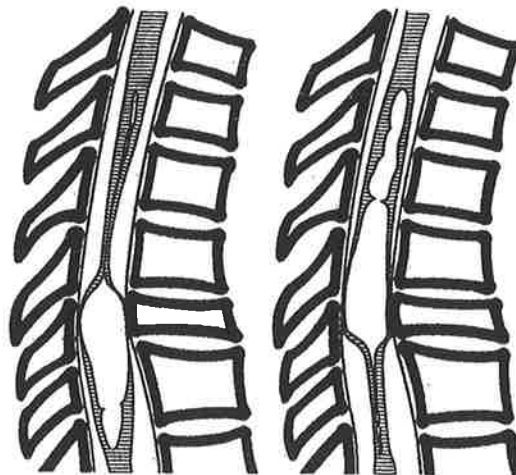


**Figure 22.** A diagram showing the mechanisms of “slosh” and “suck”. The upper part might be collapsed on the down phase as shown on the left and the lower part of the syrinx might be compressed on the phase of sloshing as shown on the right. (Adapted from Williams B: Posttraumatic syringomyelia, in Vinken PJ, Bruyn GW and Klawans HL: Handbook of clinical neurology, Amsterdam, North-Holland: 375-396, 1992.)



Although the hypothesis described above is not universally accepted as yet, it can well explain the results in this study. Certainly in rats with arachnoiditis induced by kaolin much larger syrinxes occur than in those with normal CSF flow. The subarachnoid blockage and the resulting alteration of CSF flow may be an essential prerequisite for the occurrence of syrinx in posttraumatic syringomyelia. Reports of neurological deterioration in patients after weightlifting exercise, straining, coughing or lithotripsy support this theory. The experimental study of Cho<sup>45</sup> on rabbits also confirms the critical role of subarachnoid blockage in the pathogenesis of syrinxes. Moreover, it has been reported in several clinical studies<sup>199,200</sup> that the surgical technique of subarachnoid space reconstruction and augmentation, which corrected the “suck” and “slosh” mechanism, produced radiological improvement or healing of the syrinx in 88% of the patients so treated. However, some patients with completely healed syrinxes continued to deteriorate clinically because of the irreversible pathological changes of progressive gliosis around the syrinx.<sup>199</sup> Therefore, early surgery to improve CSF flow should be considered in addition to techniques of cyst drainage.

### **3. Excitotoxic model for traumatic SCI**

Many animal models of syringomyelia produce a syrinx by dilation of the central canal (hydromyelia). This is not ideal for studying posttraumatic syringomyelia where the syrinx is usually located in the gray matter of the spinal cord. Although the weight drop method is the most widely used experimental model of posttraumatic syringomyelia, the overwhelming impact produces inconsistent results through varying combination of direct injury and ischemia or

hemorrhage from vascular injury. The photochemical method produces a cyst but it does not expand over time. Our excitotoxic model produces spinal cord cysts which are quite comparable to posttraumatic syrinxes. Moreover, it has been demonstrated that EAAs produce neuronal degeneration in a number of *in vivo* and *in vitro* studies<sup>81,201</sup> and neuronal degeneration is produced by dramatically increased EAAs in some pathological conditions, including traumatic spinal cord injury and ischemic spinal cord injury.<sup>52,71-73</sup> Furthermore, evidence for the involvement of EAAs in the pathological process following spinal cord injury has been provided by the reports of exacerbated damage to neurons in the injured cord following EAA administration and the neuroprotective effects of an EAA antagonist, following traumatic injury to the spinal cord.<sup>74,117,118</sup> Therefore, EAAs may have an important role in the production of human posttraumatic syringomyelia and are a logical choice for the development of an animal model.

#### **4. QA preparations and injection method**

QA, a potent agonist of multiple EAA receptors, was used in this animal model of posttraumatic syringomyelia due to its potent neurotoxicity and the involvement of EAAs in the secondary injury of posttraumatic syringomyelia.<sup>71</sup>

To determine the effects of QA concentration on the extent of neuron degeneration and the size of lesion, two different QA preparations were used in the experiments.<sup>81</sup> The low concentration (8.3 mM) QA solution was created by dissolving 1 mg QA powder with 0.537 ml of sterile normal saline and 0.1 ml sterile Evans Blue at 21°C. The high concentration (125 mM) QA solution used by Yeziarski et al.<sup>81</sup> could not be reproduced because it exceeded the solubility of QA. To allow injection of high-concentration QA into the spinal cord, 5mg QA

crystals were suspended in 0.170 ml of sterile normal saline and 0.041 sterile Evans Blue by sonication to produce a 23.7 mg/ml QA suspension.

In this study, we noted a decline or loss in neurotoxicity of QA solution or suspension which had either been stored for more than one day at 4°C or repeatedly frozen and thawed. This was unexpected because QA is generally considered to be quite stable.<sup>134,202</sup> McGeer et al. reported a similar fall in neurotoxicity of KA solution, which is an analogue of QA.<sup>129</sup> We found that consistent results can be obtained with aliquots of a QA solution or suspension stored at -20°C and thawed immediately before use.

Several technical difficulties were encountered during the initial stages of this study. The Hamilton 30 gauge point style 4 needle with a short bevel was still not sharp enough to penetrate the pia easily even though it was sharpened under a microscope. By contrast, the Hamilton 30 gauge point style 4 needle with a long bevel could penetrate the pia easily, but it could not deliver QA into the dorsal horn exactly and would penetrate through the spinal cord when the needle opening was completely inserted into the cord. The problem was solved by using a sharp suture needle to produce a hole in the meninges and replacing the Hamilton 30 gauge point style 4 needle with a finer SGE needle without bevel to deliver QA accurately into the dorsal horn.

It was initially difficult to inject QA into the spinal cord without leakage into the subarachnoid space because it was impossible to tell if the colorless QA solution or suspension was leaking along the needle track. Evans blue was added and this not only made any leakage very obvious but also caused discoloration within the cord, confirming appropriate location of the injectate. The leakage of QA along the track of needle into the subarachnoid space during and after the QA

injection was avoided by injecting 2 µl of QA into the spinal cord over a period of 2 minutes, leaving the injection needle in place for another 1 minute after injection and using a finer SGE needle. Wrathall et al.<sup>51</sup> described injecting a total volume of 1.68 µl over a period of 8 minutes to avoid leakage. The continuous movement of the cord due to arterial pulsation and respiration increases the risk of unwanted cord damage if the needle is left in place for this long. No obvious leakage was observed with an injection period of 2 minutes followed by a delay of 1 minute before removing the needle. Control rats in Group B receiving saline injection by the same method did not show any noticeable changes except a mild inflammatory response (Figure 8 and 9). This method of QA delivery produced very consistent results.

## **5. Limitation of this project and future work**

The combination of intraspinal QA injection and subarachnoid kaolin injection in this study has been shown to produce a useful animal model for posttraumatic syringomyelia, refining our knowledge of the pathogenesis of posttraumatic syringomyelia. The implication of subarachnoid blockage and EAAs in posttraumatic syringomyelia may suggest new treatments or improvements in currently available therapies. This approach may offer a useful method to further study the etiology of spinal cavity formation and expansion.

In this study, however, the hypothesis that CSF tracks along the perivascular spaces to gain access to the syrinx in the cord lacks direct evidence. Methods of reduction of the cyst are relatively difficult to systematically examine in this animal model due to the small size of the rat. The utility of this small animal

model in predicting syrinx formation and extension is limited by the inability to use MRI techniques because of the small size of the rat.

Further work using the CSF tracer HRP will provide information regarding the dynamics of CSF flow in both the presence and absence of subarachnoid block. Future studies will be necessary to determine if the cystic cavities enlarge after longer survival intervals. Additionally, further experiments will be performed in other species in an attempt to reproduce the results obtained in rats and to develop a larger animal model that allows trials of experimental therapies in animals and that facilitates noninvasive evaluation of the cyst volume. Sheep are suitable for this future study particularly as their cords are of similar dimension to the human.

## CONCLUSION

Inflammatory response, neuronal degeneration and spinal cavitation were observed following the intraspinal injection of the EAA receptor agonist QA. The combination of intrathecal kaolin and intraspinal injections of QA was shown to produce cavities that are much larger than those found in animals injected with QA alone. We believe the primary cyst was formed at the site of neuronal death due to QA. CSF then flowed from the subarachnoid space into the primary cyst. When the subarachnoid space was blocked by arachnoiditis, CSF tracking through the cord expanded the primary cyst producing a condition mimicking human posttraumatic syringomyelia. This excitotoxic model of posttraumatic syringomyelia in the rat may offer a useful method to study the etiology of spinal cavitation and cavity expansion.

The results of this study also support the proposal that in posttraumatic spinal cord injury, excitotoxic cell death occurring secondary to elevated levels of EAAs contributes to the pathologic process leading to the formation of spinal cavities. Subarachnoid block by arachnoiditis is one of the pathogenic factors most responsible for initiating extension of the cavity.

## APPENDICES

### 1. Fixative and buffers

#### *4% Paraformaldehyde in 0.1 M phosphate buffer (pH 7.4)*

To make 5 L of fixative:

##### Solution 1

- Dissolve 200 g paraformaldehyde in 2500 ml distilled H<sub>2</sub>O. Heat to 60° and stir.
- Add 1 mol/L NaOH by drops until clear.
- Filter.

##### Solution 2

- Dissolve 0.19 mole (26.20 g) of NaH<sub>2</sub>PO<sub>4</sub> in 2500 ml distilled H<sub>2</sub>O.
- Add 0.807 mole (114.56 g) of Na<sub>2</sub>HPO<sub>4</sub>.

Combine Solution 1 and Solution 2.

Cool down overnight.

Check pH and adjust pH to 7.4 with 5 M NaOH.

#### *Tris buffer 0.05 M, pH 7.45*

To make 1 L of buffer:

- Dissolve 6.06 g Tris in 1 L distilled H<sub>2</sub>O.
- Add 8.77 g NaCl.
- Adjust pH to 7.45
- Allow at least 10 minutes to fully dissolve and equilibrate, recheck pH.

#### *Citric acid buffer 0.05 M, pH 6.0*

To make 5 L of buffer:

- Dissolve 10.5 g citric acid monohydrate in 5 L distilled water.
- Adjust pH to 6.0.

#### *PBS 0.01 M, pH 7.45*

To make 20 L of buffer:

- Dissolve 1052 g NaCl into 3250 ml distilled water.
- Add 165.6 g NaH<sub>2</sub>PO<sub>4</sub>·H<sub>2</sub>O.
- Adjust pH to 6.33.
- Allow 2-3 minutes to ensure electrode stability, recheck pH of the stock solution.
- Dilute 660 ml of stock solution to 20 L with distilled water.

- Sample 200 ml, check pH and adjust pH to 7.45 using 5 M NaOH.
- Adjust the 20 L buffer by adding 100 times of the NaOH added to 200 ml sample.

***Ni DAB chromogen-substrate buffer 0.05 M, pH 7.45***

To make 50 ml of buffer:

- Thaw 1 ml DAB and dilute it in 50 ml Tris buffer.
- Add 500 µl of 4% NiCl<sub>2</sub>.
- Adjust pH to 7.45.
- Filter and add 50 µl of 30% hydrogen peroxide.

**2. Immunohistochemical techniques**

***GFAP immunostaining***

1. Rehydrate
  - Wash in 3 changes × 5 minutes of 100% xylene.
  - Wash in 2 changes × 3 minutes of 100% alcohol.
  - Wash in 2 changes × 3 minutes of 95% alcohol.
  - Wash in 2 changes × 2 minutes of 0.01 M PBS.
2. Block endogenous peroxidase
  - Remove an unblocked control slide to fresh 0.01 M PBS.
  - Incubate slides in 3% H<sub>2</sub>O<sub>2</sub> in PBS for 5 minutes.
  - Rinse slides in PBS.
  - Wash in 2 changes × 5 minutes of 0.01 M PBS.
  - Remove a blocked control slide to PBS with unblocked one. Store in 4 °C.
3. Autoclave
  - Slides in citric acid buffer are incubated in the autoclave for 10 minutes (134 °C, 32 psi)
  - Remove to air and cool down to 50 °C.
  - Rinse slides in 0.01 M PBS.
  - Wash in 2 changes × 5 minutes of 0.01 M PBS.
4. Make 15% NHS/PBS, pH7.45.
  - Add 5 ml NHS to 25 ml PBS.
  - Adjust pH to 7.45.
5. Add 15% NHS/PBS; incubate for 20 minutes.
6. Incubated at 4 °C overnight with the primary rabbit anti-cow polyclonal antibody, diluted in 1:1500.
7. Defrost for 2 hours at room temperature.
8. Rinse in PBS individually.
9. Wash in 2 changes × 5 minutes of 0.01 M PBS.

10. Add 1:300 dilution of the swine anti-rabbit biotinylated secondary polyclonal antibody for 1 hour.
11. Rinse in PBS individually.
12. Wash in 2 changes  $\times$  5 minutes of 0.01 M PBS.
13. Add 1:500 dilution of HRP-labelled streptavidin; incubate for 2 hours.
14. Rinse in PBS individually.
15. Wash in 2 changes  $\times$  5 minutes of 0.01 M PBS.
16. Put back the unblocked and blocked control slides.
17. Add Ni DAB; incubate for 10 minutes.
18. Rinse in PBS individually.
19. Wash in 2 changes  $\times$  5 minutes of 0.01 M PBS.
20. Counterstain using eosin for 30 seconds.
21. Rinse in PBS.
22. Wash in 90% alcohol for 1 minute.
23. Wash in 100% alcohol for 1 minute.
24. Wash in 100% xylene for 2 minutes, two times.
25. Coverslip.

### ***ED1 immunostaining***

1. Rehydrate
  - Wash in 3 changes  $\times$  5 minutes of 100% xylene.
  - Wash in 2 changes  $\times$  3 minutes of 100% alcohol.
  - Wash in 2 changes  $\times$  3 minutes of 95% alcohol.
  - Wash in 2 changes  $\times$  2 minutes of 0.01 M PBS.
2. Block endogenous peroxidase
  - Remove an unblocked control slide to fresh 0.01 M PBS.
  - Incubate slides in 3% H<sub>2</sub>O<sub>2</sub> in PBS for 5 minutes.
  - Rinse slides in PBS.
  - Wash in 2 changes  $\times$  5 minutes of 0.01 M PBS.
  - Remove a blocked control slide to PBS with unblocked one. Store in 4 °C.
3. Make 15% NHS/PBS, pH7.45.
  - Add 5 ml NHS to 25 ml PBS.
  - Adjust pH to 7.45.
4. Add 15% NHS/PBS; incubate for 20 minutes.
5. Incubated with the mouse anti-rat primary ED1 monoclonal antibody, diluted in 1:400.
6. Rinse in PBS individually.
7. Wash in 2 changes  $\times$  5 minutes of 0.01 M PBS.
8. Incubated with a 1:20 dilution of sheep anti-mouse secondary antibody linked with peroxidase for 1 hour.
9. Rinse in PBS individually.
10. Wash in 2 changes  $\times$  5 minutes of 0.01 M PBS.
11. Add Ni DAB; incubate for 10 minutes.
12. Rinse in PBS individually.
13. Wash in 2 changes  $\times$  5 minutes of 0.01 M PBS.

14. Counterstain using eosin for 30 seconds.
15. Rinse in PBS.
16. Wash in 90% alcohol for 1 minute.
17. Wash in 100% alcohol for 1 minute.
18. Wash in 100% xylene for 2 minutes, two times.
19. Coverslip.

### ***β-APP immunostaining***

1. Rehydrate
  - Wash in 3 changes × 5 minutes of 100% xylene.
  - Wash in 2 changes × 3 minutes of 100% alcohol.
  - Wash in 2 changes × 3 minutes of 95% alcohol.
  - Wash in 2 changes × 2 minutes of 0.01 M PBS.
2. Block endogenous peroxidase
  - Remove an unblocked control slide to fresh 0.01 M PBS.
  - Incubate slides in 3% H<sub>2</sub>O<sub>2</sub> in PBS for 5 minutes.
  - Rinse slides in PBS.
  - Wash in 2 changes × 5 minutes of 0.01 M PBS.
  - Remove a blocked control slide to PBS with unblocked one. Store in 4 °C.
3. Autoclave
  - Slides in citric acid buffer are incubated in the autoclave for 10 minutes (134 °C, 32 psi)
  - Remove to air and cool down to 50 °C.
  - Rinse slides in 0.01 M PBS.
  - Wash in 2 changes × 5 minutes of 0.01 M PBS.
4. Make 15% NHS/PBS, pH7.45.
  - Add 5 ml NHS to 25 ml PBS.
  - Adjust pH to 7.45.
5. Add 15% NHS/PBS; incubate for 20 minutes.
6. Incubated at 4 °C overnight with the primary anti-APP monoclonal antibody, diluted in 1:10000.
7. Defrost for 2 hours at room temperature.
8. Rinse in PBS individually.
9. Wash in 2 changes × 5 minutes of 0.01 M PBS.
10. Add 1:200 dilution of the rabbit anti-mouse biotinylated secondary antibody for 1 hour.
11. Rinse in PBS individually.
12. Wash in 2 changes × 5 minutes of 0.01 M PBS.
13. Add 1:500 dilution of streptavidin/HRP; incubate for 2 hours.
14. Rinse in PBS individually.
15. Wash in 2 changes × 5 minutes of 0.01 M PBS.
16. Put back the unblocked and blocked control slides.

17. Add Ni DAB; incubate for 10 minutes.
18. Rinse in PBS individually.
19. Wash in 2 changes  $\times$  5 minutes of 0.01 M PBS.
20. Counterstain using eosin for 30 seconds.
21. Rinse in PBS.
22. Wash in 90% alcohol for 1 minute.
23. Wash in 100% alcohol for 1 minute.
24. Wash in 100% xylene for 2 minutes, two times.
25. Coverslip.

## REFERENCE

1. Wilson SAK. Syringomyelia: syringobulbia. In: Bruce AN, ed. *Neurology*, Baltimore: Williams & Wilkins, 1955: 1187-1202.
2. Simpson JA, Weiner ESC, eds. *The Oxford English Dictionary*, 2nd ed. Oxford: Clarendon Press, 1989:
3. Milhorat TH, Capocelli AL, Jr., Anzil AP, Kotzen RM, Milhorat RH. Pathological basis of spinal cord cavitation in syringomyelia: analysis of 105 autopsy cases. *J Neurosurg* 1995; **82**: 802-812.
4. Small JA, Sheridan PH. Research priorities for syringomyelia: a National Institute of Neurological Disorders and Stroke workshop summary. *Neurology* 1996; **46**: 577-582.
5. Barnett HJ. The epilogue. In: Barnett HJM, Foster JB, Hudgson P, eds. *Syringomyelia*, London: W.B.Saunders, 1973: 302-313.
6. Finlayson AI. Syringomyelia and related conditions. In: Joynt RJ, ed. *Clinical Neurology*, Philadelphia: J.B. Lippincott Co. 1989: 1-17.
7. Foster JB, Hodgson P. Historical introduction. In: Barnett HJM, Foster JB, Hudgson P, eds. *Syringomyelia*, London: W.B.Saunders, 1973: 3-10.
8. Madsen PW, Yeziarski RP, Holets VR. Syringomyelia: clinical observations and experimental studies. *J Neurotrauma* 1994; **11**: 241-254.
9. Ballantine HT, Ojemann RG, Drew JH. Syringomyelia. In: Kraybuhl H, Maspes PE, Sweet WH, eds. *Progress in Neurological Surgery*, New York: S.Karger, 1971: 227-245.
10. Schurch B, Wichmann W, Rossier AB. Post-traumatic syringomyelia (cystic myelopathy): a prospective study of 449 patients with spinal cord injury. *J Neurol Neurosurg Psychiatry* 1996; **60**: 61-67.
11. Nurick S, Russell JA, Deck MD. Cystic degeneration of the spinal cord following spinal cord injury. *Brain* 1970; **93**: 211-222.
12. Barnett HJ, Botterell EH, Jousse AT, Wynn Jones M. Progressive myelopathy as a sequel to traumatic paraplegia. *Brain* 1966; **89**: 159-174.
13. Freeman LW. Ascending spinal paralysis. *Journal of Neurosurgery* 1959; **16**: 120-122.
14. Rossier AB, Werner A, Wildi E, Berney J. Contribution to the study of late cervical syringomyelic syndromes after dorsal or lumbar traumatic paraplegia. *J Neurol Neurosurg Psychiatry* 1968; **31**: 99-105.

15. Donauer E, Rascher K. Syringomyelia: a brief review of ontogenetic, experimental and clinical aspects. **Neurosurg Rev** 1993; **16**: 7-13.
16. Moriwaka F, Tashiro K, Tachibana S. Epidemiology of syringomyelia in Japan--the nationwide survey. **Rinsho Shinkeigaku** 1995; **35**: 1395-1397
17. Noguez MA. Syringomyelia and syringobulbia. In: Vinken PJ, Bruyn GW, Klawans HL, eds. *Handbook of Clinical Neurology*, 6th ed. Amsterdam: North-Holland, 1987: 443-464.
18. Foster JB. Neurology of syringomyelia. In: Batzdorf U, ed. *Syringomyelia: Current Concepts in Diagnosis and Treatment*. Baltimore: Williams and Wilkins, 1991: 91-115.
19. Goldstein B, Hammond MC, Stiens SA, Little JW. Posttraumatic syringomyelia: profound neuronal loss, yet preserved function. **Arch Phys Med Rehabil** 1998; **79**: 107-112.
20. Squier MV, Lehr RP. Post-traumatic syringomyelia [see comments]. **J Neurol Neurosurg Psychiatry** 1994; **57**: 1095-1098.
21. Wozniewicz B, Filipowicz K, Swiderska SK, Deraka K. Pathophysiological mechanism of traumatic cavitation of the spinal cord. **Paraplegia** 1983; **21**: 312-317.
22. Tator CH, Fehlings MG. Review of the secondary injury theory of acute spinal cord trauma with emphasis on vascular mechanisms [see comments]. **J Neurosurg** 1991; **75**: 15-26.
23. Quencer RM, Green BA, Eismont FJ. Posttraumatic spinal cord cysts: clinical features and characterization with metrizamide computed tomography. **Radiology** 1983; **146**: 415-423.
24. Barnett HJM, Botterell EH, Jousse AT. Progressive myelopathy as a sequel to traumatic paraplegia. **Brain** 1966; **89**: 159-174.
25. Reddy KK, Del Bigio MR, Sutherland GR. Ultrastructure of the human posttraumatic syrinx. **J Neurosurg** 1989; **71**: 239-243.
26. McLean DR, Miller JD, Allen PB, Ezzeddin SA. Posttraumatic syringomyelia. **J Neurosurg** 1973; **39**: 485-492.
27. Siddall P, Xu CL, Cousins M. Allodynia following traumatic spinal cord injury in the rat. **Neuroreport** 1995; **6**: 1241-1244.
28. Milhorat TH, Mu HT, LaMotte CC, Milhorat AT. Distribution of substance P in the spinal cord of patients with syringomyelia. **J Neurosurg** 1996; **84**: 992-998.

29. Barnett HJM. Syringomyelia associated with spinal arachnoiditis. In: Barnett HJM, Foster JB, Hudgson P, eds. Syringomyelia, London: W.B.Saunders, 1973: 220-244.
30. Bunge RP, Puckett WR, Becerra JL, Marcillo A, Quencer RM. Observations on the pathology of human spinal cord injury. A review and classification of 22 new cases with details from a case of chronic cord compression with extensive focal demyelination. *Adv Neurol* 1993; **59**: 75-89.
31. Conway LW. Hydrodynamic studies in syringomyelia. *J Neurosurg* 1967; **27**: 501-514.
32. Batzdorf U. Syringomyelia related to abnormalities at the level of the craniovertebral junction. In: Batzdorf U, ed. Syringomyelia: Current Concepts in Diagnosis and Treatment, Baltimore: Williams and Wilkins, 1991: 163-182.
33. Churchill's Medical Dictionary, New York: Churchill Livingstone Inc. 1989: 1846
34. Gardner WJ, Abdullah AF, McCormack LJ. The varying expressions of embryonal atresia of the fourth ventricle in adults: Arnold-Chiari malformation, Dandy-Walker syndrome, "arachnoid" cyst of the cerebellum, and syringomyelia. *Journal of Neurosurgery* 1957; 591-607.
35. Gardner WJ. Hydrodynamic mechanism of syringomyelia: its relationship to myelocoele. *J Neurol Neurosurg Psychiat* 1965; **28**: 247-258.
36. Hall PV, Muller J, Campbell RL. Experimental hydrosyringomyelia, ischemic myelopathy, and syringomyelia. *J Neurosurg* 1975; **43**: 464-470.
37. Yamada H, Yokota A, Haratake J, Horie A. Morphological study of experimental syringomyelia with kaolin-induced hydrocephalus in a canine model. *J Neurosurg* 1996; **84**: 999-1005.
38. Ghanem IB, Londono C, Delalande O, Dubousset JF. Chiari I malformation associated with syringomyelia and scoliosis. *Spine* 1997; **22**: 1313-1317.
39. Morioka T, Shono T, Nishio S, Yoshida K, Hasuo K, Fukui M. Acquired Chiari I malformation and syringomyelia associated with bilateral chronic subdural hematoma. Case report [see comments]. *J Neurosurg* 1995; **83**: 556-558.
40. Milhorat TH, Miller JI, Johnson WD, Adler DE, Heger IM. Anatomical basis of syringomyelia occurring with hindbrain lesions. *Neurosurgery* 1993; **32**: 748-754.
41. Siddiqi SN, Fehlings MG. Lhermitte-Duclos disease mimicking adult-onset aqueductal stenosis. Case report. *J Neurosurg* 1994; **80**: 1095-1098.

42. McLaurin RL, Bailey OT, Schurr PH, Ingraham FD. Myelomalacia and multiple cavitations of spinal cord secondary to adhesive arachnoiditis. **Arch Pathol** 1954; 138-146.
43. Williams B, Bentley J. Experimental communicating syringomyelia in dogs after cisternal kaolin injection: Part 1. Morphology. **J Neurol Sci** 1980; 93-107.
44. Ball MJ, Dayan AD. Pathogenesis of syringomyelia. **Lancet** 1972; 2: 799-801.
45. Cho KH, Iwasaki Y, Imamura H, Hida K, Abe H. Experimental model of posttraumatic syringomyelia: the role of adhesive arachnoiditis in syrinx formation. **J Neurosurg** 1994; 80: 133-139.
46. Kao CC, Chang LW, Bloodworth JM, Jr. The mechanism of spinal cord cavitation following spinal cord transection. Part 2. Electron microscopic observations. **J Neurosurg** 1977; 46: 745-756.
47. Zhang Z, Krebs CJ, Guth L. Experimental analysis of progressive necrosis after spinal cord trauma in the rat: etiological role of the inflammatory response. **Exp Neurol** 1997; 143: 141-152.
48. Yeziarski RP, Liu S, Ruenes GL, Busto R, Dietrich WD. Neuronal damage following intraspinal injection of a nitric oxide synthase inhibitor in the rat. **J Cereb Blood Flow Metab** 1996; 16: 996-1004.
49. Stoodley MA, Brown SA, Brown CJ, Jones NR. Arterial pulsation-dependent perivascular cerebrospinal fluid flow into the central canal in the sheep spinal cord. **J Neurosurg** 1997; 86: 686-693.
50. Stoodley MA, Jones NR, Brown CJ. Evidence for rapid fluid flow from the subarachnoid space into the spinal cord central canal in the rat. **Brain Res** 1996; 707: 155-164.
51. Wrathall JR, Choiniere D, Teng YD. Dose-dependent reduction of tissue loss and functional impairment after spinal cord trauma with the AMPA/kainate antagonist NBQX. **J Neurosci** 1994; 14: 6598-6607.
52. Liu D, Thangnipon W, McAdoo DJ. Excitatory amino acids rise to toxic levels upon impact injury to the rat spinal cord. **Brain Res** 1991; 547: 344-348.
53. Bracken MB, Shepard MJ, Collins WF, Holford TR. A randomized controlled trial of methylprednisolone or naloxone in the treatment of acute spinal cord injury. **N Engl J Med** 1990; 1405-1411.

54. Demediuk P, Daly MP, Faden AI. Effect of impact trauma on neurotransmitter and nonneurotransmitter amino acids in rat spinal cord [published erratum appears in *J Neurochem* 1990 Feb;54(2):724-5]. *J Neurochem* 1989; **52**: 1529-1536.
55. Wrathall JR, Bouzoukis J, Choiniere D. Effect of kynurenate on functional deficits resulting from traumatic spinal cord injury. *Eur J Pharmacol* 1992; **218**: 273-281.
56. Faden AI. Recent pharmacological advances in experimental spinal injury: theoretical and methodological considerations. *TINS* 1983; **6**: 375-377.
57. Headley PM, Grillner S. Excitatory amino acids and synaptic transmission: the evidence for a physiological function. *Trends Pharmacol Sci* 1990; **11**: 205-211.
58. Nadler JV, Evenson DA, Cuthbertson GJ. Comparative toxicity of kainic acid and other acidic amino acids toward rat hippocampal neurons. *Neuroscience* 1981; **6**: 2505-2517.
59. Urca G, Urca R. Neurotoxic effects of excitatory amino acids in the mouse spinal cord: quisqualate and kainate but not N-methyl-D-aspartate induce permanent neural damage. *Brain Res* 1990; **529**: 7-15.
60. Globus MY, Busto R, Martinez E, Valdes I, Dietrich WD, Ginsberg MD. Comparative effect of transient global ischemia on extracellular levels of glutamate, glycine, and gamma-aminobutyric acid in vulnerable and nonvulnerable brain regions in the rat. *J Neurochem* 1991; **57**: 470-478.
61. Benveniste H, Drejer J, Schousboe A, Diemer NH. Elevation of the extracellular concentrations of glutamate and aspartate in rat hippocampus during transient cerebral ischemia monitored by intracerebral microdialysis. *J Neurochem* 1984; **43**: 1369-1374.
62. Globus MY, Busto R, Dietrich WD, Martinez E, Valdes I, Ginsberg MD. Effect of ischemia on the in vivo release of striatal dopamine, glutamate, and gamma-aminobutyric acid studied by intracerebral microdialysis. *J Neurochem* 1988; **51**: 1455-1464.
63. Hagberg H, Lehmann A, Sandberg M, Nystrom B, Jacobson I, Hamberger A. Ischemia-induced shift of inhibitory and excitatory amino acids from intra- to extracellular compartments. *J Cereb Blood Flow Metab* 1985; **5**: 413-419.
64. Korf J, Klein HC, Venema K, Postema F. Increases in striatal and hippocampal impedance and extracellular levels of amino acids by cardiac arrest in freely moving rats. *J Neurochem* 1988; **50**: 1087-1096.
65. Faden AI, Demediuk P, Panter SS, Vink R. The role of excitatory amino acids and NMDA receptors in traumatic brain injury. *Science* 1989; **244**: 798-800.

66. Simon RP, Swan JH, Griffiths T, Meldrum BS. Blockade of N-methyl-D-aspartate receptors may protect against ischemic damage in the brain. **Science** 1984; **226**: 850-852.
67. Sheardown MJ, Nielsen EO, Hansen AJ, Jacobsen P, Honore T. 2,3-Dihydroxy-6-nitro-7-sulfamoyl-benzo(F)quinoxaline: a neuroprotectant for cerebral ischemia. **Science** 1990; **247**: 571-574.
68. Meldrum B, Garthwaite J. Excitatory amino acid neurotoxicity and neurodegenerative disease. **Trends Pharmacol Sci** 1990; **11**: 379-387.
69. Hayes RL, Jenkins LW, Lyeth BG, et al. Pretreatment with phencyclidine, an N-methyl-D-aspartate antagonist, attenuates long-term behavioral deficits in the rat produced by traumatic brain injury. **J Neurotrauma** 1988; **5**: 259-274.
70. Garthwaite G, Hajos F, Garthwaite J. Ionic requirements for neurotoxic effects of excitatory amino acid analogues in rat cerebellar slices. **Neuroscience** 1986; **18**: 437-447.
71. Panter SS, Yum SW, Faden AI. Alteration in extracellular amino acids after traumatic spinal cord injury [see comments]. **Ann Neurol** 1990; **27**: 96-99.
72. Simpson RK, Jr., Robertson CS, Goodman JC. Spinal cord ischemia-induced elevation of amino acids: extracellular measurement with microdialysis. **Neurochem Res** 1990; **15**: 635-639.
73. Marsala M, Sorkin LS, Yaksh TL. Transient spinal ischemia in rat: characterization of spinal cord blood flow, extracellular amino acid release, and concurrent histopathological damage. **J Cereb Blood Flow Metab** 1994; **14**: 604-614.
74. Faden AI, Simon RP. A potential role for excitotoxins in the pathophysiology of spinal cord injury. **Ann Neurol** 1988; **23**: 623-626.
75. Faden AI, Lemke M, Simon RP, Noble LJ. N-methyl-D-aspartate antagonist MK801 improves outcome following traumatic spinal cord injury in rats: behavioral, anatomic, and neurochemical studies. **J Neurotrauma** 1988; **5**: 33-45.
76. Wrathall JR, Teng YD, Choiniere D, Mundt DJ. Evidence that local non-NMDA receptors contribute to functional deficits in contusive spinal cord injury. **Brain Res** 1992; **586**: 140-143.
77. Gomez Pinilla F, Tram H, Cotman CW, Nieto Sampedro M. Neuroprotective effect of MK-801 and U-50488H after contusive spinal cord injury. **Exp Neurol** 1989; **104**: 118-124.

78. Martinez Arizala A, Rigamonti DD, Long JB, Kraimer JM, Holaday JW. Effects of NMDA receptor antagonists following spinal ischemia in the rabbit. **Exp Neurol** 1990; **108**: 232-240.
79. Hao JX, Watson BD, Xu XJ, Wiesenfeld Hallin Z, Seiger A, Sundstrom E. Protective effect of the NMDA antagonist MK-801 on photochemically induced spinal lesions in the rat. **Exp Neurol** 1992; **118**: 143-152.
80. Nag S, Riopelle RJ. Spinal neuronal pathology associated with continuous intrathecal infusion of N-methyl-D-aspartate in the rat. **Acta Neuropathol Berl** 1990; **81**: 7-13.
81. Yeziarski RP, Santana M, Park SH, Madsen PW. Neuronal degeneration and spinal cavitation following intraspinal injections of quisqualic acid in the rat. **J Neurotrauma** 1993; **10**: 445-456.
82. Yeziarski RP, Liu S, Ruenes GL, Kajander KJ, Brewer KL. Excitotoxic spinal cord injury: behavioral and morphological characteristics of a central pain model. **Pain** 1998; **75**: 141-155.
83. Rothman SM, Olney JW. Excitotoxicity and the NMDA receptor. **TINS** 1987; **10**: 299-302.
84. Choi DW. Ionic dependence of glutamate neurotoxicity. **J Neurosci** 1987; **7**: 369-379.
85. Choi DW. Glutamate neurotoxicity in cortical cell culture is calcium dependent. **Neurosci Lett** 1985; **58**: 293-297.
86. Garthwaite G, Garthwaite J. Mechanisms of AMPA neurotoxicity in rat brain slices. **European Journal of Neuroscience** 1991; **3**: 729-736.
87. Hartley DM, Kurth MC, Bjerkness L, Weiss JH, Choi DW. Glutamate receptor-induced  $45\text{Ca}^{2+}$  accumulation in cortical cell culture correlates with subsequent neuronal degeneration. **J Neurosci** 1993; **13**: 1993-2000.
88. Jancso G, Karcsu S, Kiraly E, et al. Neurotoxin induced nerve cell degeneration: possible involvement of calcium. **Brain Res** 1984; **295**: 211-216.
89. Young W, Koreh I. Potassium and calcium changes in injured spinal cords. **Brain Res** 1986; **365**: 42-53.
90. Schanne FAX, Kane AB, Young EE. Calcium dependence of toxic cell death: a final common pathway. **Science** 1979; 700-702.

91. Randall RD, Thayer SA. Glutamate-induced calcium transient triggers delayed calcium overload and neurotoxicity in rat hippocampal neurons. **J neurosci** 1992; 1882-1895.
92. Simon RP, Griffiths T, Evans MC, Swan JH, Meldrum BS. Calcium overload in selectively vulnerable neurons of the hippocampus during and after ischemia: an electron microscopy study in the rat. **J Cereb Blood Flow Metab** 1984; 4: 350-361.
93. Mitchell JJ, Anderson KJ. Quantitative autoradiographic analysis of excitatory amino acid receptors in the cat spinal cord. **Neurosci Lett** 1991; 124: 269-272.
94. Wallace MC, Tator CH, Frazee P. Relationship between posttraumatic ischemia and hemorrhage in the injured rat spinal cord as shown by colloidal carbon angiography. **Neurosurgery** 1986; 433-439.
95. Guha A, Tator CH, Rochon J. Spinal cord blood flow and systemic blood pressure after experimental spinal cord injury in rats. **Stroke** 1989; 372-377.
96. Guha A, Tator CH. Acute cardiovascular effects of experimental spinal cord injury. **J Trauma** 1988; 481-490.
97. Fehlings MG, Tator CH, Linden RD. The effect of nimodipine and dextran on axonal function and blood flow following experimental spinal cord injury. **J Neurosurg** 1989; 403-416.
98. Bunge MB, Holets VR, Bates ML, Clarke TS, Watson BD. Characterization of photochemically induced spinal cord injury in the rat by light and electron microscopy. **Exp Neurol** 1994; 127: 76-93.
99. Guth L, Albuquerque EX, Deshpande SS, Barrett CP. Ineffectiveness of enzyme therapy on regeneration in the transected spinal cord of the rat. **J Neurosurg** 1980; 73-86.
100. Naftchi NE, Demeny M, DeCrescito V, Tomasula JJ, Flamm ES, Campbell JB. Biogenic amine concentrations in traumatized spinal cords of cats. Effect of drug therapy. **J Neurosurg** 1974; 40: 52-57.
101. Zivin JA, Doppman JL, Reid JL, et al. Biochemical and histochemical studies of biogenic amines in spinal cord trauma. **Neurology** 1976; 26: 99-107.
102. Brodner RA, Dohrmann GJ, Roth RH, Rubin RA. Correlation of cerebrospinal fluid serotonin and altered spinal cord blood flow in experimental trauma. **Surg Neurol** 1980; 13: 337-343.

103. Salzman SK, Hirofuji E, Lladós Eckman C, MacEwen GD, Beckman AL. Monoaminergic responses to spinal trauma. Participation of serotonin in posttraumatic progression of neural damage. **J Neurosurg** 1987; **66**: 431-439.
104. Torre JC, Johnson CM, Harris LH, Kajihara K, Mullan S. Monoamine changes in experimental head and spinal cord trauma: failure to confirm previous observations. **Surg Neurol** 1974; **2**: 5-11.
105. Faden AI, Molineaux CJ, Rosenberger JG, Jacobs TP, Cox BM. Endogenous opioid immunoreactivity in rat spinal cord following traumatic injury. **Ann Neurol** 1985; **17**: 386-390.
106. Williams B. Posttraumatic syringomyelia. In: Vinken PJ, Bruyn GW, Klawans HL, eds. *Handbook of Clinical Neurology*, Amsterdam: ELSEVIER SCIENCE, 1992: 375-396.
107. Williams B. Progress in syringomyelia. **Neurol Res** 1986; **8**: 130-145.
108. Chakraborty S, Tamaki N, Ehara K, Takahashi A, Ide C. Experimental syringomyelia: late ultrastructural changes of spinal cord tissue and magnetic resonance imaging evaluation. **Surg Neurol** 1997; **48**: 246-254.
109. Yamazaki Y, Tachibana S, Ohta N, Yada K, Ohama E. Experimental model of chronic tonsillar herniation associated with early stage syringomyelia. **Acta Neuropathol Berl** 1995; **90**: 425-431.
110. Milhorat TH, Nobandegani F, Miller JI, Rao C. Noncommunicating syringomyelia following occlusion of central canal in rats. Experimental model and histological findings. **J Neurosurg** 1993; **78**: 274-279.
111. Yeziarski RP. Pain following spinal cord injury: the clinical problem and experimental studies. **Pain** 1996; **68**: 185-194.
112. Basso DM, Beattie MS, Bresnahan JC. Graded histological and locomotor outcomes after spinal cord contusion using the NYU weight-drop device versus transection. **Exp Neurol** 1996; **139**: 244-256.
113. Balentine JD. Pathology of experimental spinal cord trauma. II. Ultrastructure of axons and myelin. **Lab Invest** 1978; **39**: 254-266.
114. Ducker TB, Kindt GW, Kempf LG. Pathological findings in acute experimental spinal cord trauma. **J Neurosurg** 1971; **35**: 700-708.
115. Pisharodi M, Nauta HJ. An animal model for neuron-specific spinal cord lesions by the microinjection of N-methylaspartate, kainic acid, and quisqualic acid. **Appl Neurophysiol** 1985; **48**: 226-233.

116. Liu S, Ruenes GL, Yeziarski RP. NMDA and non-NMDA receptor antagonists protect against excitotoxic injury in the rat spinal cord. **Brain Res** 1997; **756**: 160-167.
117. Liu S, Ruenes GL, Yeziarski RP. Dose-dependent neuronal loss produced by the intraspinal injection of NMDA: blockade by MK-801 but not NBQX or a metabotropic antagonist. **Society of Neuroscience Abstract** 1995; **21**: 1904
118. Liu S, Ruenes GL, Dancausse HA, Yeziarski RP. Non-NMDA receptor antagonists protect against neurotoxic spinal cord injury in the rat. **Society for Neuroscience Abstract** 1994; **20**: 1534-1535.
119. Liu S, Ruenes GL, Yeziarski RP. Dose-dependent neuronal loss produced by the intraspinal injection of AMPA: blockade by NBQX but not MK-801 or a metabotropic antagonist. **Society of neuroscience abstract** 1996; 1904
120. Dancausse HA, Brunschwig JP, Bunge MB, Yeziarski RP. Morphological characterization of excitotoxic injury in the rat spinal cord. **Soc Neurosci Abstr** 1995; **21**: 231
121. McLennan H, Hicks TP, Hall JG. Receptors for the excitatory amino acids. In: DeFeudis FV, Mandel P, eds. *Amino acid neurotransmitters*, New York: Raven Press, 1981: 213-221.
122. Watkins JC. The NMDA receptor concept: origins and development. In: Collingridge GL, Watkins JC, eds. *The NMDA receptor*, 2nd ed. Oxford, New York, Tokyo: Oxford University Press, 1994: 1-30.
123. Collingridge GL, Singer W. Excitatory amino acid receptors and synaptic plasticity. **Trends Pharmacol Sci** 1990; **11**: 290-296.
124. Lehmann J, Schneider JA, Williams M. Excitatory amino acids and mammalian CNS function. **Annual reports in medicinal chemistry** 1987; **22**: 31-40.
125. Garthwaite J. NMDA receptors, neuronal development, and neurodegeneration. In: Collingridge GL, Watkins JC, eds. *The NMDA Receptor*, 2nd ed. Oxford, New York, Tokyo: Oxford University Press, 1994: 428-456.
126. Olney JW, Rhee V, Ho OL. Kainic acid: a powerful neurotoxic analogue of glutamate. **Brain Res** 1974; **77**: 507-512.
127. Murakoshi I, Kato F, Haginiwa J, Takemoto T. Enzymic synthesis of quisqualic acid from O-Acetylserine and 3,5-Dioxo-1,2,4-oxadiazolidine by extracts of higher plants. **Chem Pharm Bull** 1974; **22**: 473-475.

128. Watkins JC, Pook PCK, Sunter DC, Davies J, Honore T. Experiments with kainate and quisqualate agonists and antagonists in relation to the sub-classification of non-NMDA receptors. In: Ben-Ari Y, ed. Excitatory amino acids and neuronal plasticity, New York: Plenum Press, 1990: 49-55.
129. McGeer PL, McGeer EG, Hattori T. Kainic acid as a tool in neurobiology. In: McGeer EG, Olney JW, McGeer PL, eds. Kainic acid as a tool in neurobiology, New York: Raven Press, 1978: 123-138.
130. Subasinghe N, Schulte M, Roon RJ, Koerner JF, Johnson RL. Quisqualic acid analogues: synthesis of beta-heterocyclic 2-aminopropanoic acid derivatives and their activity at a novel quisqualate-sensitized site. **J Med Chem** 1992; **35**: 4602-4607.
131. Boden P, Bycroft BW, Chhabra SR, et al. The action of natural and synthetic isomers of quisqualic acid at a well-defined glutamatergic synapse. **Brain Res** 1986; **385**: 205-211.
132. Dictionary of organic compounds, 5th, suppl 5 ed. London, New York: Chapman and Hall, 1989: 553
133. Flippen JL, Gilardi RD. Quisqualic acid. **Acta Cryst** 1976; **B32**: 951-953.
134. Takemoto T, Nakajima T, Arihara S, Koike K. Studies on the constituents of quisqualic fructus. II. and structure of quisqualic acid. **Yakugaku Zasshi** 1975; **95**: 326-332.
135. Watkins JC. Excitatory amino acids. In: McGeer EG, Olney JW, McGeer PL, eds. Kainic acid as a tool in neurobiology, New York: Raven Press, 1978: 37-69.
136. Biscoe TJ, Evans RH, Headley PM, Martin MR, Watkins JC. Structure-activity relations of excitatory amino acids on frog and rat spinal neurones. **Br J Pharmacol** 1976; **58**: 373-382.
137. Biscoe TJ, Evans RH, Headley PM, Martin MR, Watkins JC. Domoic and quisqualic acids as potent amino acid excitants of frog and rat spinal neurones. **Nature** 1975; **255**: 166-167.
138. Shinozaki H, Shibuya I. A new potent excitant, quisqualic acid: effects on crayfish neuromuscular junction. **Neuropharmacology** 1974; **13**: 665-672.
139. Lodge D, Curtis DR, Johnston GA, Bornstein JC. In vivo inactivation of quisqualate: studies in the cat spinal cord. **Brain Res** 1980; **182**: 491-495.
140. Honore T, Lauridsen J, Krosgaard Larsen P. The binding of [3H]AMPA, a structural analogue of glutamic acid, to rat brain membranes. **J Neurochem** 1982; **38**: 173-178.

141. Watkins JC, Evans RH, Mewett KN, Olverman HJ, Pook PC. Recent advance in the pharmacology of excitatory amino acids. **Neurology and Neurobiology** 1987; **24**: 19-26.
142. Monaghan DT, Bridges RJ, Cotman CW. The excitatory amino acid receptors: their classes, pharmacology, and distinct properties in the function of the central nervous system. **Annu Rev Pharmacol Toxicol** 1989; **29**: 365-402.
143. Watkins JC. Pharmacology of excitatory amino acid transmitters. In: DeFeudis FV, Mandel P, eds. Amino acid neurotransmitters, New York: Raven Press, 1981: 205-212.
144. Watkins JC, Davies J, Evans RH, Francis AA, Jones AW. Pharmacology of receptors for excitatory amino acids. In: Chiara GD, Gessa GL, eds. Glutamate as a neurotransmitter, New York: Raven Press, 1981: 263-273.
145. Olney JW. kainic acid and other excitotoxins: a comparative analysis. In: Chiara GD, Gessa GL, eds. Glutamate as a neurotransmitter, New York: Raven Press, 1981: 375-384.
146. Young AB, Fagg GE. Excitatory amino acid receptors in the brain: membrane binding and receptor autoradiographic approaches. **Trends Pharmacol Sci** 1990; **11**: 126-133.
147. Barnard EA, Henley JM. The non-NMDA receptors: types, protein structure and molecular biology. **Trends Pharmacol Sci** 1990; **11**: 500-507.
148. Watkins JC. The NMDA receptor concept: origins and development. In: Watkins JC, Collingridge GL, eds. The NMDA receptor, 1st ed. Oxford, New York, Tokyo: Oxford University Press, 1989: 1-17.
149. Alexander SPH, Peters JA. 1997 receptor & ion channel nomenclature supplement. **Trends in Pharmacological Sciences** 1997; **supple1**: 36-40.
150. Aanonsen LM, Lei S, Wilcox GL. Excitatory amino acid receptors and nociceptive neurotransmission in rat spinal cord. **Pain** 1990; **41**: 309-321.
151. Pai KS, Ravindranath V. Quisqualic acid-induced neurotoxicity is protected by NMDA and non-NMDA receptor antagonists. **Neurosci Lett** 1992; **143**: 177-180.
152. Palmer E, Monaghan DT, Cotman CW. Glutamate receptors and phosphoinositide metabolism: stimulation via quisqualate receptors is inhibited by N-methyl-D-aspartate receptor activation. **Brain Res** 1988; **464**: 161-165.
153. Sladeczek F, Pin J, Recasens M, Bockaert J, Weiss S. Glutamate stimulates inositol phosphate formation in striatal neurones. **Nature** 1985; **317**: 717-719.

154. Recasens M, Guiramand J, Nourigat A, Sasseti I, Devilliers G. New quisqualate receptor subtype(sAA2) responsible for the glutamate-induced inositol phosphate formation in rat brain synaptoneuroosomes. **Neuroche Int** 1988; **13**: 463-467.
155. Garthwaite G, Garthwaite J. Differential dependence on Ca<sup>2+</sup> of N-methyl-D-aspartate and quisqualate neurotoxicity in young rat hippocampal slices. **Neurosci Lett** 1989; **97**: 316-322.
156. Davies J, Francis AA, Jones AW, Watkins JC. 2-Amino-5-phosphonovalerate (2APV), a potent and selective antagonist of amino acid-induced and synaptic excitation. **Neurosci Lett** 1981; **21**: 77-81.
157. Nag S. Vascular changes in the spinal cord in N-methyl-D-aspartate-induced excitotoxicity: morphological and permeability studies. **Acta Neuropathol Berl** 1992; **84**: 471-477.
158. Hajos F, Garthwaite G, Garthwaite J. Reversible and irreversible neuronal damage caused by excitatory amino acid analogues in rat cerebellar slices. **Neuroscience** 1986; **18**: 417-436.
159. Rothman SM, Olney JW. Glutamate and the pathophysiology of hypoxic--ischemic brain damage. **Ann Neurol** 1986; **19**: 105-111.
160. Dougherty PM, Willis WD. Modification of the responses of primate spinothalamic neurons to mechanical stimulation by excitatory amino acids and an N-methyl-D-aspartate antagonist. **Brain Res** 1991; **542**: 15-22.
161. Dougherty PM, Palecek J, Paleckova V, Sorkin LS, Willis WD. The role of NMDA and non-NMDA excitatory amino acid receptors in the excitation of primate spinothalamic tract neurons by mechanical, chemical, thermal, and electrical stimuli. **J Neurosci** 1992; **12**: 3025-3041.
162. Wilcox GL. Pharmacological studies of grooming and scratching behavior elicited by spinal substance P and excitatory amino acids. In: Colbern DL, Gispén WH, eds. Neural mechanisms and biological significance of grooming behavior, New York: The New York Academy of Sciences, 1988: 228-236.
163. Olney JW, Ho OL, Rhee V. Cytotoxic effects of acidic and sulphur containing amino acids on the infant mouse central nervous system. **Exp Brain Res** 1971; **14**: 61-76.
164. Auer RN, Siesjö BK. Biological differences between ischemia, hypoglycemia, and epilepsy. **Ann Neurol** 1988; **24**: 699-707.
165. Garthwaite J, Garthwaite G, Hajos F. Amino acid neurotoxicity: relationship to neuronal depolarization in rat cerebellar slices. **Neuroscience** 1986; **18**: 449-460.

166. Garthwaite G, Garthwaite J. In vitro neurotoxicity of excitatory acid analogues during cerebellar development. **Neuroscience** 1986; **17**: 755-767.
167. Choi DW, Maulucci Gedde M, Kriegstein AR. Glutamate neurotoxicity in cortical cell culture. **J Neurosci** 1987; **7**: 357-368.
168. Olney JW. Brain lesions, obesity, and other disturbances in mice treated with monosodium glutamate. **Science** 1969; **164**: 719-721.
169. Kohler C, Schwarcz R. Comparison of ibotenate and kainate neurotoxicity in rat brain: a histological study. **Neuroscience** 1983; **8**: 819-835.
170. Koh JY, Goldberg MP, Hartley DM, Choi DW. Non-NMDA receptor-mediated neurotoxicity in cortical culture. **J Neurosci** 1990; **10**: 693-705.
171. Olney JW. Neurotoxicity of excitatory amino acids. In: McGeer EG, Olney JW, McGeer PL, eds. *Kainic acid as a tool in neurobiology*, New York: Raven Press, 1978: 95-121.
172. Garthwaite G, Garthwaite J. Amino acid neurotoxicity: intracellular sites of calcium accumulation associated with the onset of irreversible damage to rat cerebellar neurones in vitro. **Neurosci Lett** 1986; **71**: 53-58.
173. Garthwaite J. NMDA receptors, neuronal development, and neurodegeneration. In: Watkins JC, Collingridge GL, eds. *The NMDA receptor*, 1st ed. Oxford, New York, Tokyo: Oxford University Press, 1989: 400-425.
174. Nicholls D, Attwell D. The release and uptake of excitatory amino acids [see comments]. **Trends Pharmacol Sci** 1990; **11**: 462-468.
175. Nicoletti F, Meek JL, Iadarola MJ, Chuang DM, Roth BL, Costa E. Coupling of inositol phospholipid metabolism with excitatory amino acid recognition sites in rat hippocampus. **J Neurochem** 1986; **46**: 40-46.
176. Choi DW. Calcium-mediated neurotoxicity: relationship to specific channel types and role in ischemic damage. **Trends Neurosci** 1988; **11**: 465-469.
177. Mayer ML, Miller RJ. Excitatory amino acid receptors, second messengers and regulation of intracellular Ca<sup>2+</sup> in mammalian neurons. **Trends Pharmacol Sci** 1990; **11**: 254-260.
178. Schoepp D, Bockaert J, Sladeczek F. Pharmacological and functional characteristics of metabotropic excitatory amino acid receptors. **Trends Pharmacol Sci** 1990; **11**: 508-515.

179. Schoepp DD, Johnson BG. Excitatory amino acid agonist-antagonist interactions at 2-amino-4-phosphonobutyric acid-sensitive quisqualate receptors coupled to phosphoinositide hydrolysis in slices of rat hippocampus. **J Neurochem** 1988; **50**: 1605-1613.
180. Nishizuka Y. Turnover of inositol phospholipids and signal transduction. **Science** 1984; **225**: 1365-1370.
181. Sugiyama H, Ito I, Hirono C. A new type of glutamate receptor linked to inositol phospholipid metabolism. **Nature** 1987; **325**: 531-533.
182. Garthwaite G, Garthwaite J. Quisqualate neurotoxicity: a delayed, CNQX-sensitive process triggered by a CNQX-insensitive mechanism in young rat hippocampal slices. **Neurosci Lett** 1989; **99**: 113-118.
183. Dingledine R, McBain CJ, McNamara JO. Excitatory amino acid receptors in epilepsy. **Trends Pharmacol Sci** 1990; **11**: 334-338.
184. Sacaan AI, Schoepp DD. Activation of hippocampal metabotropic excitatory amino acid receptors leads to seizures and neuronal damage. **Neurosci Lett** 1992; **139**: 77-82.
185. Griffiths T, Evans MC, Meldrum BS. Intracellular calcium accumulation in rat hippocampus during seizures induced by bicuculline or L-allylglycine. **Neuroscience** 1983; **10**: 385-395.
186. Young AB, Greenamyre JT, Hollingsworth Z, et al. NMDA receptor losses in putamen from patients with Huntington's disease. **Science** 1988; **241**: 981-983.
187. McGeer EG, McGeer PL. Duplication of biochemical changes of Huntington's chorea by intrastriatal injections of glutamic and kainic acids. **Nature** 1976; **263**: 517-519.
188. Greenamyre JT, Olson JM, Penney JB, Jr., Young AB. Autoradiographic characterization of N-methyl-D-aspartate-, quisqualate- and kainate-sensitive glutamate binding sites. **J Pharmacol Exp Ther** 1985; **233**: 254-263.
189. Meldrum B. Possible therapeutic applications of antagonists of excitatory amino acid neurotransmitters. **Clin Sci** 1985; **68**: 113-122.
190. Santoreneos S, Stoodley MA, Jones NR. A technique for in vivo vascular perfusion fixation of the sheep central nervous system. **Journal of Neuroscience** 1998; **79**: 195-199.
191. Sternberger LA, ed. Immunocytochemistry, 2nd ed. New York: John Wiley & Sons, 1979:

192. McLendon RE, Burger PC, Pegram CN. The immunohistochemical application of three anti-GFAP monoclonal antibodies to formalin-fixed, paraffin-embedded, normal and neoplastic brain tissues. **Journal of Neuropathology and Experimental Neurology** 1986; **45**: 692-703.
193. Dijkstra CD, Dopp EA, Joling P. The heterogeneity of mononuclear phagocytes in lymphoid organs: distinct macrophage subpopulations in the rat recognized by monoclonal antibodies ED1, ED2 and ED3. **Immunology** 1985; 589-599.
194. Masters CL, Beyreuther K, Trillet M, Christen Y, eds. Amyloid protein precursor in development, aging and Alzheimer's disease- research and perspectives in Alzheimer's disease, Heidelberg: Springer-Verlag, 1994:
195. Gentleman SM, Nash MJ, Sweeting CJ. Amyloid precursor protein as a marker for axonal injury after head injury. **Neuroscience Letters** 1993; 139-144.
196. Lewis SB, Finnie JW, Blumbergs PC. A head impact model of early axonal injury in the sheep. **Journal of Neurotrauma** 1996; **13**: 505-514.
197. Trauma to the spinal cord. In: Hughes JT, ed. Pathology of the spinal cord. London: LLOYD-LUKE LTD, 1966: 58-69.
198. Christian S, Gallo V. News on glutamate receptors in glial cells. **TINS** 1996; **19**: 339-345.
199. Sgouros S, Williams B. Management and outcome of posttraumatic syringomyelia [see comments]. **J Neurosurg** 1996; **85**: 197-205.
200. Verbe BP, Aurier KL, Robert R. Posttraumatic syringomyelia and posttraumatic spinal canal stenosis: a direct relationship: review of 75 patients with a spinal cord injury. **Spinal Cord** 1998; **36**: 137-143.
201. Garthwaite G, Garthwaite J. Neurotoxicity of excitatory amino acid receptor agonists in rat cerebellar slices: dependence on calcium concentration. **Neurosci Lett** 1986; **66**: 193-198.
202. Takemoto T, Takagi N, Nakajima T. Studies on the constituents of Quisqualic Fructus. I. on the amino acids. **Journal of the Pharmaceutical Society of Japan** 1975; **95**: 176-179.